8-2016

The Role the N-terminal Domain Plays in Spidroin Assembly

Krystal Audrey Cadle
Clemson University, kcadle@g.clemson.edu

THE ROLE THE N-TERMINAL DOMAIN PLAYS IN SPIDROIN ASSEMBLY

A Dissertation
Presented to
the Graduate School of
Clemson University

In Partial Fulfillment
of the Requirements for the Degree
Doctor of Philosophy
Genetics

---

by
Krystal Audrey Cadle
August 2016

Accepted by:
Dr. William Marcotte, Committee Chair
Dr. James Morris
Dr. Michael Sehorn
Dr. Kerry Smith

ABSTRACT

One of the most interesting biomaterials known to man is spider silk. These fibers, composed primarily of protein, show beneficial mechanical and biological properties that have many uses in medical and industrial fields. Spider silk proteins (spidroins) are composed of three core components that consists of a C-terminal domain (CTD), repeat domain (R), and N-terminal domain (NTD). The NTD and CTD are highly conserved and are believed to form "multimeric strands" that make up spider silk. Although it is known that the NTD undergoes a conformational change that results in stable homodimer formation at acidic pH , the way in which the NTD contributes to fiber assembly is still under investigation. .

Here we provide label-free, real-time dimerization data of the wild-type major ampullate spidroin 1 (MaSp1) NTD from *Nephila clavipes* using the Octet RED96 system. This data shows over 25-fold increase in the affinity of wild-type NTD monomers at pH 5.5 compared to pH 7.0. These results are in agreement with previous work from our lab and others that show an increase in homodimer stability at acidic pH. This information correlates with the conformational change seen as the wild-type NTD transitions from a neutral to acidic pH environment. We found that NTD variants D45K and E84K abolished the conformational change that occurs at pH 5.5 and decreased dimer stability compared to wild-type MaSp1 NTD. We also found showed that variant K70D and double variant D45K/K70D exist in an intermediate conformation between that seen at pH 5.5 and pH 7.0 for wild-type NTD. This new information provides additional evidence to support the idea that a conformational change is directly connected

to dimerization. Our data provides additional insight into which residues are necessary for this conformational change and subsequent dimerization, which allows for a better understanding of the homodimerization process.

We also demonstrate production of MaSp2 “mini spidroins” in *Saccharomyces cerevisiae*. These “mini spidroins” contained a native CTD and NTD and eight repeat units and preliminary results show that glucose and raffinose preinduction media result in better protein expression using 24 hr and 72hr induction times, respectively.

DEDICATION

For my friends and family who have been so supportive.

ACKNOWLEDGMENTS

First I would like to thank Dr. William Marcotte, Jr. for allowing me to join his lab, and guiding me and supporting me throughout my graduate career. I would also like to thank my committee members Dr. James Morris, Dr. Michael Sehorn, and Dr. Kerry Smith for their suggestions and help. This work could not have been accomplished without the invaluable help of my past and current lab members Dr. Will Gaines, Dr. Todd Lyda, Dr. Congyue (Annie) Peng, Kelly McQueeney, Mikayla Spitler, Breanna Burks and Allison Nelson.

TABLE OF CONTENTS

Page

Table of Contents (Continued)

Page

Table of Contents (Continued)

Page

LIST OF TABLES

LIST OF FIGURES

List of Figures (Continued)

Figure Page

List of Figures (Continued)

Figure Page

CHAPTER ONE
LITERATURE REVIEW

I. Types and Properties of Spider Silk

1. Spider Silk

Silks are structural proteins that are produced primarily by arthropods and have evolved multiple times in the arthropod phylum. Within this phylum are insects that can produce many different types of silks but only one type per individual species. However, another member of this phylum, the arachnid, can produce up to seven different types of silk and has been producing silks for over 450 million years(Fig 1.1) (Lewis, 2006). These silks have evolved to be used in a variety of ways including: shelter, prey capture and offspring protection (Heidebrecht and Scheibel, 2013; Lewis, 2006). Each of these different types of silk are produced in a separate gland that is located within the abdominal cavity of the spider. A liquid composed predominately of fibroin proteins is secreted into the glands. The various arachnid silks are thought to have evolved through gene duplication and differentiation (Bittencourt et al., 2012). The proteins contain highly repetitive amino acid sequences that contribute to the mechanical and functional properties of the spidroin (spider fibroin) protein (Craig, 1997; Vepari and Kaplan, 2007). The various spidroin proteins can vary greatly in size, strength, elasticity and toughness (Altman et al., 2003; Humenik et al., 2011).

The most studied group of spider silk belongs to the *Orbiculariae* clade due to the orb-web that they produce. The adult female spider of this group can produce up to seven different types of silk (Heidebrecht and Scheibel, 2013). These include pyriform (Py),

aciniform (Ac), tubiform (Tu), aggregate (Ag), flagelliform (Flag), minor ampullate (Mi) and major ampullate silk (Ma) (Fig. 1.1). Within this group of orb-weavers *Nephila clavipes* is one of the most studied spiders due to its large size and availability. *Nephila clavipes* is often referred to as the golden orb-weaving spider, due to the golden color of some of its silk. These spiders are found in parts of Central and North America. The largest variety of silks are produced by the female *Nephila clavipes* which can grow up to 10 times larger than their male counterparts (Elgar and Fahey, 1996)

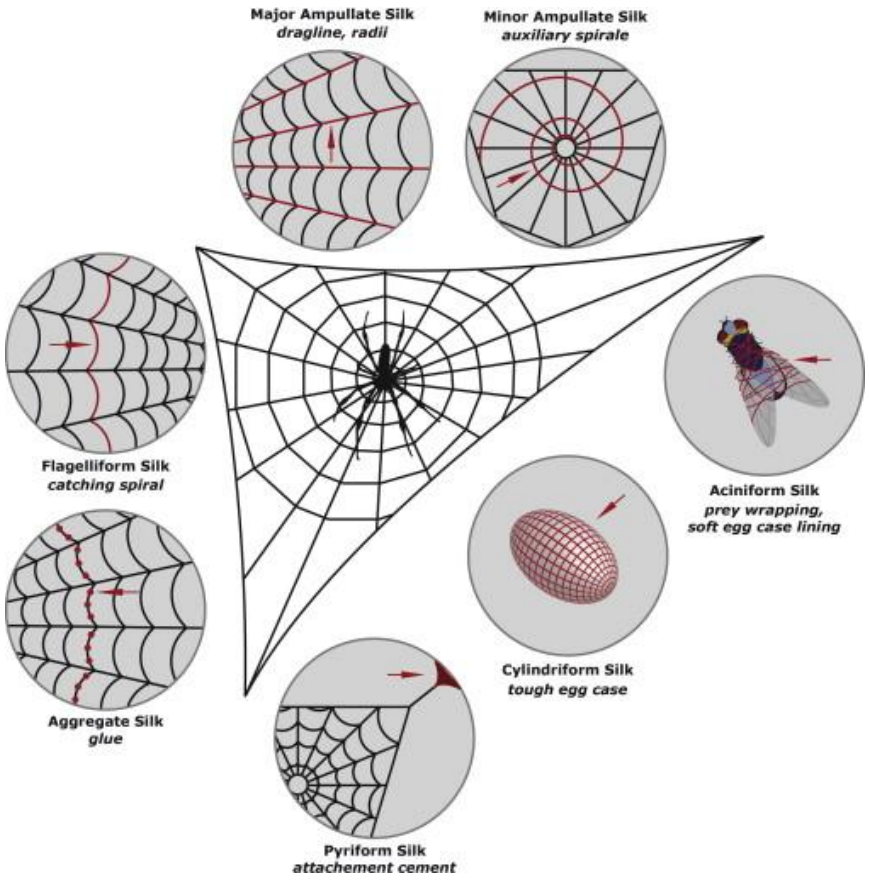

Figure 1.1 Schematic presentations of the seven different types of spider silk. From (Heidebrecht and Scheibel, 2013)

2. Pyriform

Pyriform (Py) silk is one of the least studied, yet most diverse, spider silks. This silk functions as a glue-like substance that is used to form attachment disc silks (Fig. 1.1) (Blasingame et al., 2009; Humenik et al., 2011; Perry et al., 2010). Disc silks secure major ampullate, minor ampullate, and flagelliform silk fibers to each other and to a variety of materials such as walls and tree branches (Blasingame et al., 2009; Heidebrecht and Scheibel, 2013). The pyriform silk fibers contain a large amount of polar amino acid residues as well as the highest amount of charged residues and alanine of all known spidroins. Some species have been shown to contain QQ and PXP motifs in their protein sequence although their function is still unknown (Blasingame et al., 2009; Humenik et al., 2011; Perry et al., 2010). In the black widow spider, *Latrodectus mactans*, and others, the pyriform gland is the smallest gland found in the abdomen of the spider. Unlike many of the other silk glands, which occur in a single pair, the pyriform gland can occur in more than one pair (Blasingame et al., 2009; Jeffery et al., 2011).

3. Aciniform

Aciniform silk (Ac) is used in egg casing, prey wrappings, and to reinforce the pyriform silk disks (Fig. 1.1) (Blackledge and Hayashi, 2006). It displays almost two-fold greater toughness than other silks (Blackledge and Hayashi, 2006). The aciniform spidroin 1 protein (AcSp1) is composed of about 200 amino acids consisting of 14 repeats (Hayashi et al., 2004; Heidebrecht and Scheibel, 2013; Lewis, 2006). The most common subrepeat is poly-serine, however the repeats do not show significant similarity to other spidroin repetitive regions (Humenik et al., 2011). The aciniform and pyriform

glands are believed to be the closest in appearance to primitive spider silk glands which are simple pear–shaped or spherical glands that occur in some mylalomorph spiders (Jeffery et al., 2011; Shultz, 1987).

4. Tubuliform

Tubuliform silk (Tu), also known as cylindriform silk, is only produced in the adult female spider and is used as the tough outer coat for the egg sack (Fig 1.1) (Lin et al., 2009). It contains S_n, $(SA)_n$, $(SQ)_n$, and GX motifs where X represents Q, N, I, L, A, V, Y, F, or D (Humenik et al., 2011; Lewis, 2006). These motifs likely contribute to a large amount of β-sheet structures turn produces a silk with a more brittle nature when compared to other spider silks (Lewis, 2006). This brittle characteristic is believed to be well suited to the protection of the egg case. Harm to the eggs contained within is reduced because the casing will not deform due to changes in pressure (Humenik et al., 2011).

5. Aggregate

The silk that is produced in the aggregate gland is used as a glue to coat the capture spirals of the web to apprehend prey (Fig. 1.1) (Heidebrecht and Scheibel, 2013; Vasanthavada et al., 2012). This glue behaves as a viscoelastic solid and primarily contains two glycoproteins named ASG-1 and ASG-2, which have a molecular weight of 38 kDa and 65 kDa respectively (Humenik et al., 2011; Sahni et al., 2011). Uniquely ASG-1 and ASG-2 are the only known glycosylated silk proteins (Humenik et al., 2011). Glycosylation may be a large contributor to the adhesive property of the aggregate silks. Unlike cobweb-weaving spiders, orb-weaving spider aggregate silk responds to changes

in humidity to prevent water evaporation of the fiber that attaches to the aggregate silk (Perea et al., 2013; Sahni et al., 2011; Vollrath et al., 1990). This is thought to occur because the aggregate silk of the orb-weaver sequesters water through its high concentration of hygroscopic salt. This water uptake causes the aggregate protein to spread out across the capture spiral, which is composed of flagelliform silk (Fig. 1.1) and maintain its hydration. The glands are very large, when compared to other silk glands and have a relatively large duct connecting the gland to the spinneret, which is located on the abdomen and is where the silk is extruded (Jeffery et al., 2011).

6. Flagelliform

Flagelliform silk (Flag), also capture or viscid silk, is used in the spiral of the web to capture prey (Fig. 1.1) (Humenik et al., 2011). It was also the first spider silk gene to be sequenced and is believed to be the most recently evolved spider silk (Humenik et al., 2011; Lewis, 2006). Unlike other spider silks the gene for flagelliform silk is separated into 13 exons instead of the one large exon that is common in other spider silk genes (Humenik et al., 2011). The flagelliform fiber (~500 kDa) contains the GPGGX and GGX motifs that are believed to be involved in β-turn spirals. The flagelliform spidroin also has a spacer motif that has numerous charged and hydrophilic amino acids (Lewis, 2006). This spacer motif provides strength due to lack of poly-alanine motifs present in dragline silk and gives flagelliform silk the highest elasticity of all the spider silks with an extensibility of up to 475% of its original length (Heidebrecht and Scheibel, 2013; Humenik et al., 2011; Lee et al., 2007). Major ampullate silk, the major ampullate silk is not nearly as extensible (Fig. 1.2) and when both major ampullate and flagelliform silks

are exposed to stress, a higher strain is observed from the flagelliform silk. However, the major ampullate silk can withstand more than twice the stress before it registers even a sixth of the strain.

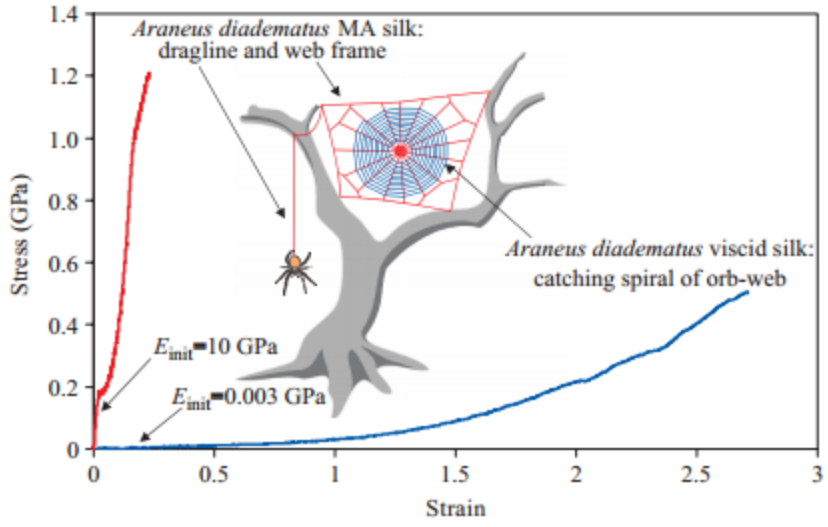

Figure 1.2 Stress-strain curves for major ampullate (red) and viscid (blue) silks form *Araneus diadematus.* From (Gosline et al., 1999)

7. Minor Ampullate

Minor Ampullate silks consist of two proteins, approximately 250 kDa each, labeled MiSp1 and MiSp2, that are used as a support spiral during web construction (Fig 1.1) (Heidebrecht and Scheibel, 2013). The minor ampullate silk, shows large similarities to the major ampullate silk; however, there are some significant differences (Humenik et al., 2011). For instance *N. clavipes*, major and minor ampullate spidroins have similar repetitive region motifs GGXGGY and $(GA)_y(A)_z$ for Sp1; $(GGX)_n$ and GAGA for Sp2 (Colgin and Lewis, 1998). However, the repetitive regions are broken by non-repetitive serine-rich spacers for minor ampullate spidroins. Additionally, the poly-alanine motifs

are shorter for minor ampullate spidroins (Lewis, 2006). Unlike major ampullate spider silk, the minor ampullate silk does not supercontract in water (Chen et al., 2012).

7. Major Ampullate

Major ampullate silk, known as the dragline silk, is used as lifeline for the spider, and is used as the radial threads in the web construction (Fig 1.1) (Heidebrecht and Scheibel, 2013). It is the most studied type of silk and consists of at least two major ampullate (Ma) spidroins. The two types of major ampullate silk are denoted as MaSp1 and MaSp2 and have a molecular weight of between 200 kDa and 350 kDa. The major difference between the two types of major ampullate silk is that MaSp2 is rich in prolines and the length of the repeats is variable. The ratio of MaSp1 to MaSp2 can vary among spider species and has been shown to change based on the level of starvation and available food sources experienced by the spider (Brooks et al., 2005; Guehrs et al., 2008; Tso et al., 2005). Both MaSp1 and MaSp2, along with many other types of spider silks, contain a repetitive domain that is flanked on either side by a non-repetitive amino-terminal (NTD) and carboxy-terminal domain (CTD). The repeat domain consists of amino acid sequences that can be repeated up to one hundred times.

II. Major Ampullate Silk Components

1. Overview

Spider dragline silk is the "toughest biopolymer on Earth" (Tokareva et al., 2013). Therefore, it is no surprise that it is the most studied of all the spider silks and although some mysteries still remain, much information has been gathered on this biomaterial.

Over 90% of the dry mass of major ampullate fiber is composed of protein dominated by two proteins known as major ampullate spidroin 1 (MaSp1) and major ampullate spidroin 2 (MaSp2) (Lewis, 2006). In *Nephila clavipes* there are two distinct MaSp1 genes (MaSp1A and MaSp1B) (Gaines and Marcotte, 2008). It is possible that the different ratios of MaSp1 to MaSp2 are the reason for the differences seen in the strength and extension of these fibers between species. Within the core of the fibers, the MaSp1 and MaSp1 are arranged in a way that the MaSp1 is found in both the core and periphery while the MaSp2 forms clusters only within the core (Tokareva, et al., 2013). The MaSps are between 250 to 350 kDa and are composed of three parts: 1) N-terminal domain; 2) repeat domain; 3) C-terminal domain (Sponner et al., 2007).

2. Shell

In addition to MaSp1 and MaSp2, there are other components that make up the natural dragline fiber. Outside of the core MaSp1 and MaSp2 proteins there is a 150-250 nm thick shell made up of lipids, glycoproteins and minor ampullate silk proteins (Fig. 1.3) (Augsten et al., 2000; Sponner et al., 2007). This shell helps to carry pheromones, which are used for sexual communication, protect the fiber from the surroundings including microorganisms, regulate the water balance in the fiber, and support and add plasticity to the fiber (Schulz, 2013; Augsten et al., 2000; Heidebrecht and Scheibel, 2013; Romer and Scheibel, 2008; Sponner et al., 2007).

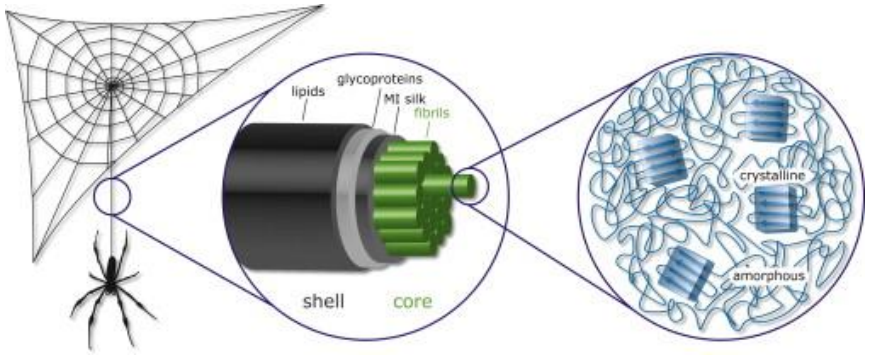

Figure 1.3 Core–shell structure of the dragline silk.. From (Heidebrecht and Scheibel, 2013)

3. C-terminal Domain

The C-terminal domain (CTD) is a non-repetitive sequence of about 150 amino acids. The CTDs of all silk types are conserved with at least 30% identity (Challis et al., 2006). Additionally, the predicted secondary structures and physical properties are alike. Originally, it was believed that the CTDs were not present in dragline fiber due to cleavage. However, through the use of polyclonal antibodies major ampullate filaments were shown to contain CTDs (Sponner et al., 2004). The structure of the CTD is composed of a bundle of five parallel α-helices. A single cysteine residue in the middle of the C-terminal sequence is highly conserved and is responsible for the covalent dimerization of CTDs through disulfide bond linkage with another CTD (homo-dimerization, Fig. 1.4) (Hedhammar et al., 2008; Ittah et al., 2007; Sponner et al., 2004). While in this folded state, the hydrophobic residues are buried and the hydrophilic residues are exposed (Romer and Scheibel, 2008). This arrangement is believed to be important in the solubility of the silk and subsequent fiber self-assembly (Gao et al., 2013; Sponner et al., 2004).

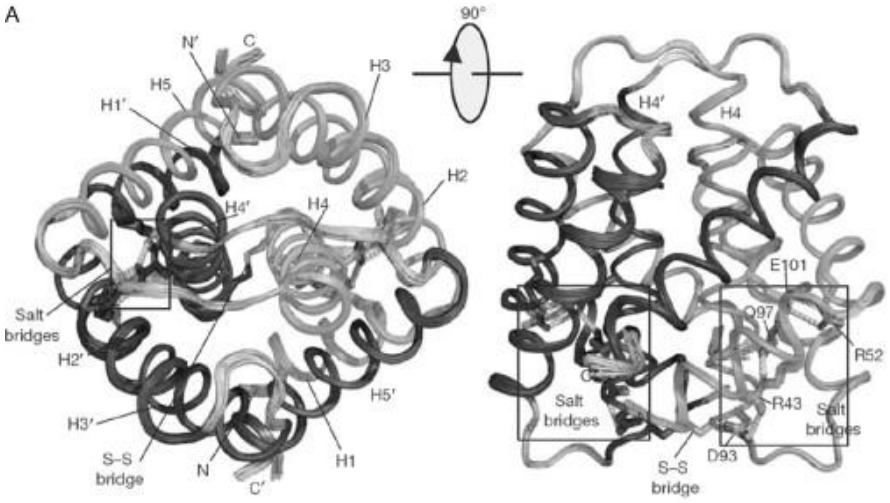

Figure 1.4 NMR structure of the C-terminal domain dimer, from *Euprosthenops australis,* with monomers in light and dark grey. Regions involved in salt bridges are denoted by boxes. From (Humenik et al., 2011)

4. Repeat Domain

More than 90% of spidroin protein is composed of repeat domain (R) amino acid sequences (Romer and Scheibel, 2008). Single repeat units vary in length from about 20-40 amino acids and a repeat section can be repeated over a hundred times within the dragline silk spidroin (Ayoub et al., 2007; Keten and Buehler, 2010; Xu and Lewis, 1990). The repeat domain varies greatly between the different types of silks. Thus, the repeat domain is believed to be responsible for the majority of the differences in mechanical properties of various silk types. Within the dragline silk, MaSp1 and MaSp2 differ primarily in their repeat domains. Both contain poly-alanine $(A)_n$ motifs, however, MaSp1 contains GA and GGX motifs where X is often A, Y, L, or Q (Gatesy et al., 2001; Hu et al., 2006; Keten and Buehler, 2010; Xu and Lewis, 1990). MaSp2 is proline-rich (~15%) and contains GPGXX where X is usually glutamine, glycine or tyrosine. The poly-alanine motifs, also called tails as they usually occur at the end of a repeat, form β-

sheets during fiber formation. The GPGXX motifs of MaSp2 form β-turn spirals that are believed to provide fiber extensibility (Hayashi et al., 1999). The GGX motifs of MaSp1 are thought to form an amorphous matrix that connects the crystalline regions (Hayashi et al., 1999; Scheibel, 2004).

5. N-terminal Domain

Due to the repetitive nature of the MaSps it has been difficult to obtain the sequence of the N-terminal domain (NTD) (Gaines et al., 2010; Romer and Scheibel, 2008). This domain is the most highly conserved domain and consists of five parallel α-helices (Fig. 1.5) (Askarieh et al., 2010; Hedhammar et al., 2008; Motriuk-Smith et al., 2005).

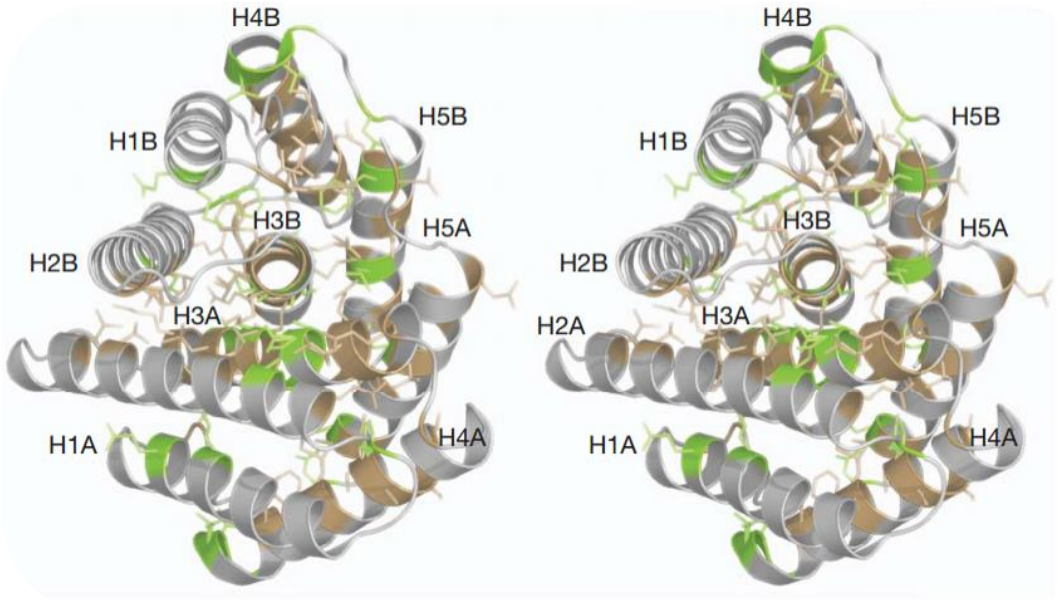

Figure 1.5 Ribbon structure of N-terminal domain dimer, from *E. australis*, showing five α-helixes as H1-H5 with subunits A and B. Highly conserved residues shown in green and brown. From (Askarieh et al., 2010)

The NTD dimerizes in an anti-parallel orientation due to the dipolar nature of the NTD (Askarieh et al., 2010; Humenik et al., 2011; Jaudzems et al., 2012). This homo-dimerization is believed to happen when a pH induced conformational change between pH 7 and pH 6 occurs in the duct during spridroin fiber assembly (Askarieh et al., 2010; Gaines et al., 2010; Motriuk-Smith et al., 2005; Wallace and Shen, 2012).

III. Fiber Assembly

1. The Major Ampullate Gland

Each of the different spider silks previously discussed are secreted and stored in their own glands (Kovoor, 1987). These glands contain dope, a liquid crystalline protein solution, until it is needed by the spider (Hu et al., 2006). Most of the glands are present in a single pair and contain three main parts: the tail, sac (ampulle) and duct (Fig 1.6).

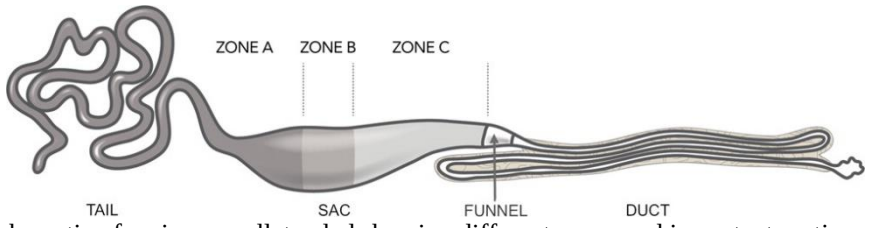

Figure 1.6 Schematic of major ampullate glad showing different zones and important sections. From (Andersson et al., 2013)

The tail of the gland is where the majority of the protein is secreted by glandular cells after which these proteins are stored at very high concentrations (30- 50% w/v) in the ampulle (Chen et al., 2002; Hijirida et al., 1996; Vollrath and Knight, 1999). The tail and sac are composed of three different epithelial cell types that differentiate the tail and

sac into three zones labeled A, B and C (Fig. 1.6) (Andersson et al., 2013; Vollrath and Knight, 1999). In zone A, which includes the tail and the beginning of the sac, the cells are characterized by large irregularly shaped intracellular granules that vary in electron density. In zone B the granules are smaller, more evenly sized and are more dense than in zone A. In zone C the granules are small and have areas of high and low electron density. While zone A secretes the majority of the silk protein, zone B also shows some secretion. This secretion forms a skin-like layer over the zone A protein secretions. Zone C does not show the same secretory behavior and attaches to the funnel of the gland.

The funnel acts as a transition point between the sac and the duct of the gland (Lefevre et al., 2008). The duct is highly elongated and has a two stage hyperbolic geometry where it becomes increasingly narrower as it progresses toward the spinneret (Knight and Vollrath, 1999). The "highly elongated" nature of the duct, which is five times longer than is needed to connect the sac to the spinneret, forms three "limbs" that form an S shape on its way to the valve and is useful to change the environment in which the spidroin protein is found (Fig.1.6) (Bell and Peakall, 1969; Hijirida et al., 1996). The duct epithelial cells are lined with profuse amounts of microvilli and while the cells of the first and second limb are similar, the third limb differs in that the cells are taller and form a single layer (Andersson et al., 2013). The end of the duct attaches to a muscular valve which controls flow rate, fiber diameter and reinitiation upon fiber breakage (Lefevre et al., 2008; Lewis, 2006). The valve is attached to the spigot and spinneret of the spider. (Knight and Vollrath, 1999). The spinnerets are located on the lower abdomen of the spider and have a selection of spigots from which the silk is pulled (Humenik et al.,

2011). There are three pairs of spinnerets called anterior, median and posterior (Lewis, 2006). These spinnerets are innervated and muscular and help to control the fiber diameter and the rate at which it is drawn (Craig, 1997). The number and arrangement of the spigots can vary between the sex, age, and species of spider (Humenik et al., 2011).

2. Mechanical Forces for Fiber Assembly

As spider silk proteins moves from the ampulle and along the duct, they are subjected to mechanical forces that help to align the proteins and create the dragline fiber (Greving et al., 2012). As the duct narrows the protein inside is subject to an increase in flow velocity causing shear forces (Breslauer et al., 2009; Eisoldt et al., 2010; Leclerc et al., 2013). These shear forces act as a catalyst for aggregate or nuclear formation which promotes oligomerization and transitions the protein from a storage state to a "spinnable" state (Leclerc et al., 2013; Li et al., 2001). These shear forces are also thought to be responsible for transitioning the α-helical form of the poly-alanine tail found in the ampulle to the β-sheet structures that lead to crystallite formation in the fiber (Gosline et al., 1986; Knight et al., 2000).

3. Chemical Forces for Fiber Assembly:

As the duct narrows, the protein is not only subject to shear forces but there are also chemical changes including a drop in pH and an alteration of ion concentrations (Andersson et al., 2014; Knight, 2001). Ion changes include a decrease in Na^+ and Cl^- and an increase in K^+, P and S (Knight, 2001). It is worth noting that while most of these changes occur in a linear like fashion along the duct and are believed to affect the solubility and aggregation of spidroin protein allowing for fiber formation (Eisoldt et al.,

2010). Because the protein is highly concentrated in the dope it is also believed that the salt levels in the ampulle help to prevent premature aggregation (Leclerc et al., 2013). The protein fiber is also thought to undergo oxidation conditions as it travels along the duct (Romer and Scheibel, 2008; Sponner et al., 2005; Szela et al., 2000). These oxidation conditions help to create the disulfide bonds in the CTD and reduce methionine to help with β-sheet assembly.

The decrease in pH that occurs along the duct is thought to play an important role in fiber formation as it causes changes in the terminal domain, of the spidroin proteins, most notably a conformational change in the NTD (Andersson et al., 2014). This reduction of pH is caused by *carbonic anhydrase* that generates CO_2 and H^+. Originally the pH was thought to decrease from 7.2/6.9 to 6.3. However, with the use of microelectrodes and Intelligent Sensor Management (ISM) probes, the measured pH drops from 7.6 in the tail to 5.7 in the duct (Fig. 1.7) (Andersson et al., 2014; Dicko et al., 2004; Knight, 2001). At the midpoint of the duct the diameter becomes too small to obtain an accurate pH reading and it is believed that the pH may continue to drop.

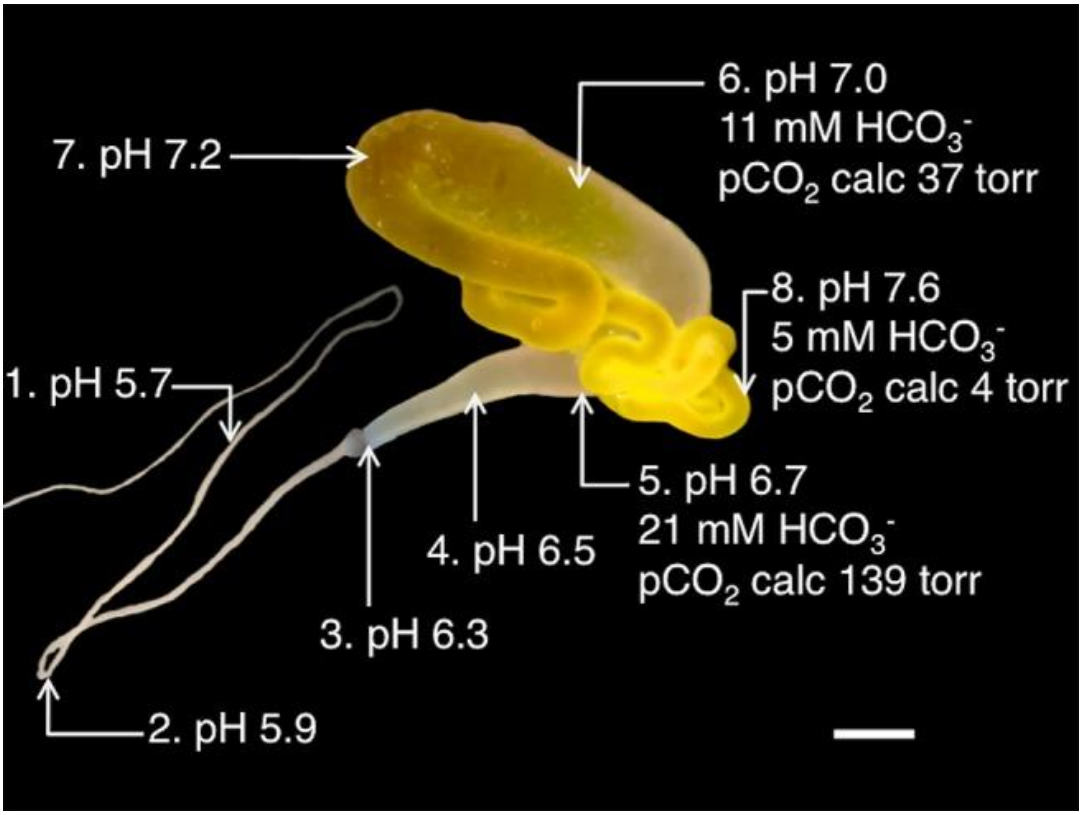

Figure 1.7 Picture of a major ampullate gland where pH, and HCO_3^- measurements were taken and the pCO2 values were determined. Data for all there are at locations indicated. From (Andersson et al., 2014)

4. Domain Roles in Fiber Assembly:

a. Repeat Domain:

The poly-alanine tails are thought to transition to β-sheets due to shear forces. These β-sheets allow interlocking of the alanine residues with the nearby chain by copious amounts of hydrogen bonds (Hayashi et al., 1999; Papadopoulos et al., 2009; Scheibel, 2004). Although shear forces predominate the mechanism by which the repeat domain influences fiber formation, phosphate is also known to cause aggregation of repeat domains at very high concentrations (Hedhammar et al., 2008).

b. C-terminal Domain:

The C-terminal domain creates a spidroin dimer through disulfide bond linkage with another C-terminal domain. Through flow rate and shear forces experienced in the duct the spidroin proteins, connected by the CTD dimers, will align in the duct to form a fiber. The CTD was proposed to play a role in protein solubility in the ampulle, thus preventing early aggregation too early in the fiber forming process (Eisoldt et al., 2010; Sponner et al., 2005b). This is believed to be done by an "unfolding" of the CTD through ionization state changes by some amino acid side chain groups (Sponner et al., 2005b). When the CTD is at neutral pH, it is in a folded state where the hydrophobic residues reside within the core of the protein leaving the hydrophilic residues on the outside keeping the protein soluble (Gauthier et al., 2014; Hagn et al., 2010). CTD has a high concentration of charged and polar amino acids and as the pH drops in the duct the acidic charged residues, like aspartate and glutamate, go from a negative to neutral charge. The change in charge cause the CTD to partially unfold leaving the CTD more hydrophobic than either the folded or completely unfolded state (Hagn et al., 2010). This results in a decrease in repulsion forces and an increase in hydrophobic interactions that help with the formation of β-sheets and thus precipitation by increasing the parallel alignment of the spidroins (Andersson et al., 2014; Hu et al., 2006; Sponner et al., 2005a).

c. N-terminal Domain:

The role of the NTD in fiber assembly is dependent on its pH-induced conformational change that causes NTD dimerization (Fig. 1.8) (Askarieh et al., 2010; Gaines et al., 2010; Kronqvist et al., 2014). This conformational change occurs between

pH 7 and 6, and from experiments done monitoring tryptophan fluorescence, the change appears to be abrupt. Salt has an effect on dimerization wherein higher salt concentrations require a lower pH to induce dimerization as key salt bridges in the monomer are weakened (Gaines et al., 2010; Gronau et al., 2013). Although this conformational change and dimerization occurs at a lower pH, weak NTD-NTD interactions are observed at higher pHs. Using tryptophan fluorescence, dynamic light scattering, electrospray ionization mass spectrometry (ESI-MS), hydrogen-deuterium exchange (HDX)-MS, circular dichroism (CD) and nuclear magnetic resonance (NMR) spectroscopy were used to determine which residues in the NTD are responsible for the conformational and dimerization (Askarieh et al., 2010; Jaudzems et al., 2012; Kronqvist et al., 2014). Some of the suggested residues include D40, R60, K65, E79, E84 and E119 in *Euprosthenops australis* MaSp1 (Kronqvist et al., 2014). Previous reports suggested, based that two residues, E79 and E119, act as a "trap-and-trigger" mechanism. For instance at neutral pH the residues are deprotonated and form a "trap" but as the pH drops, the trap is "triggered" due to the protonation of the residues helping to form a stable dimer needed for silk formation (Kronqvist et al., 2014).

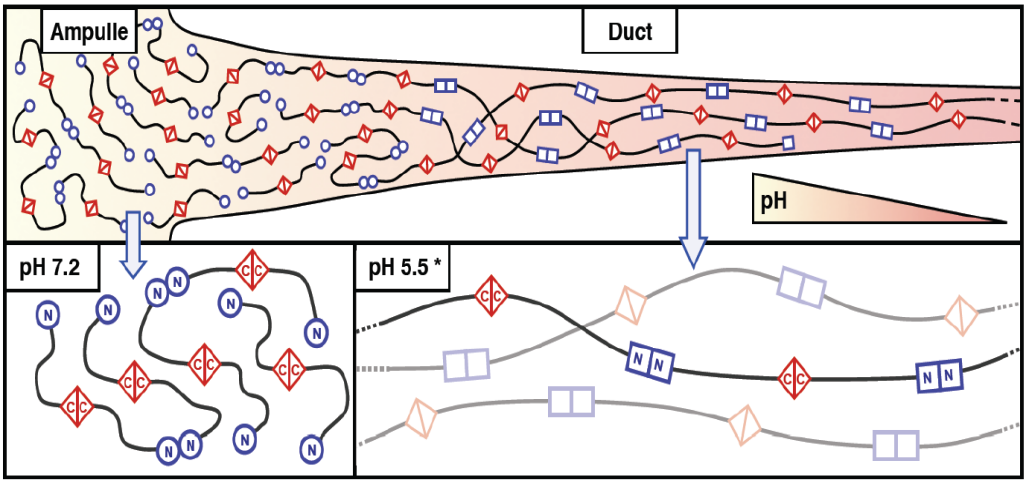

Figure 1.8 Model of MaSp multimeric spidroin assembly. Showing pH change in gland where at pH 7.5 NTD is weakly associated and pH 5.5 NTD undergoes conformation change and dimer stabilization. From (Gaines et al., 2010)

6. Overview

The dope of the major ampullate silk gland exists as a liquid crystal formed from micelle-like structures (Fig. 1.9) (Silvers et al., 2010). During this storage phase the CTDs are covalently linked though a disulfide bond forming dimers of NTD-R-CTD-CTD-R-NTD (Hedhammar et al., 2008; Hu et al., 2006). Although unstable, the NTDs will experience transient interactions with proximal NTDs from neighboring spidroin dimers (Askarieh et al., 2010; Gaines et al., 2010). Once the proteins initiate movement through the duct, changes in pH, salt concentrations, flow speed and shear forces influence the spidroin proteins to self-assembly into a fiber. Compression of the micelles aligns the proteins and intramolecular and intermolecular β-sheets interactions initiate. Transient NTD interactions at more neutral pH allow resolution of tangles to prevent "knots" from forming which could clog the duct, but upon acidification the pH dependent

conformational change, leads to the formation of salt bridges connecting negatively and positively charges residues at the dimerization interface (Knight et al., 2000; Lefevre et al., 2008; van Beek et al., 2002). Once the NTD dimers are set, multimeric strands of connected spidroins proteins are formed.

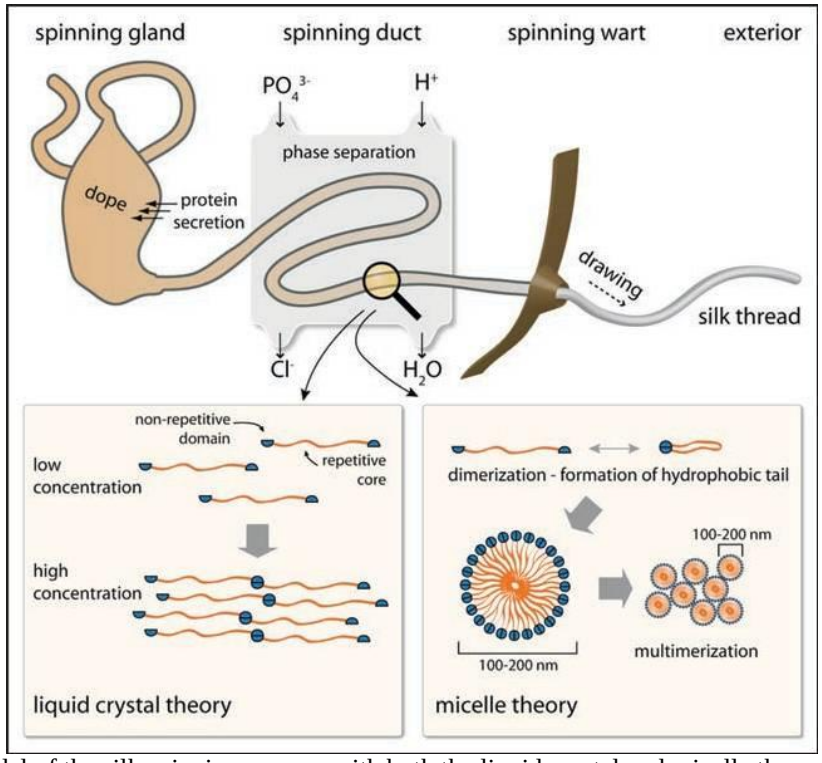

Figure 1.9 Model of the silk spinning process with both the liquid crystal and micelle theory shown. From (Romer and Scheibel, 2008)

IV. Expression Systems

1. Natural Expression System

With as many spiders as there are in the world and with as many different types of silks that they can produce, farming would be a preferential way to obtain silk. However, due to the cannibalistic nature farming of spiders, has proven difficult. Also, while spider

silking apparati have been created, even as far back as 1830, silking still remains tedious and impractical (Lewis, 1996). Also, there is the issue of uniformity. The same type of silk can vary between individuals of the same species and can be further exacerbated by the individual diet of the spider (Heidebrecht and Scheibel, 2013). One scientist, Dr. Wilder, had a spider that produced 150 yards of silk (Lewis, 1996). From this it was determined that it would take 5,000 spiders to retrieve enough material for a single dress. As a further example, a golden cape was recently created from the silk of about 1.2 million golden orb spiders and took about 8 years to complete (Chung et al., 2012). Due to these overwhelming odds, other expression systems have been explored to create spider silk in a more practical and cost effective manner.

Recombinant gene expression and gene mimicry are two methods commonly used for the expression of spidroin proteins (Humenik et al., 2011). Two major factors have traditionally impeded progress: codon usage optimization and repetitive sequence tolerance (Heidebrecht and Scheibel, 2013). Therefore, a range of organisms from unicellular bacterium *Escherichia coli* to mammals, such as goats (Table 1.1), have been used as spidroin expression system hosts. Each of the different expression systems have strengths and weaknesses that would have to be taken into account if industrial scale spider silk production was attempted.

Host	Type of silk produced	Spider	M_w [kDa]	Yield [mg/L]
Prokaryotes				
Bacteria				
Escherichia coli	MaSp1	*Nephila clavipes*	15-285	1.2-95
	MaSp1	*Euprosthenops australis*	10-28	25-150
	MaSp2	*Argiope aurantia*	63-71	
	MaSp2		31-112	
	MaSp1 and MaSp2	*Nephila clavipes*	15-163	
	MaSp1 and MaSp2	*Latrodectus hesperus*	14	
	MaSp2/Flag	*Nephila clavipes*	58,62	7-10
	TuSp1	*Nephila antipodiana*	12-15	
	TuSp1	*Latrodectus hesperus*	33, 45	4.8-7.2
	ADF3, ADF4	*Araneus diadematus*	34-106	
	Flag	*Nephila clavipes*	14-94	11.6
Salmonella typhimurium	ADF1, ADF2, ADF3, ADF4	*Araneus diadematus*	25-56	
Eukaryotes				
Yeasts				
Pichia pastoris	MaSp1	*Nephila clavipes*	94	300
	MaSp1	*Nephila madagascariensis*	113	
	MaSp1 and MaSp2	*Nephila clavipes*	33-61	
Insects				
Bombyx mori	MaSp1	*Nephila clavipes*	70-83	6
Cells-Bombyx mori	MaSp1	*Nephila clavipes*	70	
Cells-Bombyx mori	Flag	*Nephila clavipes*	37	12.3
Cells-*Spodoptera frugiperda*	ADF3, ADF4	*Araneus diadematus*	35-105	50
	Flag	*Araneus ventricosus*	28-61	
Plants				
Arabidopsis thaliana	MaSp1	*Nephila clavipes*	64, 127	
Nicotiana tabacum	MaSp1	*Nephila clavipes*	13-100	80
	MaSp2	*Nephila clavipes*	65	
	MaSp1 and MaSp2	*Nephila clavipes*	60	0.3-3
Solanum tuberosum	MaSp1	*Nephila clavipes*	13-100	80
Mammals				
Cells-COS-1	MaSp1	*Euprosthenops sp.*	22,25	
Cells-MAC-T and BHK	MaSp1 and MaSp2	*Nephila clavipes*	60-140	
Cells-MAC-T and BHK	ADF3	*Araneus diadematus*	60-140	25-50
Transgenic mice	MaSp1 and MaSp2	*Nephila clavipes*	31-66	8-12
Transgenic goat	MaSp1 and MaSp2	*Nephila clavipes*	50	
	ADF3	*Araneus diadematus*	60	

Table 1.1 Summary of expression of native spider silk genes from assorted host organisms. Modified from (Heidebrecht and Scheibel, 2013)

2. Prokaryotes

Because it is well studied and widely used, *E. coli* is often used as a host organism for protein production of recombinant spider silk (Table 1.1) (Heidebrecht and Scheibel, 2013). *E. coli* is also inexpensive, fast growing, easily screenable for correct inserts and can be scaled up using bioreactors which make it advantageous for large scale production. However, for all the positive benefits there are some negative qualities that must be addressed when using *E. coli* as an expression system. Due to the large size and repetitive nature of spider silk protein, *E. coli* has a difficult time with protein production. In addition, *E.coli* is unable to perform most eukaryotic post-translational modifications, like phosphorylation and glycosylation, which could be important in the natural spider silk fiber formation (Heidebrecht and Scheibel, 2013). Even with these obstacles, strides are being made in recombinant spider silk protein production using *E. coli*. Recently, a group was able to express and purify near native recombinant dragline silk in *E. coli.* The 284.9 kDa protein was expressed using metabolically engineered *E. coli* where glycyl-tRNA sythetase was overexpressed and glycyl-tRNA pool was increased (Xia et al., 2010). While the protein production does significantly vary some groups have been able to produce up to 150 mg/L of protein, although these were not full length proteins (Heidebrecht and Scheibel, 2013).

While *E. coli* is by far the predominately used prokaryote for spider silk protein production, other bacteria have also been used. *Salmonella* is the most notable of these mainly due to its ability to secrete proteins (Table 1.1) (Widmaier and Voigt, 2010). This attribute could be very useful in spider silk production as it would help with purification.

Secretion is accomplished using the type III secretion system that is found in Gram - bacteria but is shown to be hampered by sequences larger than 628 amino acids as well as charged sequences (Widmaier and Voigt, 2010).

3. Eukaryotes:

a. Yeast

As a unicellular alternative to the prokaryotic *E. coli*, *Pichia pastoris* has great potential. Not only is it inexpensive, fast growing and easily scalable, like *E. coli*, it also has the ability to secrete proteins and can be grown at high cell densities (Cregg et al., 2000). While *E. coli* is largely used to produce protein, yeast has the ability to produce more protein per liter than *E. coli* (Heidebrecht and Scheibel, 2013). *P. pastoris*, has been shown to grow to cell densities greater than 100 g/L of dry cell mass and can produced at up to 300 mg/L of and MaSp1 and 1-3 g/L of spider-like protein (Fahnestock and Bedzyk, 1997; Werten et al., 2008). One advantage it has over *E.coli* is that yeast can modify proteins post translational (Table 1.1). Nevertheless, *Pichia* is not a perfect expression system because expression significantly decreases with larger proteins. (Heidebrecht and Scheibel, 2013).

b. Insects:

While using prokaryotes and single celled eukaryotes have proven useful in producing some recombinant spider silk proteins, the use of insects as expression hosts could be better suited due to their closer relation to spiders than other expression systems (Huemmerich et al., 2004). Insect expression systems do not seem to exhibit the truncation that is a problem in other cell expression systems, (Huemmerich et al., 2004;

Miao et al., 2006; Wen et al., 2010; Zhang et al., 2008). This truncation seen in other systems could be caused by limitation in translational machinery resulting early termination of mRNA synthesis (Xia et al., 2010; Fahnestock et al., 2000). Most commonly, researchers have used *Bombyx mori*, silkworms, as either cell lines or transgenic animals, however the insect cell line Sf9 from *Spodptera frugiperda*, the Fall Armyworm, has also been used (Table 1.1) (Huemmerich et al., 2004). The important advantages of this system, are that silkworms already produce a silk protein, form the protein into fibers and have established farming practices. This system, unfortunately, is not as easily manipulated as the bacterial and yeast systems and thus a baculovirus or a *piggyback*-based vector was used in the BmN and Sf9 cell lines and transgenic silkworms (Huemmerich et al., 2004; Miao et al., 2006; Wen et al., 2010; Zhang et al., 2008). Both BmN and Sf9 cell lines along with transgenic silkworms were able to express recombinant spider silk proteins at up to 50 mg/L (Table 1.1)

c. Plants

One of the larger drawbacks of producing recombinant spider silk has been the ability to acquire enough material to be useful for medical or industrial purposes. Plants are a good option to solve this problem as they are larger organisms and can be grown on a large scale through farming. Four plants that have been used to produce recombinant spider silks are *Arabidopsis thaliana* (Arabidopsis), *Glycine max* (soybean), *Solanum tuberosum* (potato) and *Nicotiana tabacum* (tobacco) (Table 1.1) (Augsten et al., 2000; Barr et al., 2004; Chung et al., 2012; Heim et al., 2009; Peng et al., 2016; Scheller et al., 2001; Scheller and Conrad, 2005; Yang et al., 2005). Plants do, however, take longer to

grow and are also harder to genetically manipulate than other organisms, like bacteria and yeast. For Arabidopsis, a synthetic analogue of dragline silk called DP1B was expressed in the apoplast, ER lumen and vacuole of cells to help with higher protein yields of 6.7-8.2% total soluble protein in leaves and seeds (Yang et al., 2005). DP1B was also introduced into somatic soybean embryos, although instead of using Agrobacterium, which was used in Arabidopsis, particle bombardment was employed (Barr et al., 2004; Yang et al., 2005). Agrobacterium was also used to transfect tobacco and potato plants that were able to produce synthetic spider silk modeled after MaSp1 at about 2% of total soluble protein (Scheller et al., 2001). The amount of protein produced in tobacco and potato plants did not seem to decrease as the size of the proteins, from 12.9 kDa to 99.8 kDa, were increased, which is important since many spider silk proteins are quite large. However, plants also have longer generation times, are more expensive (due to the price of land or greenhouse space, and require more space than previously mentioned systems.

d. Mammals

There are two ways in which mammals can be used to produce spider silk protein: 1) cell cultures; 2) transgenic animals. Three of the cell lines that have been used in silk production are bovine mammary epithelial alveolar cells with large T (MAC-T) cells, baby hamster kidney cells (BHK) and fibroblast-like cells derived from monkey kidney tissue (COS-1). Two transgenic animals that have been used are *Mus musculus* (mouse) and BELE goats (Table 1.1) (Grip et al., 2006; Heidebrecht and Scheibel, 2013; Heim et al., 2009; Lazaris et al., 2002; Xu et al., 2007). With mammalian cells, it is possible to produce spider silk of a high molecular weight, although larger yields are difficult,

possibly due to the repetitive nature of spider silk (Grip et al., 2006; Lazaris et al., 2002). Transgenic animals have the potential to produce large quantities of protein, especially if it is secreted during lactation. However, making transgenic mammals is very difficult as mammals have a longer generation interval when compared to other expression systems (Heidebrecht and Scheibel, 2013; Heim et al., 2009; Xu et al., 2007).

V. Uses for Spider Silk

1. Historical Uses for Spider Silk:

Man has been using spider silks for thousands of years (Kluge et al., 2008). Spider silks were originally used to dress wounds, stop bleeding, make fishing nets and even to produce cloth (Forrest, 1982; Lewis, 1996). These historical took advantage of the exceptional properties of spider silk: strength, elasticity and biocompatibility. There is even support suggesting that spider silk has antimicrobial properties (Wright and Goodacre, 2012). Because spider silk is so fine, up until World War II, spider silks were used for crosshairs in optical devices such as telescopes, microscopes, gun scopes and bomb guiding systems (Lewis, 1996).

2. Different Forms of the Spider Silk Protein:

The uses for spider silk protein are as varied as the different silks themselves and while fibers are understandably the most recognized form of these proteins it is not the only type of product that can be produced. Silk proteins can be processed into many different forms including the well-known fiber, as well as, sponges, films, capsules and gels (Fig. 1.10) (Kluge et al., 2008; Omenetto and Kaplan, 2010; Spiess et al., 2010). Within each of these individual forms, alterations in size and composition of the protein

can give rise to a wide range of novel materials for use in industry and medicine. Fibers can be created using different methods to produce nano to micron-scale fibers (Kluge et al., 2008). Films can also be manufactured with a thickness from several micrometers to a few nanometers while their mechanical and chemical characteristics will change depending on the type of process used to create them (Romer and Scheibel, 2008). The form the silk takes is not the only thing that can be changed, however. Native silk is biodegradable and recombinant silk protein can be altered so that the time it takes to degrade is either longer or shorter, depending on need (Doblhofer and Scheibel, 2015; Hardy et al., 2013; Hofer et al., 2012; Lammel et al., 2011). With current technology, the different motifs that are found in spider silks can be rearranged, added to or subtracted from to change the physical characteristics of the formed protein. Other non-native protein sequences can also be added to the ends or middle of the spidroin protein sequence to supplement a particular trait. The different forms the fiber can take, along with the ability to create novel silk proteins using recombinant DNA techniques, can further expand the use of this protein.

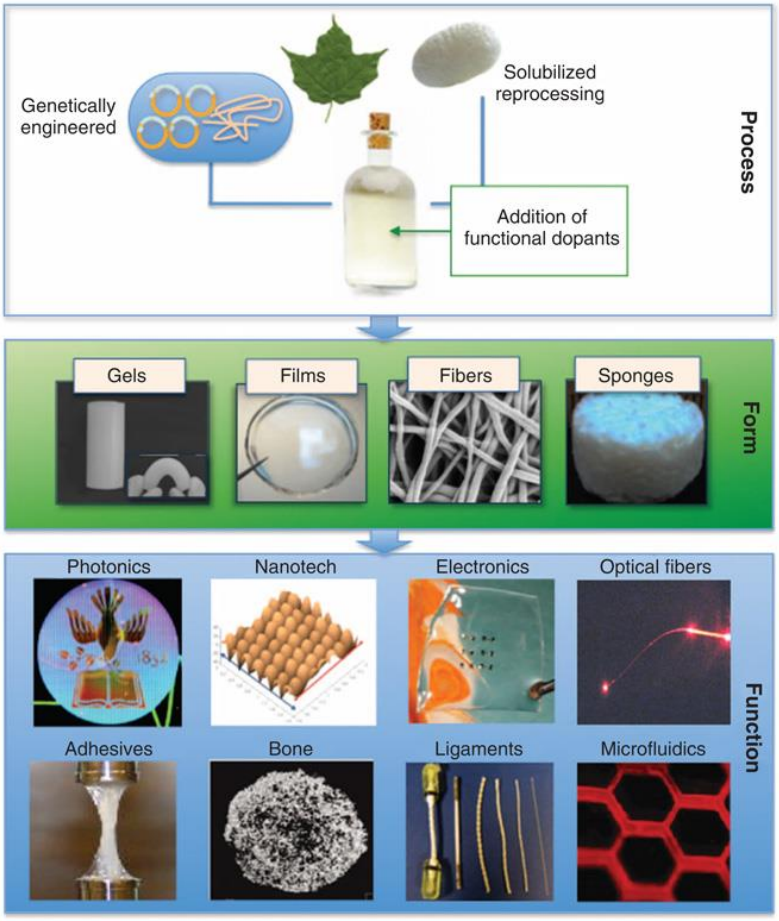

Figure 1.10 Silk forms and uses that the different forms can give rise to. From (Omenetto and Kaplan, 2010)

2. Medical Uses:

Because of the many forms that spider silk can take, there are great opportunities to use it as a biomaterial. A biomaterial is "any substance (other than a drug) or combination of substances synthetic or natural in origin, which can be used any time, as a whole or as a part of a system which treats, augments, or replaces any tissue, organ or function of the body" (Von Recum and Laberge, 1995). One aspect that makes spider silk

such a useful biomaterial is its biocompatibility. This allows the spider silk to be used for applications like drug release materials, cell supporting scaffolds, and muscle and organ repair. Recombinant spider silk can also be recombinantly engineered to produce an antimicrobial property which is very useful in the medical field (Gomes et al., 2011).

For drug delivery, one method is to create submicroparticles to be used as drug carriers (Lammel et al., 2011). These submicroparticles, created from the spider silk protein eADF4 (C16), were shown to have a constant release rate over a period of two weeks using incorporated small molecules with positive net-charge. Electrospinning is another method that allows drugs, such as antibiotics, proteins, small molecules and DNA to be loaded into the matrices through pre-spinning embedment, post-spinning coating, or conjugating/coaxial spinning, which encapsulate bioactive agents (Zhang et al., 2009). This way, as the fiber degrades the drug is slowly released. The silk protein could also be formed into films that could incorporate other materials such as polyesters or polyurethane (Hardy et al., 2013). This would allow for different release times for the drugs, which could be useful for drugs that need to be maintained at a constant concentration in the body over a long period of time. It was also shown that this drug delivery could not only be used with small drugs but with larger ones as well. One study used lysozyme, which is about 15 kDa, as a model protein to look at analyte loading into silk particles (Hofer et al., 2012). Not only were the researchers able to load lysozyme at a high concentration of up to about 30% (w/w) they were able to show that different pHs and ionic strengths can change the release rate of the protein.

When using silks for cell supporting scaffolds, it is important that the necessary cells will attach and grow on the silk scaffold. Using native spider silks, chondrocytes, Schwann cells and mouse fibroblasts were shown to attach and grow along the silk (Gomes et al., 2011; Wendt et al., 2011; Widhe et al., 2012). Fibroblasts, keratinocytes, endothelial cells, Schawann cells, bone marrow stem cells, human (NT2) model neurons and human osteosarcoma cells were also shown to attach and grow along recombinant spider silk protein (Roloff et al., 2014; Widhe et al., 2013; Wohlrab et al., 2012; Zhang et al., 2014). Other biomedical applications of spider silk include using them as replacements for nylon sutures and common wound dressings (Baoyong et al., 2010; Hennecke et al., 2013; Kuhbier et al., 2011; Schneider et al., 2009). In the case of silk sutures, it was shown that braided silk fibers are comparable to conventional sutures in terms of tensile strength and superior in terms of fatigue properties (Hennecke et al., 2013).

3. Industrial Uses:

Medical applications dominate the research focus done of spider silk proteins, however industrial applications have been found. One example, would be in the textile industry either on its own or as a composite material (table 1.2) (Kluge et al., 2008).

Material	Stiffness, E_{init} (Gpa)	Strength, σ_{max} (Gpa)	Extensibility, $£_{max}$	Toughness (MJ m^{-3})	Hysteresis (%)
***Araneus* MA**	10	1.1	0.27	160	65
***Araneus* Flag**	0.003	0.5	2.7	150	65
***A. diadematus* MA**	6	0.7	30	150	
***A. trifasciata* Ma**	9.3	1.29	22	145	
***A. trifasciata* MI**	8.5	0.342	54	148	
***A. diadematus* Flag**	0.003	0.5	270	150	
***A. bruennichi* Cyl**	9.1	0.39	40	128	
***A. trifasciata* Aci**	9.6	0.687	86	367	
***Bombyx mori* cocoon silk**	7	0.6	0.18	70	
Tendon Collagen	1.5	0.15	0.12	7.5	
Bone	20	0.16	0.03	4	
Wool, 100% RH	0.5	0.2	0.5	60	
Elastin	0.001	0.002	1.5	2	10
Resilin	0.002	0.003	1.9	4	6
Synthetic rubber	0.001	0.05	8.5	100	
Nylon fiber	5	0.95	0.18	80	
Kevlar 49 fiber	130	2.6	0.027	50	
Carbon Fiber	300	4	0.013	25	
Copper (soft)	120	0.2	40		
High-Tensile steel	200	1.5	0.008	6	

Table 1.2 Different mechanical properties of natural and synthetic materials. Reproduced from (Gosline et al., 1999; Heidebrecht and Scheibel, 2013; Heim et al., 2009) (MA- Major Ampullate, MI- Minor Ampullate, Flag- Flagelliform, Cyl- Cylindriform, Aci- Aciniform silks)

With the wide range of uses for spider silk, it is understandable why there would be such variability between the silk types and properties. Differences in mechanical properties are the easiest traits to observe and quantify. As a general rule spider silks provide a great mixture of strength and toughness (Altman et al., 2003). These qualities along with spider silks extensibility and resistance to failure in compression are often higher than other natural and synthetic materials (Table 1.1). This is important since

many synthetic materials must tradeoff between strength and toughness (Ritchie, 2011). For example many man-made materials including Kevlar, carbon fiber, and high-tensile steel sacrifice toughness at the exspense of strength (Table 1.2) (Gosline et al., 1999; Romer and Scheibel, 2008).

A novel use for spider silk is its use as violin string cores (Osaki, 2012). The strings, created from natural spider silk from *Nephila maculata*, were packaged in bundles of approximately 9000, 12000, and 15000 for the A, D, and G strings respectively. The sound created by the strings was of a "soft and profound timbre" (Osaki, 2012). Recent research has analyzed the ability to use spider silk protein as nonwoven meshes to enhance the efficiency of air filter devices (Lang et al., 2013). While this application is still in the early stages it does show promise.

VI. References

Altman, G.H., Diaz, F., Jakuba, C., Calabro, T., Horan, R.L., Chen, J., Lu, H., Richmond, J., and Kaplan, D.L. (2003). Silk-based biomaterials. Biomaterials *24,* 401-416.

Andersson, M., Chen, G., Otikovs, M., Landreh, M., Nordling, K., Kronqvist, N., Westermark, P., Jornvall, H., Knight, S., Ridderstrale, Y., *et al.* (2014). Carbonic Anhydrase Generates CO2 and H+ That Drive Spider Silk Formation Via Opposite Effects on the Terminal Domains. PLoS Biol. *12,* e1001921.

Andersson, M., Holm, L., Ridderstrale, Y., Johansson, J., and Rising, A. (2013). Morphology and composition of the spider major ampullate gland and dragline silk. Biomacromolecules *14,* 2945-2952.

Askarieh, G., Hedhammar, M., Nordling, K., Saenz, A., Casals, C., Rising, A., Johansson, J., and Knight, S.D. (2010). Self-assembly of spider silk proteins is controlled by a pH-sensitive relay. Nature *465,* 236-238.

Augsten, K., Muhlig, P., and Herrmann, C. (2000). Glycoproteins and skin-core structure in *Nephila clavipes* spider silk observed by light and electron microscopy. Scanning *22,* 12-15.

Ayoub, N.A., Garb, J.E., Tinghitella, R.M., Collin, M.A., and Hayashi, C.Y. (2007). Blueprint for a high-performance biomaterial: full-length spider dragline silk genes. PLoS One *2,* e514.

Baoyong, L., Jian, Z., Denglong, C., and Min, L. (2010). Evaluation of a new type of wound dressing made from recombinant spider silk protein using rat models. Burns *36,* 891-896.

Barr, L.A., Fahnestock, S.R., and Yang, J. (2004). Production and purification of recombinant DP1B silk-like protein in plants. Mol. Breed. *13,* 345-356.

Bell, A.L., and Peakall, D.B. (1969). Changes in fine structure during silk protein production in the ampullate gland of the spider *Araneus sericatus*. J. Cell Biol. *42,* 284-295.

Bittencourt, D., Oliveira, P.F., Prosdocimi, F., and Rech, E.L. (2012). Protein families, natural history and biotechnological aspects of spider silk. Genet. Mol. Res. *11,* 2360-2380.

Blackledge, T.A., and Hayashi, C.Y. (2006). Silken toolkits: biomechanics of silk fibers spun by the orb web spider Argiope argentata (Fabricius 1775). J. Exp. Biol. *209,* 2452-2461.

Blasingame, E., Tuton-Blasingame, T., Larkin, L., Falick, A.M., Zhao, L., Fong, J., Vaidyanathan, V., Visperas, A., Geurts, P., Hu, X., La Mattina, C., and Vierra, C. (2009). Pyriform spidroin 1, a novel member of the silk gene family that anchors dragline silk fibers in attachment discs of the black widow spider, *Latrodectus hesperus*. J. Biol. Chem. *284,* 29097-29108.

Breslauer, D.N., Lee, L.P., and Muller, S.J. (2009). Simulation of flow in the silk gland. Biomacromolecules *10,* 49-57.

Brooks, A.E., Steinkraus, H.B., Nelson, S.R., and Lewis, R.V. (2005). An investigation of the divergence of major ampullate silk fibers from *Nephila clavipes* and *Argiope aurantia*. Biomacromolecules *6,* 3095-3099.

Challis, R.J., Goodacre, S.L., and Hewitt, G.M. (2006). Evolution of spider silks: conservation and diversification of the C-terminus. Insect Mol. Biol. *15,* 45-56.

Chen, G., Liu, X., Zhang, Y., Lin, S., Yang, Z., Johansson, J., Rising, A., and Meng, Q. (2012). Full-length minor ampullate spidroin gene sequence. PLoS One *7,* e52293.

Chen, X., Knight, D.P., and Vollrath, F. (2002). Rheological characterization of nephila spidroin solution. Biomacromolecules *3,* 644-648.

Chung, H., Kim, T.Y., and Lee, S.Y. (2012). Recent advances in production of recombinant spider silk proteins. Curr. Opin. Biotechnol. *23,* 957-964.

Colgin, M.A., and Lewis, R.V. (1998). Spider minor ampullate silk proteins contain new repetitive sequences and highly conserved non-silk-like "spacer regions". Protein Sci. *7,* 667-672.

Craig, C.L. (1997). Evolution of arthropod silks. Annu. Rev. Entomol. *42,* 231-267.

Cregg, J.M., Cereghino, J.L., Shi, J., and Higgins, D.R. (2000). Recombinant protein expression in *Pichia pastoris*. Mol. Biotechnol. *16,* 23-52.

Dicko, C., Vollrath, F., and Kenney, J.M. (2004). Spider silk protein refolding is controlled by changing pH. Biomacromolecules *5,* 704-710.

Doblhofer, E., and Scheibel, T. (2015). Engineering of recombinant spider silk proteins allows defined uptake and release of substances. J. Pharm. Sci. *104,* 988-994.

Eisoldt, L., Hardy, J.G., Heim, M., and Scheibel, T.R. (2010). The role of salt and shear on the storage and assembly of spider silk proteins. J. Struct. Biol. *170,* 413-419.

Elgar, M.A., and Fahey, B.F. (1996). Sexual cannibalism, competition, and size dimorphism in the orb-weaving spider *Nephila plumipes Latreille* (Araneae: Araneoidea). Behav. Ecol. *7,* 195-198.

Fahnestock, S.R., and Bedzyk, L.A. (1997). Production of synthetic spider dragline silk protein in *Pichia pastoris*. Appl. Microbiol. Biotechnol. *47,* 33-39.

Fahnestock, S.R., Yao, Z., and Bedzyk, L.A. (2000). Microbial production of spider silk proteins. Rev Mol Biotechnol *74,* 105-119.

Forrest, R.D. (1982). Early history of wound treatment. J. R. Soc. Med. *75,* 198-205.

Gaines, W.A.,4th, and Marcotte Jr, W.R. (2008). Identification and characterization of multiple Spidroin 1 genes encoding major ampullate silk proteins in *Nephila clavipes*. Insect Mol. Biol. *17,* 465-474.

Gaines, W.A., Sehorn, M.G., and Marcotte Jr, W.R. (2010). Spidroin N-terminal domain promotes a pH-dependent association of silk proteins during self-assembly. J. Biol. Chem. *285,* 40745-40753.

Gao, Z., Lin, Z., Huang, W., Lai, C.C., Fan, J., and Yang, D. (2013). Structural characterization of minor ampullate spidroin domains and their distinct roles in fibroin solubility and fiber formation. PloS One *8,* e56142.

Gatesy, J., Hayashi, C., Motriuk, D., Woods, J., and Lewis, R. (2001). Extreme diversity, conservation, and convergence of spider silk fibroin sequences. Science *291,* 2603-2605.

Gauthier, M., Leclerc, J., Lefèvre, T., Gagné, S.M., and Auger, M. (2014). Effect of pH on the structure of the recombinant C-terminal domain of *Nephila clavipes* dragline silk protein. Biomacromolecules *15,* 4447-4454.

Gomes, S.C., Leonor, I.B., Mano, J.F., Reis, R.L., and Kaplan, D.L. (2011). Antimicrobial functionalized genetically engineered spider silk. Biomaterials *32,* 4255-4266.

Gosline, J.M., DeMont, M.E., and Denny, M.W. (1986). The structure and properties of spider silk. Endeavour *10,* 37-43.

Gosline, J.M., Guerette, P.A., Ortlepp, C.S., and Savage, K.N. (1999). The mechanical design of spider silks: from fibroin sequence to mechanical function. J. Exp. Biol. *202,* 3295-3303.

Greving, I., Cai, M., Vollrath, F., and Schniepp, H.C. (2012). Shear-induced self-assembly of native silk proteins into fibrils studied by atomic force microscopy. Biomacromolecules *13,* 676-682.

Grip, S., Rising, A., Nimmervoll, H., Storckenfeldt, E., Mcqueen-Mason, S.J., Pouchkina-Stantcheva, N., Vollrath, F., Engström, W., and Fernandez-Arias, A. (2006). Transient expression of a major ampullate spidroin 1 gene fragment from *Euprosthenops* sp. in mammalian cells. Cancer Genomics-Proteomics *3,* 83-87.

Gronau, G., Qin, Z., and Buehler, M.J. (2013). Effect of sodium chloride on the structure and stability of spider silk's N-terminal protein domain. Biomater. Sci. *1,* 276-284.

Guehrs, K., Schlott, B., Grosse, F., and Weisshart, K. (2008). Environmental conditions impinge on dragline silk protein composition. Insect Mol. Biol. *17,* 553-564.

Hagn, F., Eisoldt, L., Hardy, J.G., Vendrely, C., Coles, M., Scheibel, T., and Kessler, H. (2010). A conserved spider silk domain acts as a molecular switch that controls fibre assembly. Nature *465,* 239-242.

Hardy, J.G., Leal-Egana, A., and Scheibel, T.R. (2013). Engineered spider silk protein-based composites for drug delivery. Macromol. Biosci. *13,* 1431-1437.

Hayashi, C.Y., Shipley, N.H., and Lewis, R.V. (1999). Hypotheses that correlate the sequence, structure, and mechanical properties of spider silk proteins. Int. J. Biol. Macromol. *24,* 271-275.

Hayashi, C.Y., Blackledge, T.A., and Lewis, R.V. (2004). Molecular and mechanical characterization of aciniform silk: uniformity of iterated sequence modules in a novel member of the spider silk fibroin gene family. Mol. Biol. Evol. *21,* 1950-1959.

Hedhammar, M., Rising, A., Grip, S., Martinez, A.S., Nordling, K., Casals, C., Stark, M., and Johansson, J. (2008). Structural properties of recombinant nonrepetitive and repetitive parts of major ampullate spidroin 1 from *Euprosthenops australis*: implications for fiber formation. Biochemistry *47,* 3407-3417.

Heidebrecht, A., and Scheibel, T. (2013). Recombinant production of spider silk proteins. Adv. Appl. Microbiol. *82,* 115-153.

Heim, M., Keerl, D., and Scheibel, T. (2009). Spider silk: from soluble protein to extraordinary fiber. Angewandte Chemie International Edition *48,* 3584-3596.

Hennecke, K., Redeker, J., Kuhbier, J.W., Strauss, S., Allmeling, C., Kasper, C., Reimers, K., and Vogt, P.M. (2013). Bundles of spider silk, braided into sutures, resist basic cyclic tests: potential use for flexor tendon repair. PLoS One *8,* e61100.

Hijirida, D.H., Do, K.G., Michal, C., Wong, S., Zax, D., and Jelinski, L.W. (1996). 13C NMR of *Nephila clavipes* major ampullate silk gland. Biophys. J. *71,* 3442-3447.

Hofer, M., Winter, G., and Myschik, J. (2012). Recombinant spider silk particles for controlled delivery of protein drugs. Biomaterials *33,* 1554-1562.

Hu, X., Vasanthavada, K., Kohler, K., McNary, S., Moore, A.M., and Vierra, C.A. (2006). Molecular mechanisms of spider silk. Cell Mol. Life Sci. *63,* 1986-1999.

Huemmerich, D., Scheibel, T., Vollrath, F., Cohen, S., Gat, U., and Ittah, S. (2004). Novel assembly properties of recombinant spider dragline silk proteins. Curr. Biol. *14,* 2070-2074.

Humenik, M., Scheibel, T., and Smith, A. (2011). Spider silk understanding the structure-function relationship of a natural fiber. Prog. Mol. Biol. Transl. Sci. *103,* 131-185.

Ittah, S., Michaeli, A., Goldblum, A., and Gat, U. (2007). A model for the structure of the C-terminal domain of dragline spider silk and the role of its conserved cysteine. Biomacromolecules *8,* 2768-2773.

Jaudzems, K., Askarieh, G., Landreh, M., Nordling, K., Jörnvall, H., Rising, A., Knight, S.D., and Johansson, J. (2012). pH-Dependent Dimerization of Spider Silk N-Terminal Domain Requires Relocation of a Wedged Tryptophan Side Chain. J. Mol. Biol. *422,* 477-487.

Jeffery, F., La Mattina, C., Tuton-Blasingame, T., Hsia, Y., Gnesa, E., Zhao, L., Franz, A., and Vierra, C. (2011). Microdissection of black widow spider silk-producing glands. J. Vis. Exp. *(47). pii: 2382. doi,* 10.3791/2382.

Keten, S., and Buehler, M.J. (2010). Nanostructure and molecular mechanics of spider dragline silk protein assemblies. J. R. Soc. Interface *7,* 1709-1721.

Kluge, J.A., Rabotyagova, O., Leisk, G.G., and Kaplan, D.L. (2008). Spider silks and their applications. Trends Biotechnol. *26,* 244-251.

Knight, D., and Vollrath, F. (1999). Liquid crystals and flow elongation in a spider's silk production line. Proceedings of the Royal Society of London.Series B: Biological Sciences *266,* 519-523.

Knight, D.P., Knight, M.M., and Vollrath, F. (2000). Beta transition and stress-induced phase separation in the spinning of spider dragline silk. Int. J. Biol. Macromol. *27,* 205-210.

Knight, D.D.P. (2001). Changes in element composition along the spinning duct in a Nephila spider. Naturwissenschaften *88,* 179-182.

Kovoor, J. (1987). Comparative structure and histochemistry of silk-producing organs in arachnids. In Ecophysiology of spiders, Springer) pp. 160-186.

Kronqvist, N., Otikovs, M., Chmyrov, V., Chen, G., Andersson, M., Nordling, K., Landreh, M., Sarr, M., Jornvall, H., Wennmalm, S., *et al.* (2014). Sequential pH-driven dimerization and stabilization of the N-terminal domain enables rapid spider silk formation. Nat. Commun. *5,* 3254, 1-11.

Kuhbier, J.W., Reimers, K., Kasper, C., Allmeling, C., Hillmer, A., Menger, B., Vogt, P.M., and Radtke, C. (2011). First investigation of spider silk as a braided microsurgical suture. Journal of Biomedical Materials Research Part B: Applied Biomaterials *97,* 381-387.

Lammel, A., Schwab, M., Hofer, M., Winter, G., and Scheibel, T. (2011). Recombinant spider silk particles as drug delivery vehicles. Biomaterials *32,* 2233-2240.

Lang, G., Jokisch, S., and Scheibel, T. (2013). Air filter devices including nonwoven meshes of electrospun recombinant spider silk proteins. J. Vis. Exp. *(75):e50492. doi,* e50492.

Lazaris, A., Arcidiacono, S., Huang, Y., Zhou, J.F., Duguay, F., Chretien, N., Welsh, E.A., Soares, J.W., and Karatzas, C.N. (2002). Spider silk fibers spun from soluble recombinant silk produced in mammalian cells. Science *295,* 472-476.

Leclerc, J., Lefevre, T., Gauthier, M., Gagne, S.M., and Auger, M. (2013). Hydrodynamical properties of recombinant spider silk proteins: Effects of pH, salts and shear, and implications for the spinning process. Biopolymers *99,* 582-593.

Lee, K.S., Kim, B.Y., Je, Y.H., Woo, S.D., Sohn, H.D., and Jin, B.R. (2007). Molecular cloning and expression of the C-terminus of spider flagelliform silk protein from *Araneus ventricosus*. J. Biosci. *32,* 705-712.

Lefevre, T., Boudreault, S., Cloutier, C., and Pézolet, M. (2008). Conformational and orientational transformation of silk proteins in the major ampullate gland of *Nephila clavipes* spiders. Biomacromolecules *9,* 2399-2407.

Lewis, R. (1996). Unraveling the weave of spider silk. Bioscience 636-638.

Lewis, R.V. (2006). Spider silk: ancient ideas for new biomaterials. Chem. Rev. *106,* 3762-3774.

Li, G., Zhou, P., Shao, Z., Xie, X., Chen, X., Wang, H., Chunyu, L., and Yu, T. (2001). The natural silk spinning process. European Journal of Biochemistry *268,* 6600-6606.

Lin, Z., Huang, W., Zhang, J., Fan, J.S., and Yang, D. (2009). Solution structure of eggcase silk protein and its implications for silk fiber formation. Proc. Natl. Acad. Sci. U. S. A. *106,* 8906-8911.

Miao, Y., Zhang, Y., Nakagaki, K., Zhao, T., Zhao, A., Meng, Y., Nakagaki, M., Park, E.Y., and Maenaka, K. (2006). Expression of spider flagelliform silk protein in *Bombyx mori* cell line by a novel Bac-to-Bac/BmNPV baculovirus expression system. Appl. Microbiol. Biotechnol. *71,* 192-199.

Motriuk-Smith, D., Smith, A., Hayashi, C.Y., and Lewis, R.V. (2005). Analysis of the conserved N-terminal domains in major ampullate spider silk proteins. Biomacromolecules *6,* 3152-3159.

Omenetto, F.G., and Kaplan, D.L. (2010). New opportunities for an ancient material. Science *329,* 528-531.

Osaki, S. (2012). Spider silk violin strings with a unique packing structure generate a soft and profound timbre. Phys. Rev. Lett. *108,* 154301-154305.

Papadopoulos, P., Sölter, J., and Kremer, F. (2009). Hierarchies in the structural organization of spider silk—a quantitative model. Colloid Polym. Sci. *287,* 231-236.

Peng, C.A., Russo, J., Gravgaard, C., McCartney, H., Gaines, W., and Marcotte Jr, W.R. (2016). Spider silk-like proteins derived from transgenic *Nicotiana tabacum*. Transgenic Res. 1-10.

Perea, G.B., Plaza, G.R., Guinea, G.V., Elices, M., Velasco, B., and Perez-Rigueiro, J. (2013). The variability and interdependence of spider viscid line tensile properties. J. Exp. Biol. *216,* 4722-4728.

Perry, D.J., Bittencourt, D., Siltberg-Liberles, J., Rech, E.L., and Lewis, R.V. (2010). Piriform spider silk sequences reveal unique repetitive elements. Biomacromolecules *11,* 3000-3006.

Ritchie, R.O. (2011). The conflicts between strength and toughness. Nat. Mater. *10,* 817-822.

Roloff, F., Strauß, S., Vogt, P.M., Bicker, G., and Radtke, C. (2014). Spider Silk as Guiding Biomaterial for Human Model Neurons. BioMed Research International *2014,* 1-7

Romer, L., and Scheibel, T. (2008). The elaborate structure of spider silk: structure and function of a natural high performance fiber. Prion *2,* 154-161.

Sahni, V., Blackledge, T.A., and Dhinojwala, A. (2011). Changes in the adhesive properties of spider aggregate glue during the evolution of cobwebs. Sci. Rep. *1,* 41, 1-8.

Scheibel, T. (2004). Spider silks: recombinant synthesis, assembly, spinning, and engineering of synthetic proteins. Microb. Cell. Fact. *3(14),* 1-10.

Scheller, J., and Conrad, U. (2005). Plant-based material, protein and biodegradable plastic. Curr. Opin. Plant Biol. *8,* 188-196.

Scheller, J., Guhrs, K.H., Grosse, F., and Conrad, U. (2001). Production of spider silk proteins in tobacco and potato. Nat. Biotechnol. *19,* 573-577.

Schneider, A., Wang, X., Kaplan, D., Garlick, J., and Egles, C. (2009). Biofunctionalized electrospun silk mats as a topical bioactive dressing for accelerated wound healing. Acta Biomaterialia *5,* 2570-2578.

Shultz, J.W. (1987). The origin of the spinning apparatus in spiders. Biological Reviews *62,* 89-113.

Schulz, S. (2013). Spider pheromones–a structural perspective. J. Chem. Ecol. *39,* 1-14.

Silvers, R., Buhr, F., and Schwalbe, H. (2010). The molecular mechanism of spider-silk formation. Angew. Chem. Int. Ed Engl. *49,* 5410-5412.

Spiess, K., Lammel, A., and Scheibel, T. (2010). Recombinant spider silk proteins for applications in biomaterials. Macromol. Biosci. *10,* 998-1007.

Sponner, A., Schlott, B., Vollrath, F., Unger, E., Grosse, F., and Weisshart, K. (2005a). Characterization of the protein components of *Nephila clavipes* dragline silk. Biochemistry (N. Y.) *44,* 4727-4736.

Sponner, A., Vater, W., Rommerskirch, W., Vollrath, F., Unger, E., Grosse, F., and Weisshart, K. (2005b). The conserved C-termini contribute to the properties of spider silk fibroins. Biochem. Biophys. Res. Commun. *338,* 897-902.

Sponner, A., Unger, E., Grosse, F., and Weisshart, K. (2004). Conserved C-termini of Spidroins are secreted by the major ampullate glands and retained in the silk thread. Biomacromolecules *5,* 840-845.

Sponner, A., Vater, W., Monajembashi, S., Unger, E., Grosse, F., and Weisshart, K. (2007). Composition and hierarchical organisation of a spider silk. PLoS One *2,* e998.

Szela, S., Avtges, P., Valluzzi, R., Winkler, S., Wilson, D., Kirschner, D., and Kaplan, D.L. (2000). Reduction-oxidation control of β-sheet assembly in genetically engineered silk. Biomacromolecules *1,* 534-542.

Tokareva, O., Michalczechen-Lacerda, V.A., Rech, E.L., and Kaplan, D.L. (2013). Recombinant DNA production of spider silk proteins. Microb. Biotechnol. *6,* 651-663.

Tso, I.M., Wu, H.C., and Hwang, I.R. (2005). Giant wood spider *Nephila pilipes* alters silk protein in response to prey variation. J. Exp. Biol. *208,* 1053-1061.

van Beek, J.D., Hess, S., Vollrath, F., and Meier, B.H. (2002). The molecular structure of spider dragline silk: folding and orientation of the protein backbone. Proc. Natl. Acad. Sci. U. S. A. *99,* 10266-10271.

Vasanthavada, K., Hu, X., Tuton-Blasingame, T., Hsia, Y., Sampath, S., Pacheco, R., Freeark, J., Falick, A.M., Tang, S., Fong, J., *et al.* (2012). Spider glue proteins have distinct architectures compared with traditional spidroin family members. J. Biol. Chem. *287,* 35986-35999.

Vepari, C., and Kaplan, D.L. (2007). Silk as a biomaterial. Progress in Polymer Science *32,* 991-1007. Nature

Vollrath, F., Fairbrother, W.J., Williams, R.J., Tillinghast, E.K., Bernstein, D.T., Gallagher, K.S., and Townley, M.A. (1990). Compounds in the droplets of the orb spider's viscid spiral.Nature 345, 526-528.

Vollrath, F., and Knight, D.P. (1999). Structure and function of the silk production pathway in the spider Nephila edulis. Int. J. Biol. Macromol. *24,* 243-249.

Von Recum, A.F., and Laberge, M. (1995). Educational goals for biomaterials science and engineering: prospective view. J. Appl. Biomater *6,* 137-144.

Wallace, J.A., and Shen, J.K. (2012). Unraveling A Trap-and-Trigger Mechanism in the pH-Sensitive Self-Assembly of Spider Silk Proteins. J. Phys. Chem. Lett. *3,* 658-662.

Wen, H., Lan, X., Zhang, Y., Zhao, T., Wang, Y., Kajiura, Z., and Nakagaki, M. (2010). Transgenic silkworms (*Bombyx mori*) produce recombinant spider dragline silk in cocoons. Mol. Biol. Rep. *37,* 1815-1821.

Wendt, H., Hillmer, A., Reimers, K., Kuhbier, J.W., Schafer-Nolte, F., Allmeling, C., Kasper, C., and Vogt, P.M. (2011). Artificial skin--culturing of different skin cell lines for generating an artificial skin substitute on cross-weaved spider silk fibres. PLoS One *6,* e21833.

Werten, M.W., Moers, A.P., Vong, T., Zuilhof, H., van Hest, J.C., and de Wolf, F.A. (2008). Biosynthesis of an amphiphilic silk-like polymer. Biomacromolecules *9,* 1705-1711.

Widhe, M., Johansson, J., Hedhammar, M., and Rising, A. (2012). Invited review current progress and limitations of spider silk for biomedical applications. Biopolymers *97,* 468-478.

Widhe, M., Johansson, U., Hillerdahl, C.O., and Hedhammar, M. (2013). Recombinant spider silk with cell binding motifs for specific adherence of cells. Biomaterials *34,* 8223-8234.

Widmaier, D.M., and Voigt, C.A. (2010). Quantification of the physiochemical constraints on the export of spider silk proteins by Salmonella type III secretion. Microb. Cell. Fact. *9,* 78-90.

Wohlrab, S., Muller, S., Schmidt, A., Neubauer, S., Kessler, H., Leal-Egana, A., and Scheibel, T. (2012). Cell adhesion and proliferation on RGD-modified recombinant spider silk proteins. Biomaterials *33,* 6650-6659.

Wright, S., and Goodacre, S.L. (2012). Evidence for antimicrobial activity associated with common house spider silk. BMC Res. Notes *5,* 326-332.

Xia, X.X., Qian, Z.G., Ki, C.S., Park, Y.H., Kaplan, D.L., and Lee, S.Y. (2010). Native-sized recombinant spider silk protein produced in metabolically engineered *Escherichia coli* results in a strong fiber. Proc. Natl. Acad. Sci. U. S. A. *107,* 14059-14063.

Xu, H.T., Fan, B.L., Yu, S.Y., Huang, Y.H., Zhao, Z.H., Lian, Z.X., Dai, Y.P., Wang, L.L., Liu, Z.L., Fei, J., and Li, N. (2007). Construct synthetic gene encoding artificial spider dragline silk protein and its expression in milk of transgenic mice. Anim. Biotechnol. *18,* 1-12.

Xu, M., and Lewis, R.V. (1990). Structure of a protein superfiber: spider dragline silk. Proc. Natl. Acad. Sci. U. S. A. *87,* 7120-7124.

Yang, J., Barr, L.A., Fahnestock, S.R., and Liu, Z.B. (2005). High yield recombinant silk-like protein production in transgenic plants through protein targeting. Transgenic Res. *14,* 313-324.

Zhang, W., Zhu, C., Ye, D., Xu, L., Zhang, X., Wu, Q., Zhang, X., Kaplan, D.L., and Jiang, X. (2014). Porous silk scaffolds for delivery of growth factors and stem cells to enhance bone regeneration. PLoS One *9,* e102371.

Zhang, X., Reagan, M.R., and Kaplan, D.L. (2009). Electrospun silk biomaterial scaffolds for regenerative medicine. Adv. Drug Deliv. Rev. *61,* 988-1006.

Zhang, Y., Hu, J., Miao, Y., Zhao, A., Zhao, T., Wu, D., Liang, L., Miikura, A., Shiomi, K., Kajiura, Z., and Nakagaki, M. (2008). Expression of EGFP-spider dragline silk fusion protein in BmN cells and larvae of silkworm showed the solubility is primary limit for dragline proteins yield. Mol. Biol. Rep. *35,* 329-335.

CHAPTER 2

TRYPTOPHAN FLOURESCENCE OF N-TERMINAL DOMAIN VARIANTS

I. Abstract

Spiders produce an array of different silks with varying properties that allow them to survive. However, the way in which the spider produce these silks is still under investigation. The N-terminal domain (NTD) component of spider silk has been shown to undergo a conformational change as the environmental pH is lowered, which is correlated to the formation of a stable NTD homodimer. This NTD dimerization is believed to be vital for the fiber self-assembly process and understanding this process could lead to the development of better artificial silks. In the following experiments, we examine the potential contribution of specific amino acids to the conformational change using tryptophan fluorescence. Alteration of some of these residues show substantial differences from the wild-type NTD with at least one that abolishes the conformational change completely. D45 and K70 variants were shown in other labs to be important in the conformational change which is in agreement with our data, which shows that these residues are vital as least among two different spider species and could be universally necessary among spider species and different silk types.

II. Introduction

While silks can be produced by the Insecta, Arachnida, and Myriapoda classes, the Arachnida class is of particular interest because of one of their members, spiders (Craig, 1997). Unlike most other silk producing organisms, spiders can produce up to seven different types of silk and are dependent on silk production throughout their lives (Craig, 1997; Lewis, 2006). These silks are predominantly composed of fibrous proteins (spidroins) and have highly repetitive amino acid sequences (Craig, 1997). These different types of silk display a variety of properties, such as elasticity in flagelliform silk, that is used in the web spiral for catching prey and strength in major ampullate silk, which is used for the radials of the web, as well as, the lifeline thread of the spider (Heidebrecht and Scheibel, 2013; Lewis, 2006). The mechanisms involved in the transition from a highly concentrated liquid protein solution are largely unknown.

The three main components to spider silk protein are the block repeat domain (R), the C-terminal Domain (CTD) and the N-terminal Domain (NTD) (Fig. 2.1). All three domains are involved in fiber formation. The repeat domain forms β-sheets during fiber formation that allows for hydrogen bonding of the abundant alanine and glycine residues (Hayashi et al., 2004; Papadopoulos et al., 2009; Scheibel, 2004). It is variability in the amino acid sequence of the repeat domain that imparts different characteristics to the different silks that the spider can produce (Challis et al., 2006; Gaines et al., 2010; Keten and Buehler, 2010; Xu and Lewis, 1990). The CTD forms a disulfide-bonded homodimer with another CTD through its conserved cysteine residue (Hedhammar et al., 2008; Ittah et al., 2007; Sponner et al., 2004). The NTD was recently characterized and is thought to

help fiber formation by forming NTD homodimers through salt-bridges at acidic pH (Andersson et al., 2014; Askarieh et al., 2010; Gaines et al., 2010; Hagn et al., 2011; Jaudzems et al., 2012; Kronqvist et al., 2014).

A.

B.

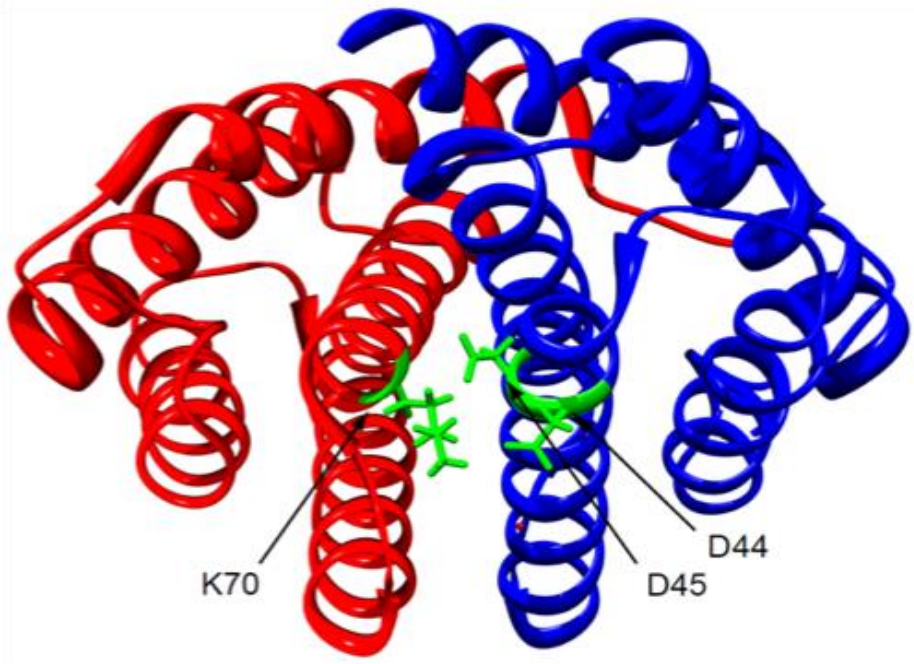

Figure 2.1 A. Schematic structure of MaSp1 domains: NTD, repeats and CTD. B. Crystal structure of *E. australis* MaSp1-NTD homodimer (one monomer in red and one monomer in blue) with three residues believed to be involved in possible salt bridges in green. (Courtesy of M. Hennig MUSC)

The pH dependence of NTD dimerization might be important for regulating fiber formation. In the gland of the spider, where the protein is stored, the environment has a neutral pH (Andersson et al., 2014; Dicko et al., 2004; Knight, 2001). However, as the spider needs the fiber, it pulls the thread from a spigot at the base of its abdomen and the protein within the gland migrates down a narrowing S-shaped duct (Andersson et al., 2013; Bell and Peakall, 1969; Vollrath and Knight, 1999). Along this duct the pH decreases from neutral to approximately pH 5.7 near the middle of the duct (Andersson et al., 2014). The NTD goes from a more monomeric state at neutral pH to a more dimeric state in response to acidification (Gaines et al., 2010). The conformational change is believed to be associated with the stability of NTD-NTD homodimerization (Gaines et al., 2010; Kronqvist et al., 2014). It is worth noting that the NTD is highly conserved, suggesting the conformation change and dimerization may occur in different species of spiders.

While research regarding the mechanism of the NTD conformation change and dimerization is still ongoing, quite a few studies have delved into this mechanism. One such computational study theorizes that the NTD, at neutral pH, forms a "trap" where certain amino acid residues are deprotonated (Wallace and Shen, 2012). This leads to water penetration and a weakened attraction of the monomers. However, as the pH becomes more acidic the residues are protonated thus triggering the dimerization. This "trap-and trigger" theory assumes that the dimer state is always favored and becomes stable at low pH. Other studies have examined this mechanistic problem by mutating conserved residues and looking at the changes that occur. These conserved residues help

with dimerization by creating salt bridges between the NTDs thus stabilizing the dimer and/or by inducing the conformation change thus helping to align residues that form the salt bridges (Jaudzems et al., 2012; Kronqvist et al., 2014). Based on some of this research, the conformation change that aids in dimer formation, occurs through the relocation of helices 3 and 5 thus moving helix 3 closer to helix 1 and providing a relatively flat surface to allow for dimerization (Fig. 2.1B) (Jaudzems et al., 2012).

In this study, we created variants of the wild-type NTD from the species *Nephila clavipes* and evaluated them for the ability to undergo the pH-induced conformational change. These variants may help identify residues that are important in conformation change and dimerization either directly or indirectly. Since there is only one tryptophan in the NTD, we were able to use tryptophan fluorescence to look at the conformation change, which not only has been used in our lab previously, to look at the wild-type NTD, but in other labs as well, thus making it a good tool for comparison (Askarieh et al., 2010; Kronqvist et al., 2014).

III. Material and Methods

1. Wild Type NTD and Variant Protein Purification

a. Cloning

Plasmid containing wild-type Major Ampullate Spidroin 1 (MaSp1) NTD coding region from *N. clavipes*, with a GST tag, was previously described (Gaines et al., 2010). Nine NTD variants were created by designing primers so that the reverse primer was complementary to the template wild-type NTD DNA and the forward primer was complementary with the exception of 1-2 nucleotide changes on the 5´ end (Table 2.1).

Variant	Forward Primer	Reverse Primer
D44N	AATGATATGTCTACCATCGG	AAGTTGATCCGCAGTAA
D45K	AAAATGTCTACCATCGGAG	ATCAAGTTGATCCGCA
D58N	AACAAAATGGCGAGAAG	CATCGCCGTTTTAATT
K70E	GAGTTGCAAGCTCTTAAC	TCCTTTTGAACTCTTGTT
K70D	GAGTTGCAAGCTCTTAAC	TCCTTTTGAACTCTTGTT
E84K	AAAATTGCTGCAGTAGGAA	CGCCATTGATGAAGCG
E84Q	CAAATTGCTGCAGTAGAACAA	CGCCATTGATGAAGCG
E124Q	CAATCAGAAGCTTAATTAAC	ATTGACAAACTGTGGG
E139Q	CAAGTATCTTACGGTGGTT	ATTTGCAGAAGATTGG

Table 2.1 Forward and reverse primers used to create *N. clavipes* MaSp1 variants.

The primers were kinase treated using PNK (NEB catalog number M0201S) and Phusion Hot Start II (Fisher) was used for PCR. The PCR product was ligated and transformed into DH5-α electro-competent *E. coli* cells. Sequencing was used to confirm introduction of the desired mutations.

b. Cell Growth and Lysis

Plasmids encoding variant NTDs were transformed into electro-competent BL21 *E. coli* cells. Cells containing plasmids were grown to an OD_{600} of approximately 0.8, induced with 0.5 mM IPTG, grown overnight at 16-20°C and pelleted by centrifugation (Gaines et al., 2010). Cells were lysed by lysozyme (20 mg/ml) in a buffer consisting of 1X PBS, protease inhibitors (0.5 mM PMSF, 0.05 mM TLCK and 0.5 mM EDTA), 1% triton X-100, 10 mM $MgCl_2$ and 20 U DNAse.

c. Protein Purification

Proteins were affinity purified using glutathione Sepharose 4B (Bioworld catalog number 20181050) by rotating glutathione resin with cell lysate end over end at 4°C for

30 minutes. Bound resin was poured into an empty column, and washed with PBS, Glutathione S-transferase (GST)-NTD fusion protein was eluted with 15 mM reduced glutathione and concentrated using a 3 kDa Amicon centrifugal filter (Millipore). The protein sample was then buffer exchanged into PreScission protease buffer containing PBS at pH 7.0, 1 mM EDTA and 1 mM DTT and digested with PreScission protease (gifted from Sehorn Lab). Released GST and PreScission Protease were removed by binding to glutathione sepharose resin and NTD was collected as flow through. Purified MaSp1-NTD was concentrated using a 3 kDa Amicon centrifugal filter. Residual GST was removed by acid wash by adding nine volume of buffer containing 10 mM MES, 10 mM citrate, 100 mM NaCl at pH 3.8 to one volume concentrated protein. Protein solution was then incubated at room temperature and spun in a microcentrifuge at 16,000 x g for 30 minutes. Supernatant was then concentrated and buffer exchanged using a 3 kDa Amicon centrifugal filter. Protein purity was assessed by SDS-PAGE and stained by Coomassie Brilliant Blue dye. Protein was also run on SDS-PAGE gels and immunodetected. Immunodetected was done by electro-transfer from SDS-PAGE to PVDF membrane. The membrane was then blocked using 5% milk (Carnation instant nonfat dry milk) in TBST for one hour. The membrane was washed with TBST and then a polyclonal rabbit anti-NTD antibody (Rockland Immunochemicals, Inc.), used as the primary antibody, was added to TBST buffer containing 1% milk and allowed to incubate with the membrane for one hour. The membrane was subsequently washed with TBST and allowed to incubate for one hour. with TBST buffer containing 1% milk and an alkaline phosphatase (AP) conjugated goat anti-rabbit secondary antibody. The

membrane was then washed with TBST and imaged (Fujifilm LAS-1000plus imager) using chemiluminescence after washing with Immun-Star™ AP (BioRad)

2. Tryptophan Fluorescence

Tryptophan fluorescence experiments were performed on a spectrofluorometer (Photon Technologies International model 814) using a 1cm x 1cm quartz cuvette as previously described (Gaines et al., 2010). Buffer contained 10 mM HEPES, 10 mM MES and 100 mM NaCl at pH 5.5, 6.0, 6.5, 7.0 or 7.5. Excitation was at 295 nm, emission was measured from 310 nm to 380 nm with 2 nm steps. The corresponding pH buffer was used as a blank and protein was added at 3 µM final concentration. Readings were taken using each variant and wild-type-NTD for each buffered pH. Data was processed separately for each variant by subtracting buffer alone readings and normalizing to highest intensity. Tryptophan data was then plotted directly as relative fluorescence vs. wavelength and as the ratio of reading at 320 nm to reading at 338 nm at pH 7.5, 7.0, 6.5, 6.0, and 5.5 for wild-type NTD and each variant.

IV. Results

1. Cloning and recombinant protein expression and purification

The amino acids chosen for alteration were determined based on sequence conservation between NTDs. The amino acids were converted into amino acids of either opposite charge or neutral charge and the new amino acid was kept as close to the original in size and shape as possible. These variants were D44N, D45K, D58N, K70E, K70D, E84K, E84Q, E124Q, and E139Q, (Fig 2.2).Once the original nine variants were created, a second amino acid was changed in the D45K variant to produce “double

variants" (K70E/D45K and K70D/D45K). Choices for the double variants were made dependent on preliminary tryptophan fluorescence data of the single variants and predicted salt bridge partners based on crystal structure (Fig. 2.1) (Jaudzems et al., 2012).

MaSp1 NTD Wild-Type Amino Acid Sequence

Figure 2.2. *N clavipes* MaSp1 wild-type N-terminal domain amino acid sequence with predicted helices bolded and amino acids chosen for alteration in red.

All variants were successfully expressed and purified using glutathione-Sepharose affinity chromatography after which the glutathione-S-transferase was removed (see Materials and Methods for details). The variants and wild-type NTD were run on a SDS-PAGE gel and visualized by immunodetection (Fig. 2.3).

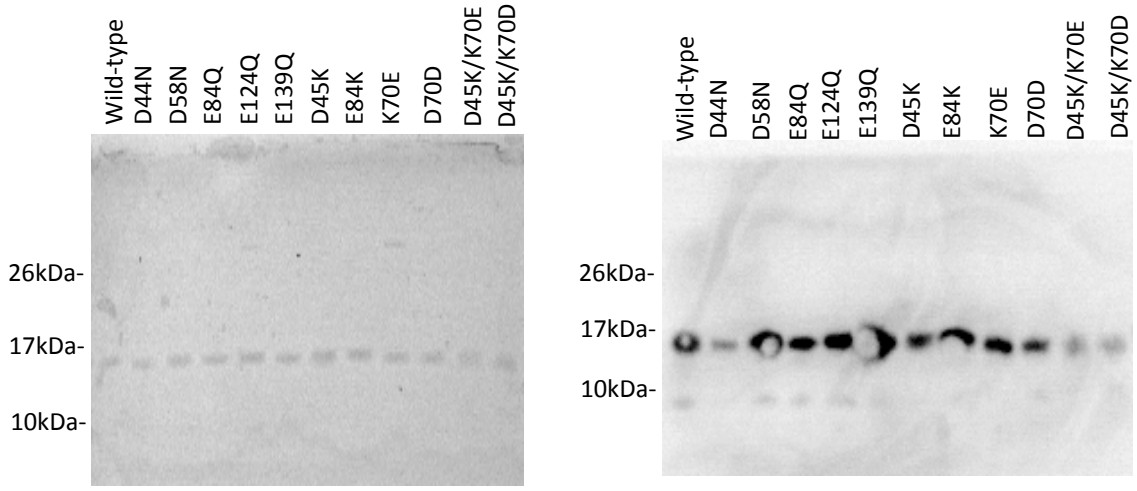

Figure 2.3 Coomassie-stained SDS-PAGE gel (Left) and immunodetected membrane (Right) showing purified MaSp1 NTD (15 kDa) wild-type and variants. Gel was stained with Coomassie blue dye and membrane immunodecteted with anti-NTD primary antibody.

2. Tryptophan Fluorescence

Wild-type NTD and all variants were analyzed by tryptophan fluorescence. Scans were collected at half pH step decreases from pH 7.5 to 5.5. For the wild-type NTD traces at pH 7.5, 7.0 and 6.5 show a high fluorescence with a peak around 320 nm (Fig. 2.3A). The magnitude of fluorescence signal decreases slightly with each stepdown in pH. Between pH 6.5 and 6.0 there is a significant drop in signal strength accompanied by a shift in the peak wavelength of the pH 6.0 trace to around 338 nm both of which are even more pronounced at pH 5.5 (Fig 2.4A). This quenching of fluorescence signal and red shift is indicative of a change in the position of the Trp residue from the interior of the protein to a solvent-exposed position. Hereafter, the conformation having high relative fluorescence and a peak emission around 320 nm will be referred to as

Conformation I and that having lower relative fluorescence and a peak emission around 338nm will be referred to as Conformation II. These experiments were repeated with each of the single and double variants for comparison to the wild-type NTD (Fig. 2.4-2.6).

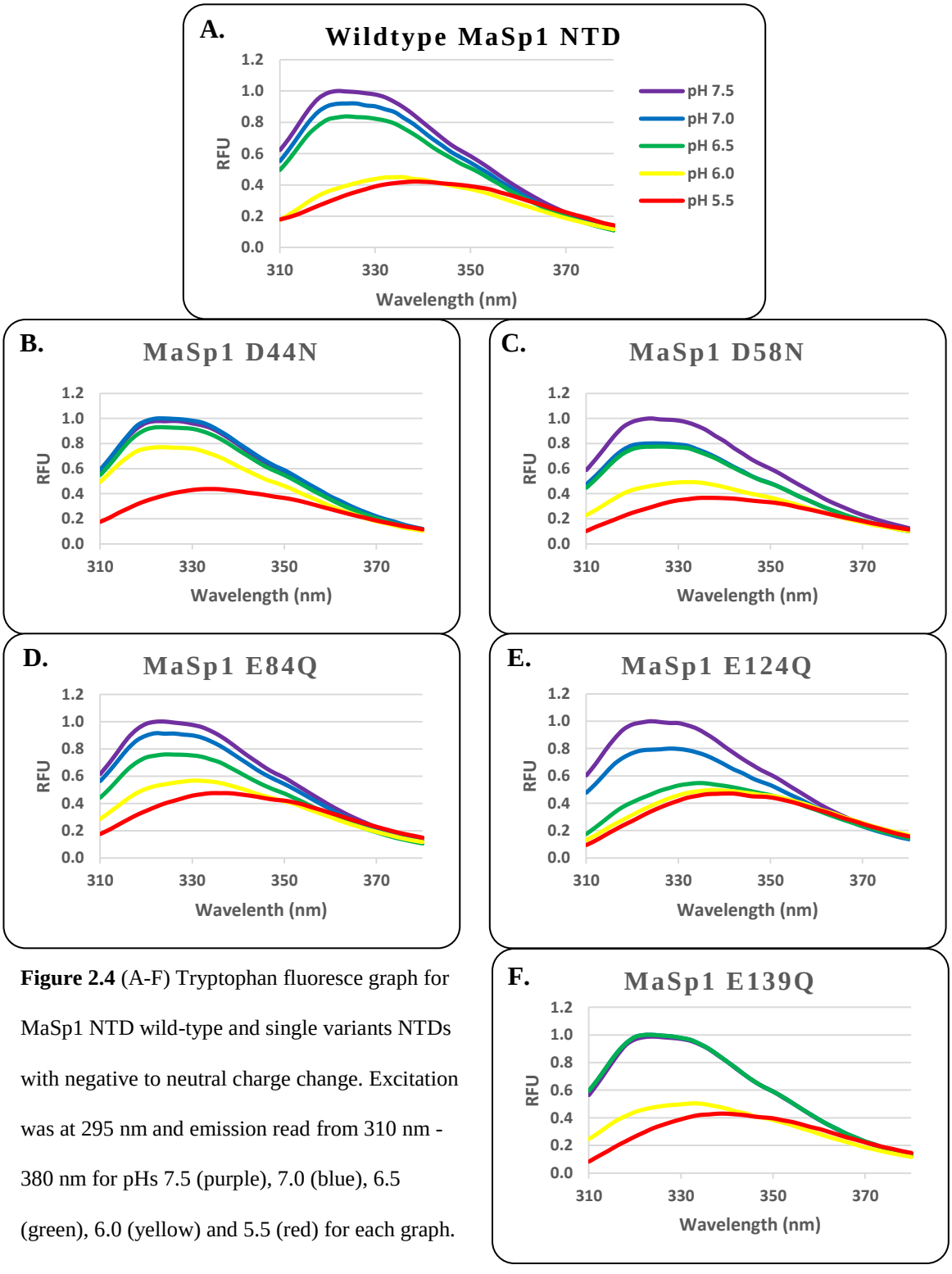

Figure 2.4 (A-F) Tryptophan fluoresce graph for MaSp1 NTD wild-type and single variants NTDs with negative to neutral charge change. Excitation was at 295 nm and emission read from 310 nm - 380 nm for pHs 7.5 (purple), 7.0 (blue), 6.5 (green), 6.0 (yellow) and 5.5 (red) for each graph.

Some of the variants failed to show a visually significant change compared to the wild-type. This was predominately seen for variants with a negative-to-neutral charge change and included two D-to-N modifications. D44N like wild-type NTD, shows both Conformation I and II, but it only goes into Conformation II at pH 5.5 (Fig 2.4B). Of note is that traces at pH 7.5, 7.0 and 6.5 do not show much decrease in fluorescence at pH 6.0. This is in contrast to the gradual decrease in fluorescence for pH 7.5, 7.0 and 6.5 and then drastic decrease and shift for pH 6.0 and 5.5, seen with wild-type NTD. Variant D58N is also a negative-to-neutral charge change and showed a similar trend to wild-type with conversion from Conformation I to Conformation II occurring between pH 6.5 and 6.0 (Fig 2.4C). The decrease in fluorescence between pH 7.5 and 6.5, however, occurred almost completely between pH 7.5 and 7.0.

Three variants were generated with E-to-Q modifications (also negative-to-neutral charge changes). E84Q shows a very gradual change from Conformation I to Conformation II with no abrupt change between any two pH steps (Fig. 2.4D). E124Q shows greater divergence from the wild-type (Fig. 2.4E). This variant has a less abrupt shift from Conformation I to Conformation II and it occurs between pH 7.0 and 6.5 instead of between pH 6.5 to 6.0. Also, traces at pH 6.5, 6.0 and 5.5 have a great deal of overlap and a red shift closer to that of wild-type. Variant E139Q, shows a conformation change similar to wild-type between pH 6.5 and 6 (Fig. 2.4F). Differences from the wild-type NTD include a complete overlap of traces for pH 7.5, 7.0 and 6.5.

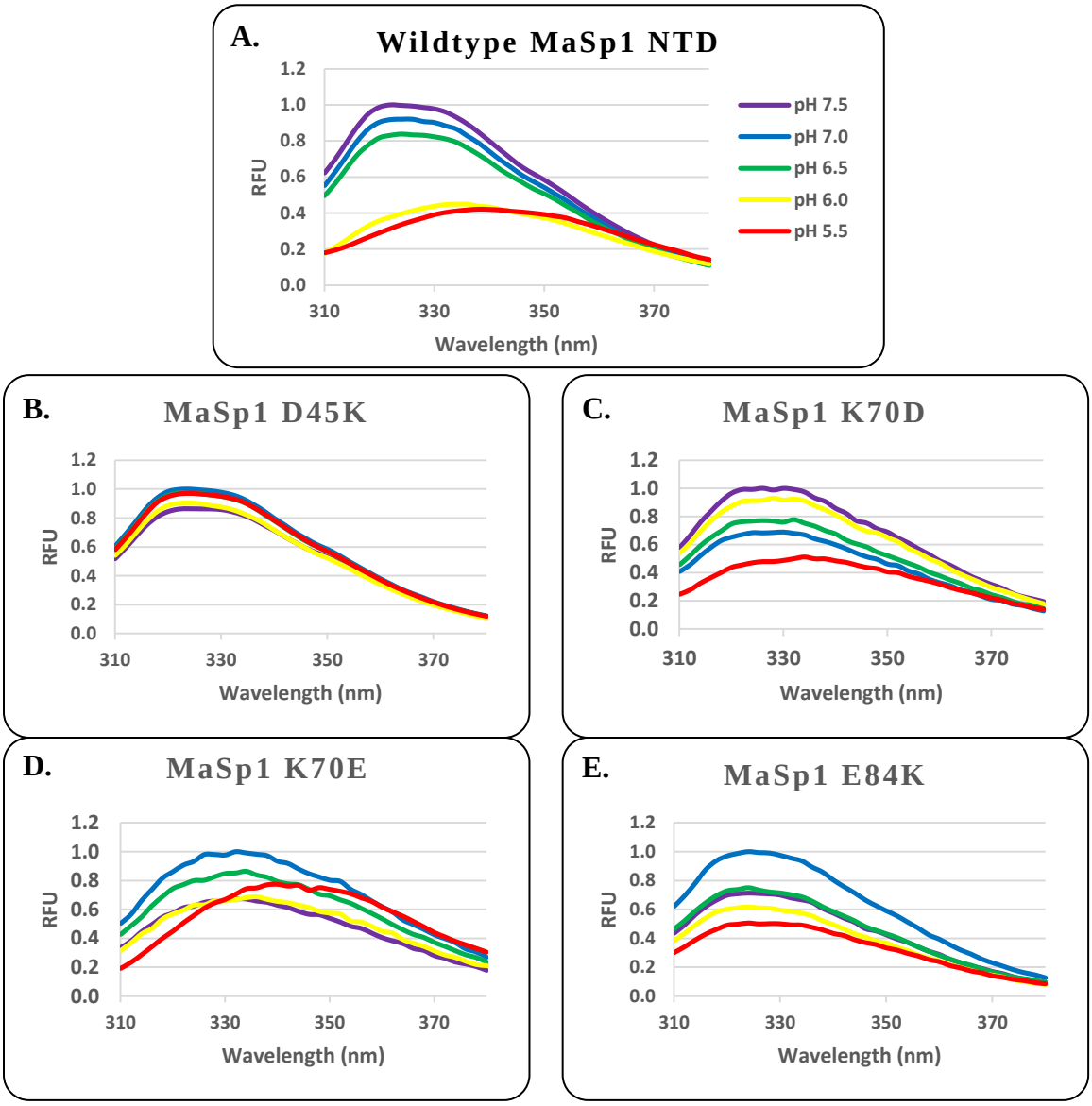

Figure 2.5 (Fig. A-E) Tryptophan fluoresce graph for MaSp1 NTD wild-type and single variants with negative-to-positive or positive-to-negative charge change. Excitation was at 295nm and emission read from 310nm -380nm for pHs 7.5 (purple), 7.0 (blue), 6.5 (green), 6.0 (yellow) and 5.5 (red) for each graph.

D45K shows a very drastic difference when compared to wild-type, and the other single variants (Fig. 2.5B). This negative-to-positive charge change shows complete abolishment of Conformation II. All traces are indicative of Conformation I displaying high fluorescence, with the maximum near 320 nm, and no red shift. K70D is a positive-to-negative charge change and displays a pattern of fluorescence that is different from any of the other variants (Fig. 2.5C). Fluorescence was highest at pH 7.5, decreases dramatically at pH 7.0 and then increases between pH 7.0 and pH 6.0. This variant does have a slight red shift at pH 5.5 but does not shift to the right as much as wild-type. The lysine at position 70 was also changed into a glutamate in variant K70E (Fig. 2.3D). This variant, like K70D, does not show a stepwise decrease in fluorescence, with decreasing pH. Fluorescence intensity is initially low at pH 7.5, increases at pH 7.0 and then decreases between pH 7.0 and 6.0. There is a red shift at pH 5.5 but fluorescence intensity rises rather than falls. It is also noteworthy that all traces for the K70E variant have a maximum wavelength that are shifted to a longer wavelength which suggests that this variant might be in a modified Conformation II and never actually exists in Conformation I. Variant E84K is the last single variant with a negative-to-positive charge change. This variant also did not have a clear shift into Conformation II, unlike wild-type (Fig. 2.5E). This variant had the highest fluorescence trace at pH 7.0 not 7.5, and the pH 6.5 trace is essentially superimposed on the pH 7.5 trace. While there is a general drop in fluorescence between pH 6.5 and 5.5, it is smaller in magnitude than wild-type and is not accompanied by a red shift.

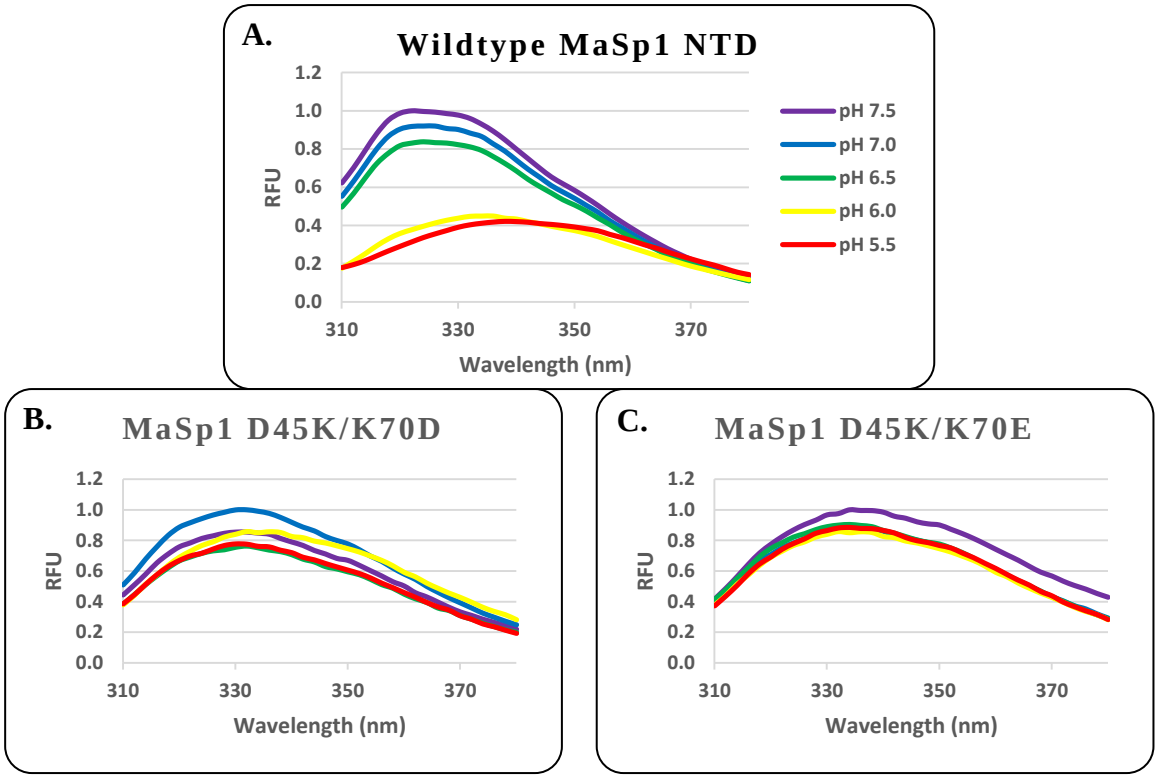

Figure 2.6 (A-C) Tryptophan fluoresce graph for MaSp1 NTD wild-type and double variants consisting of one positive-to-negative and one negative-to-positive charge change. A-C excitation was at 295nm and emission read from 310nm -380nm for pHs 7.5 (purple), 7.0 (blue), 6.5 (green), 6.0 (yellow) and 5.5 (red) for each graph.

With two of the more drastic changes occurring at positions D45 and K70 and the suggestion that these two residues form a salt bridge that stabilizes the dimer form of the NTD we created two double variants to determine if a second alteration would show a conformation of one of the variants, a mix between the two or something new (Fig. 2.1B, Fig. 2.6 B and C) (Jaudzems et al., 2012). It is also important to note that based on crystal structure these two positions are in relatively close proximity to each other at less than 4 Å (Gronau,G. 2013). Both double mutants contain a negative-to-positive charge change,

as well as, a positive-to-negative charge change. The first double variant is D45K/K70D (Fig. 2.6B). As was mentioned D45K shows no change into Conformation II and K70D shows some quenching and a small red shift. This double variant seems to assume an intermediate conformation that is neither Conformation I nor Conformation II. There is only a slight decrease in fluorescence among the traces with pH 7.5 and 7.0 traces reversed compared to wild type. Traces for pH 6.5, 6.0 and 5.5 are all very close together and all wavelengths do show a small red shift. The other double mutant, D45K/K70E is quite similar with only modest quenching and all traces showing a small red shift (Fig. 2.6C).

In the wild-type NTD, Conformation I has a maximum fluorescence around 320 nm, however, in Conformation II maximum fluorescence is seen around 338 nm (Fig. 2.4). By looking at the ratio of these two numbers the tryptophan fluorescence data can be analyzed in a different way to acquire a better understanding of the conformational change in the wild-type NTD. This can be used to compare the wild-type NTD to the NTD variants and their conformational states at different pHs. The ratio of these numbers for wild-type NTD is 1.16, 1.15, 1.13, 0.82 and 0.69 for pH 7.5, 7.0, 6.5, 6.0 and 5.5 respectively (Table 2.2). Numbers larger than 1, more specifically in the 1.1 range, show a larger fluorescence signal at 320 which is indicative of Conformation I. Ratios around 0.7-0.8 show a larger fluorescence signal around 338 nm and indicate that the tryptophan residue has become solvent-exposed and thus has entered Conformation II.

Tryptophan Fluorescence 320 nm/338 nm Ratio Table

	pH 7.5	pH 7	pH 6.5	pH 6	pH 5.5
Wild-type	1.16	1.15	1.13	0.82	0.69
D44N	1.15	1.15	1.15	1.16	0.80
D58N	1.13	1.14	1.11	0.92	0.68
E84Q	1.16	1.15	1.11	0.95	0.73
E124Q	1.13	1.07	0.76	0.63	0.58
E139Q	1.14	1.15	1.13	0.92	0.62
D45K	1.13	1.16	1.16	1.16	1.14
E84K	1.15	1.13	1.18	1.15	1.07
K70E	0.89	0.89	0.91	0.85	0.58
K70D	1.07	1.05	1.07	1.03	0.88
D45K/K70E	0.78	0.81	0.84	0.81	0.79
D45K/K70D	0.93	0.93	0.92	0.91	0.91

Table 2.2: Tryptophan Fluorescence 320 nm:/338 nm ratio table with Wild-type NTD and variants at pH 7.5, 7.0. 6.5, 6.0, and 5.5. .

As shown in the tryptophan fluorescence traces, the ratios show that many of the variants have a profile similar to wild-type (Fig. 2.7A). Variants D58N, E84Q, and E139Q show ratios that almost overlay with those of wild-type at the same respective pH (Appendix B, Fig. B-1C, D and F). Variants D44N and E124Q show a similar trend to that of wild-type with a distinct Conformation I and Conformation II (Fig. 2.7A) However, D44N remains in Conformation I until the pH drops below 6.0 unlike the wild-type where Conformation II occurs below pH 6.5 (Appendix A, Fig. B-1B). Conversely E124Q shifts into Conformation II earlier at pH 6.5 (Appendix A, Fig. B-1E).

Based on the tryptophan fluorescence graphs D45K does not shift into Conformation II (Fig. 2.5B).This is further demonstrated with the 320/338 nm graphs

where the ratio values never drop below 1.13, which is also the lowest value that wild-type NTD exhibits while in Conformation I (Table 2.2). This is represented in the graph by an almost straight line that nearly overlaps wild-type at pH 7.5, 7.0, and 6.5 (Appendix A, Fig. B-1F) Variant E84K also shows an almost straight line with near overlap with wild-type at pH 7.5, 7.0, and 6.5 (Appendix A, Fig. B-1G). The ratio of variant E84K also stay around the 1.1 range which correlates with the tryptophan fluorescence graph showing no change into Conformation II.

The K70D variant, shows a slightly lower ratio, when compared to wild-type, at pH 7.5, 7.0, 6.5 and 6.0 with numerical values around 1 (Table 2.2). At pH 5.5, the ratio does drop to 0.88 which indicates that the protein is in Conformation I until pH 5.5 and then shifts into a more intermediate conformation between I and II. The more drastic jumps that were observed, between pH 7.5 and 6.0 in the tryptophan fluorescence are not as pronounced in the ratio graph (Appendix A, Fig. B-1I). K70E also shows an intermediate conformation with ratios around 0.9 for pH 7.5, 7.0, and 6.5 with a drop to 0.85 and 0.58 at pH 6.0 and 5.5, respectively (Table 2.2). The three upper pH values lie in a range between strictly Conformation I and Conformation II, although closer to Conformation II, while at pH 6.0 the ratio places the protein in Conformation II (Appendix A, Fig. B-1H). At pH 5.5, the ratio is actually lower than that of wild-type at the same pH. This is congruent with the tryptophan fluorescence graph where the K70E variant never appears to enter Conformation I. When looked at as a whole the variants with charge changes seem to either maintain Conformation I or have an intermediate conformation between I and II with the negative-to-positive charge changes maintaining

Conformation I and the positive-to-negative charge changes existing in a more intermediate state.

The D45K/K70D variant has tryptophan fluorescence ratios and subsequent traces that lie almost perfectly in between Conformation I and Conformation II (Table 2.2 and Fig. 2.7C). This indicates an intermediate conformation along the observed pH range. While D45K/K70E shows a trace, along the pH range, that is in line with the wild-type pH 6.0 point at around 0.8 (Table 2.2). This indicates that D45K/K70E exists in Conformation II from pH 7.5 to pH 5.5 and does not enter Conformation I.

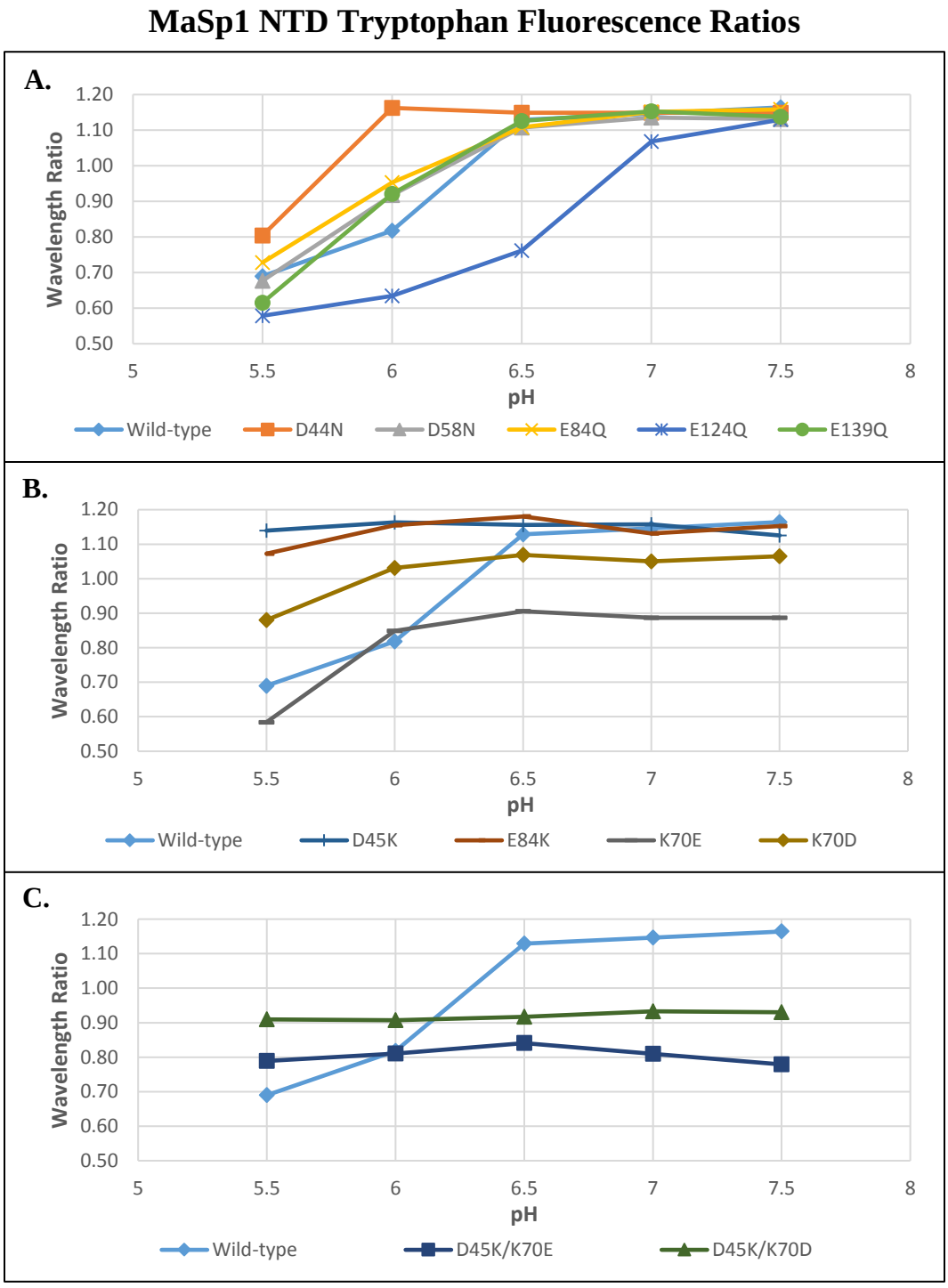

Figure 3.7 Graphs of tryptophan fluorescence readings at 320 nm divided by the reading at 338 nm for each pH (5.5, 6.0, 6.5, 7.0, and 7.5). A) Wild-type NTD, D44N, D58N, E84Q, E124Q, E139Q B) Wild-type NTD, D45K, E84K, K70E, K70D C) Wild-type NTD, D45K/K70E, D45K/K70D

V. Discussion

When excited the fluorescence of Trp residues depends on the micro-environment. When a Trp residue is buried within a protein in a hydrophobic environment, such as in the MaSp1 NTD at neutral pH, the emission signal is strong and displays a wavelength maximum of ~320 nm. However, if the Trp residue is exposed to the solvent fluorescence emission becomes quenched and the maximum is at a longer wavelength (~338 nm). As earlier research in our lab has shown, the wild-type NTD undergoes a conformational change upon acidification and the pH range at which this occurs is physiologically relevant (Andersson et al., 2014; Gaines et al., 2010). Since we see the wild-type conformation change in NTDs from other spider species (Gaines et al., 2010; Jaudzems et al., 2012; Kronqvist et al., 2014), focusing on conserved residues helped to narrow the choices of amino acids for the generation of variants. The second criterion of ionizable side chains was dictated by the pH responsiveness with which conformational change and NTD dimerization occurs (Gaines et al., 2010; Gronau et al., 2013; Humenik et al., 2011; Knight et al., 2000). For our variants, we chose to alter specific amino acids that fit both of these criteria because the NTD has a negative and positively charged pole along its axis. When the NTD forms a dimer, these poles lie opposite to each other thus creating a better environment for the creation of salt bridges (Askarieh et al., 2010; Kronqvist et al., 2014; Rising and Johansson, 2015; Wallace and Shen, 2012). These poles are thought to form a trap where the dimer state is always favored but it is unable to form until certain residues are protonated and thus "trigger" the formation of the dimer (Wallace and Shen, 2012). This "trap and trigger" mechanism is

in part due to the change in pK_a values of certain residues on the pole, when the NTD is in monomer or dimer form (Wallace and Shen, 2012). The dimer that forms at acidic pH is important for the creation of multimeric strands of spidroin protein where the CTDs are linked by disulfide bonds and the NTDs are linked by salt bridges (Gaines et al., 2010; Sponner et al., 2004). The information about residues conservation and charge led us to the creation of nine single variant NTDs and two double variant NTDs.

As detailed in the Results section, some of our variants did not show a strong deviation from wild-type MaSp1 NTD. Variant D44N does not show a large effect on conformation as D45K. The largest difference between D44N and wild-type is that a lower pH is necessary to move the D44N variant into Conformation II. This may be due to the less severe variation in charge change, from negative-to-neutral verses negative to positive charge for D45K. Variant D58N, near the C-terminal end of helix 2 is another residue that showed very little deviation from wild-type. D58 is not highly conserved and is not an exposed residue nor is it near other exposed polar residues (Askarieh et al., 2010). This makes the lack of variation from the wild-type very reasonable since all NTDs are believed to undergo the same conformation change.

Variant E84 is a position that was changed from a negative-to-neutral or negative-to-positive charge and does not show a severe phenotype for the negative to neutral charge change. When looking at the tryptophan fluorescence the E84K variant shows a decrease in fluoresce signal but does not show a red shift, which is indicative of a change into Conformation II. Looking at the 320/338 nm ratio graph the lack of shift into Conformation II is more apparent. E84 is located on helix 3, however, it is not exposed.

Since it is in such close proximity to the other acidic residues it could contribute to the overall negative pole (Askarieh et al., 2010; Flocco and Mowbray, 1995; Kronqvist et al., 2014). This could explain the decrease in fluoresce but no actual shift into conformation II.

Variant E124Q is located near the negative pole on helix 5. Though it does not show a substantial change from wild type, it might contribute to the overall negative charge of the pole. Variant E139Q, is located on the C-terminal end of the NTD, after helix 5, which is located at the end of the NTD. It is not near the NTD poles where the dimer interface occurs and thus unlikely to be a part of electrostatic interactions. This is supported by the near wild-type change from Conformation I to Conformation II seen for this variant.

From our Trp fluorescence and ratio data we have, however, determined some residues that, when changed, appear to affect the conformational change. The D45 position is one of the more extreme examples with the change into Conformation II being completely abolished. D45 is located on helix 2 and it, along with D44, are part of the negative NTD pole. This D45 residue has been shown in other labs to also be important in conformational change, although this is the first time this has been done using the *N. clavipes* NTD (Askarieh et al., 2010; Kronqvist et al., 2014). Since this residue is part of the negative pole it is likely also be involved in dimerization, although only further studies would be able to confirm this.

On the other end of the NTD is the positive pole which has K70, the theorized partner for residue D45. K70 is located toward the beginning of helix 3. While we do not

see the drastic change with K70D that is seen with D45K, at a lower pH (pH 5.5) K70D does shift into an intermediated conformation. Variant K70E, however, displays a large change and the protein exists between Conformation I and Conformation II for pH 7.5-6.5 and Conformation II at pH 6.0 and 5.5. This striking difference between the two different variants is surprising considering the only difference between K70E and K70D is a single methylene group and thus a slight shift in position of the charged side chain and pKa. This is significant because at pH 5.5 the maximum fluorescence signal is shifted slightly to the right which is more indicative of Conformation II but Conformation II also is quenched due to exposure of the Trp to the solvent. However, the maximum RFU of the pH 5.5 trace for K70E is above both pH 6 and 7.5 traces.

Double variants were generated based on the NTD crystal structure, amino acid conservation, single variant tryptophan fluorescence and their potential involvement in salt bridge formation (Askarieh et al., 2010; Wallace and Shen, 2012). D45K/K70D appeared to be between the Conformation I and Conformation II arrangement. For this double variant, by placing opposite charges in each of the poles of the protein, there is a sticking occurring between the two conformations and the protein was not able to fully enter one conformation or the other. Like in the single K70 variants, K70E shows a more pronounced change by causing a larger red shift. The extra CH_2 seems to cause a change by either shifting the side chain out further, causing a greater hindrance to Conformation I arrangement or otherwise affecting the surrounding environment of the other residues.

One thing that could affect the conformational changes seen in the variants is the change in pKa of surrounding residues due to a change in local charge. It has been shown

that environment greatly affects the pKa value of the residues side chain (Flocco and Mowbray, 1995; Pace et al., 2009). The average pKa of aspartic acid is around 2.5. However, it can have as low or as high pKa value as 0.5 and 9.2. Even if the residue itself is not directly involved in the conformation change it might affect the pKa values of neighboring residues which could lead to a preference of Conformation I or Conformation II. This theory was brought to light in other labs since only the histidine residue has a normal pKa value that is between 7.5 and 5.5, where the conformation change occurs (Askarieh et al., 2010; Kronqvist et al., 2014). This has been computational analyzed and changes in pK_a values were determined for the *E. australis* NTD, with the side chains for D45 and E84, changing about 0.5-2.3 pK_a values.

While these residues have provided us with positions that are important in conformation change. To further our understanding, other residues need to be changed and analyzed. Other labs have looked at residues equivalent to E89 and K65, in *N. clavipes*, and have shown them to be important in conformation change and would be a good starting point (Askarieh et al., 2010; Jaudzems et al., 2012; Kronqvist et al., 2014; Landreh et al., 2010; Schwarze et al., 2013; Wallace and Shen, 2012). Using the tryptophan fluorescence we have shown that there are multiple residues that are involved in conformation change. While these measurements can only be accurately attributed to the Trp residue, many groups have been able to show that this change is not only a local, but also a global change and thus Trp fluorescence is a good approximation of overall conformational change (Jaudzems et al., 2012; Kronqvist et al., 2014; Parnham et al., 2011). One theory as to this global change is that it allows helix 3 and 5 to come into

closer interaction with one another thus allowing for a better fit for dimerization (Jaudzems et al., 2012). From our data, we are able to further support the idea that all the NTDs undergo this conformational change, as many of the residues researched in other labs that were shown in *E. australis* to cause a change in conformation transition also occur in our data from *N. clavipes*. The use of only two species we cannot make a sweeping claim, it does lead to the idea that like D45 some of these residues are absolutely necessary for conformation change but others might have some flexibility and that this could apply not only across the board for different spider species but also different spider silk types as well.

VI. References

Andersson, M., Chen, G., Otikovs, M., Landreh, M., Nordling, K., Kronqvist, N., Westermark, P., Jornvall, H., Knight, S., Ridderstrale, Y., *et al.* (2014). Carbonic Anhydrase Generates CO2 and H+ That Drive Spider Silk Formation Via Opposite Effects on the Terminal Domains. PLoS Biol. *12,* e1001921.

Andersson, M., Holm, L., Ridderstrale, Y., Johansson, J., and Rising, A. (2013). Morphology and composition of the spider major ampullate gland and dragline silk. Biomacromolecules *14,* 2945-2952.

Askarieh, G., Hedhammar, M., Nordling, K., Saenz, A., Casals, C., Rising, A., Johansson, J., and Knight, S.D. (2010). Self-assembly of spider silk proteins is controlled by a pH-sensitive relay. Nature *465,* 236-238.

Bell, A.L., and Peakall, D.B. (1969). Changes in fine structure during silk protein production in the ampullate gland of the spider *Araneus sericatus*. J. Cell Biol. *42,* 284-295.

Challis, R.J., Goodacre, S.L., and Hewitt, G.M. (2006). Evolution of spider silks: conservation and diversification of the C-terminus. Insect Mol. Biol. *15,* 45-56.

Craig, C.L. (1997). Evolution of arthropod silks. Annu. Rev. Entomol. *42,* 231-267.

Dicko, C., Vollrath, F., and Kenney, J.M. (2004). Spider silk protein refolding is controlled by changing pH. Biomacromolecules *5,* 704-710.

Flocco, M.M., and Mowbray, S.L. (1995). Strange bedfellows: interactions between acidic side-chains in proteins. J. Mol. Biol. *254,* 96-105.

Gaines, W.A., Sehorn, M.G., and Marcotte, Jr., W.R.. (2010). Spidroin N-terminal domain promotes a pH-dependent association of silk proteins during self-assembly. J. Biol. Chem. *285,* 40745-40753.

Gronau, G., Qin, Z., and Buehler, M.J. (2013). Effect of sodium chloride on the structure and stability of spider silk's N-terminal protein domain. Biomater. Sci. *1,* 276-284.

Hagn, F., Thamm, C., Scheibel, T., and Kessler, H. (2011). pH-dependent dimerization and salt-dependent stabilization of the N-terminal domain of spider dragline silk--implications for fiber formation. Angew. Chem. Int. Ed Engl. *50,* 310-313.

Hayashi, C.Y., Blackledge, T.A., and Lewis, R.V. (2004). Molecular and mechanical characterization of aciniform silk: uniformity of iterated sequence modules in a novel member of the spider silk fibroin gene family. Mol. Biol. Evol. *21,* 1950-1959.

Hedhammar, M., Rising, A., Grip, S., Martinez, A.S., Nordling, K., Casals, C., Stark, M., and Johansson, J. (2008). Structural properties of recombinant nonrepetitive and repetitive parts of major ampullate spidroin 1 from *Euprosthenops australis*: implications for fiber formation. Biochemistry *47,* 3407-3417.

Heidebrecht, A., and Scheibel, T. (2013). Recombinant production of spider silk proteins. Adv. Appl. Microbiol. *82,* 115-153.

Humenik, M., Scheibel, T., and Smith, A. (2011). Spider silk understanding the structure-function relationship of a natural fiber. Prog. Mol. Biol. Transl. Sci. *103,* 131-185.

Ittah, S., Michaeli, A., Goldblum, A., and Gat, U. (2007). A model for the structure of the C-terminal domain of dragline spider silk and the role of its conserved cysteine. Biomacromolecules *8,* 2768-2773.

Jaudzems, K., Askarieh, G., Landreh, M., Nordling, K., Jörnvall, H., Rising, A., Knight, S.D., and Johansson, J. (2012). pH-Dependent Dimerization of Spider Silk N-Terminal Domain Requires Relocation of a Wedged Tryptophan Side Chain. J. Mol. Biol. *422,* 477-487.

Keten, S., and Buehler, M.J. (2010). Nanostructure and molecular mechanics of spider dragline silk protein assemblies. J. R. Soc. Interface *7,* 1709-1721.

Knight, D.P., Knight, M.M., and Vollrath, F. (2000). Beta transition and stress-induced phase separation in the spinning of spider dragline silk. Int. J. Biol. Macromol. *27,* 205-210.

Knight, D.D.P. (2001). Changes in element composition along the spinning duct in a Nephila spider. Naturwissenschaften *88,* 179-182.

Kronqvist, N., Otikovs, M., Chmyrov, V., Chen, G., Andersson, M., Nordling, K., Landreh, M., Sarr, M., Jornvall, H., Wennmalm, S., *et al.* (2014). Sequential pH-driven dimerization and stabilization of the N-terminal domain enables rapid spider silk formation. Nat. Commun. *5,* 3254, 1-11.

Landreh, M., Askarieh, G., Nordling, K., Hedhammar, M., Rising, A., Casals, C., Astorga-Wells, J., Alvelius, G., Knight, S.D., Johansson, J., Jornvall, H., and Bergman, T. (2010). A pH-dependent dimer lock in spider silk protein. J. Mol. Biol. *404,* 328-336.

Lewis, R.V. (2006). Spider silk: ancient ideas for new biomaterials. Chem. Rev. *106,* 3762-3774.

Pace, C.N., Grimsley, G.R., and Scholtz, J.M. (2009). Protein ionizable groups: pK values and their contribution to protein stability and solubility. J. Biol. Chem. *284,* 13285-13289.

Papadopoulos, P., Sölter, J., and Kremer, F. (2009). Hierarchies in the structural organization of spider silk—a quantitative model. Colloid Polym. Sci. *287,* 231-236.

Parnham, S., Gaines, W.A., Duggan, B.M., Marcotte Jr, W.R., and Hennig, M. (2011). NMR assignments of the N-terminal domain of *Nephila clavipes* spidroin 1. Biomol. NMR Assignments *5,* 131-133.

Rising, A., and Johansson, J. (2015). Toward spinning artificial spider silk. Nature Chem. Biol. *11,* 309-315.

Romer, L., and Scheibel, T. (2008). The elaborate structure of spider silk: structure and function of a natural high performance fiber. Prion *2,* 154-161.

Scheibel, T. (2004). Spider silks: recombinant synthesis, assembly, spinning, and engineering of synthetic proteins. Microb. Cell. Fact. *3,* 14, 1-10.

Schwarze, S., Zwettler, F.U., Johnson, C.M., and Neuweiler, H. (2013). The N-terminal domains of spider silk proteins assemble ultrafast and protected from charge screening. Nat. Commun. 4,2815,1-7

Sponner, A., Unger, E., Grosse, F., and Weisshart, K. (2004). Conserved C-termini of Spidroins are secreted by the major ampullate glands and retained in the silk thread. Biomacromolecules *5,* 840-845.

Vollrath, F., and Knight, D.P. (1999). Structure and function of the silk production pathway in the spider Nephila edulis. Int. J. Biol. Macromol. *24,* 243-249.

Wallace, J.A., and Shen, J.K. (2012). Unraveling A Trap-and-Trigger Mechanism in the pH-Sensitive Self-Assembly of Spider Silk Proteins. J. Phys. Chem. Lett. *3,* 658-662.

Xu, M., and Lewis, R.V. (1990). Structure of a protein superfiber: spider dragline silk. Proc. Natl. Acad. Sci. U. S. A. *87,* 7120-7124.

CHAPTER 3

OCTET OPTIMIZATION AND HOMODIMERIZATION OF WILD TYPE NTD FROM MAJOR AMPULLATE SPIDROIN 1

I. Abstract

The ability to produce spider silk has been the goal of many labs. However, the ability to spin the protein into fiber is also a concern. Understanding the mechanisms that are used in fiber formation could help with this process. The homodimerization of the NTD, which is involved in native fiber formation, is not well-understood. We used the FortéBio Octet system, which uses Bio-layer Interferometry to monitor the label free homodimerization of the *Nephila clavipes* major ampullate spidroin 1 NTD in real time. The use of streptavidin biosensors with buffer containing BSA and Tween 20, along with a free biotin blocking step was found to give the most accurate data. From this, we observed greater than a 25-fold increase in K_d for wild-type MaSp1 NTD homodimerization at pH 5.5 compared to pH 7.0, congruent with non-quantitative data previously obtained in our lab and others showing a more stable homodimer at acidic pH. This is the first instance of quantitative kinetic data for the MaSp1 wild-type NTD from *N. clavipes.*

II. Introduction

Spiders are a very diverse group with a remarkable ability to create silks that can be used to capture prey, protect offspring, and to create a lifeline (Bittencourt et al., 2012; Kluge et al., 2008; Romer and Scheibel, 2008). However, spiders have the ability to produce up to seven different types of silk, each with their own distinctive properties and functions. These silks are composed almost entirely of protein and each type of silk is produced by its own set of glands in the abdomen of the spider (Stauffer et al., 1994). The female *Nephila clavipes* is a spider from the orb-weaver family that produces a golden dragline silk. This dragline silk from the major ampullate (Ma) gland will be the focus of this study.

Dragline silk is the toughest of all spider silks, which means it can absorb the most energy of all the silks before breaking (Tokareva et al., 2013). When compared to the more commonly known silkworm silk, spider dragline silk is over twice as tough (Gosline et al., 1999; Heidebrecht and Scheibel, 2013; Heim et al., 2009). Dragline silk is used as a lifeline for the spider during controlled descents and for the radial threads and frame of web construction (Heidebrecht and Scheibel, 2013). This fiber is predominately made up of two spidroin (spider fibroin) proteins called major ampullate spidroin 1 and major ampullate spidroin 2 (MaSp1 and MaSp2, respectively). MaSp1 and MaSp1 proteins are composed of three major domains that are the C-terminal domain (CTD), the repeat domain (R) and the N-terminal domain (NTD). The proteins are stored in the major ampullate gland at very high concentrations of 30-50% (w/v) and, as they are needed, the spider pulls the fiber from the spinnerets, which are located on the lower

abdomen (Chen et al., 2002; Hijirida et al., 1996; Humenik et al., 2011; Vollrath and Knight, 1999). During the pulling process, the protein dope, used for fiber spinning, progresses from the storage portion of the gland to the spinneret through a long narrowing S-shaped duct where, the environment is drastically changed (Bell and Peakall, 1969; Hijirida et al., 1996; Knight and Vollrath, 1999). As such, the proteins are subject to mechanical shear force and chemical changes in ion concentration and a pH drop (Andersson et al., 2014; Breslauer et al., 2009; Eisoldt et al., 2010; Knight, 2001; Leclerc et al., 2013).These mechanical forces, such as shear force, help to align the fiber and transition the poly-alanine tails in the repeat domain from α-helixes to β-sheets (Gosline et al., 1986; Greving et al., 2012; Knight et al., 2000). Changes in ion concentration, including an increase in K^+, P, and S and a drop in Na^+ and Cl^- are thought to affect the aggregation and solubility of the spidroin proteins (Eisoldt et al., 2010; Knight, 2001). A drop in pH occurs along the duct of the gland which connects the sac to the spinneret. In the sac, the pH is around 7.2 and at about the midpoint of the duct the pH has been determined to be about 5.7 (Andersson et al., 2014). This pH change was shown to play a role during fiber formation by "unfolding" the CTD, thus affecting protein solubility, and by causing a conformational change in the NTD which results in stable homodimer formation (Sponner et al., 2005; Gaines,W.A. 2010; Kronqvist,N. 2014; Askarieh,G. 2010).

The CTD is a highly conserved sequence of about 150 amino acids and forms a disulfide bond with another CTD in the lumen of the gland by way of a conserved cysteine residue creating a tail-to-tail dimer (Hedhammar et al., 2008; Hu et al., 2006;

Ittah et al., 2007; Sponner et al., 2004). The repeat domain of the protein is the largest component and contains imperfect tandem repeat segments of about 20-40amino acids that can be repeated over a hundred times (Ayoub et al., 2007; Keten and Buehler, 2010; Xu and Lewis, 1990). The repeat domain of MaSp1 and MaSp2, as well as other silk types, are characterized by poly-alanine tracts (Xu,M. 1990; 230 Keten,S. 2010). As mentioned earlier, they go from an α-helical conformation to a β-sheet conformation, which allows for interlocking of nearby β-sheets through hydrogen bonds (Hayashi et al., 1999; Papadopoulos et al., 2009; Scheibel, 2004). Recombinantly-produced repeat domains can form fibers and are believed to contribute to fiber formation through the generation of extensive β-sheet structure (Hayashi et al., 1999; Papadopoulos et al., 2009; Scheibel, 2004). The N-terminal Domain (NTD) of dragline protein is like the CTD in that it is highly conserved and is about 150 amino acids in size. However, it undergoes a conformational change and homodimer stabilization as the pH is lowered from neutral to acidic pH specifically between pH 6.5 and 6 (Gaines et al., 2010; Rising et al., 2006). Separate dimerizations of the NTD and CTD are predicted to create long multimeric strands of repeating spidroin units that form the silk fiber (Gaines et al., 2010). This NTD conformational change has been observed using tryptophan fluorescence and 2-D NMR while dimer stabilization has been observed using pull down methodologies. Based on 2-D NMR and size exclusion experiments, this dimer shows a 1:1 interaction that is fully reversible when the pH is brought back to neutral pH from 5.5 (Askarieh et al., 2010; Gaines et al., 2010; Jaudzems et al., 2012). This dimer occurs between the positive and negative poles of the NTD, created from the clustering of polar amino acid side chains,

and while the exact mechanism is still unknown, some researchers have suggested a "trap and trigger" mechanism (Kronqvist et al., 2014). In this mechanism, the pH drop causes protonation of certain residues that help to "trigger" the NTD dimer stabilization. We decided to use a relatively new technology called Bio-Layer Interferometry (BLI) via the Octet RED96 system to look more closely at the rate at which the NTDs associate and dissociate in buffered environmental backgrounds set at pH 5.5 and 7.0. The BLI used by the Octet system is as a label-free way to monitor biomolecular interactions in real time. It is an analytical technique that uses reflected white light to determine the number of molecules that bind to a biosensor tip surface. Given that the BLI is a relatively new technology and the mechanism behind NTD homodimerization with associated conformational change at lowing pH has not been confirmed, extensive experimental assay refinement was necessary to obtain meaningful data. Here we give a brief overview of the experiments performed, which resulted in obtaining the association rate, dissociation rate and affinity constants of the wild-type MaSp1 NTD. These results showed a stronger homodimerization at pH 5.5 than pH 7.0, which agrees with the conclusions in the current literature.

III. Material and Methods

1. Wild Type NTD Protein Purification

a. Expression Plasmid Construction

Plasmids containing wild-type *N. clavipes* MaSp1-NTD sequence fusedwith glutathione S-transferase (GST) tag, was generated previously in our lab (Gaines et al., 2010) and used as a template to produce an NTD-His_6 protein coding region by PCR. The

Forward primer 5'-TAAGAAGCATGCTAGGGCCCCTGGGATCCC-3' and the reverse primer 5'-GCAAATGAAGTATCTTACGGTGGTAGATCTTAAGCA-3' were used to add restriction sites SphI and BglII (underlined) for cloning into the pQE-70 plasmid. M15 cells containing pREP4 were transformed with the pQE-70 MaSp1 NTD-His_6 plasmid.

b. Cell Growth and Lysis

Plasmid-containing BL21 *E. coli* cells were grown in Luria-Bertani broth (LB) at 37°C to an OD_{600} of about 0.8 and induced by addition of IPTG to a concentration of 0.5 mM. After induction and overnight growth at 16-20°C, cells were pelleted by centrifugation (Gaines et al., 2010). Cells containing GST-NTD construct were lysed by the addition of lysozyme (20 mg/ml) in a buffer consisting of 1X phosphate buffered saline (PBS), protease inhibitors (0.5 mM PMSF, 0.05 mM TLCK and 0.5 mM EDTA), 1% triton X-100, 10 mM $MgCl_2$ and 20 U DNAse. Cell lysate was clarified by centrifugation at 30,000 x g for 30 min. and then supernatant was filtered through 0.45 μm filter. GST-NTD protein was purified as described below.

Cells containing NTD-His_6 were grown to an OD_{600} of 1.0 in terrific broth (TB) and induced by addition of IPTG to a concentration of 1 mM. Cells were grown for 24 hours at 16-20°C and pelleted by centrifugation. Cells containing NTD-His_6 were resuspended in 50 mM $NaPO_4$ (pH 8) buffer containing 500 mM NaCl, 0.5 mM PMSF and 0.05 mM TLCK. Cells were lysed by three passes in a French pressure cell at ~120 MPa. Cell lysate was clarified by centrifugation and filtered through 0.45 μm filter. NTD-His_6 protein was purified as described below.

c. Protein Purification

GST-NTD proteins were affinity purified using glutathione Sepharose 4B (GE Healthcare) and GST tags were removed using PreScission protease (generous gift from the Sehorn Lab) digestion. Clarified lysate was added to glutathione resin and agitated for 30 minutes at 4°C. The resin mixture was then poured into an empty column and washed with 1X PBS. The protein was then eluted from the resin with 1X PBS plus 15 mM reduced glutathione, concentrated and buffer exchanged into PreScission Protease buffer containing 1X PBS, 1 mM EDTA and 1 mM DTT using 3 kDa centrifugal filter (Millipore UFC903008). The protein was digested with PreScission protease at 4°C overnight, rebound to glutathione resin and washed with 1X PBS. Flow through was concentrated using a 3 kDa centrifugal filter. Protein was further purified by an acid wash with 9 volumes of 10 mM MES, 10 mM citrate and 100 mM NaCl at pH 3.8 to 1 volume of concentrated protein. The solution was incubated for one hour at room temperature, spun for 30 minutes, and then supernatant was concentrated and buffer exchanged into 10 mM MES, 10 mM HEPES, and 100 mM NaCl buffer (pH 8) using 3 kDa centrifugal filter.

NTD-His_6 proteins were purified by passing clarified lysate containing 5 mM imidazole over Ni^{2+} resin (Roche). The resin was then washed with 50 mM $NaPO_4$ buffer (pH 8) containing 5 mM imidazole and 500 mM NaCl. Imidazole was increased to 23 mM and NaCl was increased to 1M and the resin was rewashed. Protein was eluted with 50 mM $NaPO_4$ buffer (pH 8) containing 500 mM NaCl and 500 mM imidazole, concentrated and buffer exchanged into 1X PBS by 3 kDa centrifugal filter. Concentrated

protein was acid washed as described for GST-NTD protein, then concentrated and buffer exchanged into 25 mM Tris HCl buffer. Mini anion-exchange spin columns (Thermo Scientific 90010) were used to further purify the sample. Protein was loaded onto the column, spun at 2,000 x *g* for 5 minutes and washed with 25 mM Tris-HCl and spun again. The wash step was repeated and protein was eluted with 25 mM Tris HCl buffer containing 500 mM NaCl by spinning at 2,000 x *g* for 5 minutes. The protein was then concentrated and buffer exchanged into 10 mM MES, 10 mM HEPES, and 100 mM NaCl buffer at pH 8.

Purified proteins were run on 15% SDS-polyacrylamide gels and either stained by Coomassie Brilliant Blue dye or immunodetected. The immunodection was completed by electro-transfer from a SDS- polyacrylamide gel onto a PVDF membrane. The membrane was blocked using 5% milk (Carnation instant nonfat dry milk) in tris-bufferd saline containing 0.1% Tween 20 (TBST) for one hour. The membrane was washed with TBST and a solution containing 1% milk and primary antibody anti-NTD (Rockland Immunochemicals, Inc.) from rabbit, was added for one hour. The membrane was washed with TBST and solution containing 1% milk and alkaline phosphatase (AP) conjugated goat anti-rabbit secondary antibody was added and allowed to incubate for one hour. Membrane was then washed and Immun-Star imaging substrate (BioRad) was added before imaging (Fujifilm LAS-1000plus imager).

d. NTD-His_6 biotinylation

NTD-His_6 was biotinylated using a protocol to preferentially biotinylate the N-terminal α-amino group (Selo et al., 1996). The protein was diluted into 50 mM

phosphate buffer (pH 6.5) and biotin (Thermo Scientific 21455) was added to a 5:1 ratio of NHS-PEG4-biotin to NTD-His_6. The solution was incubated for 24 hrs at 4°C. Unreacted biotin was removed using a desalting spin column (Thermo Scientific).

2. Octet Experiments

a. Experiments setup-initial

An Octet RED96 instrument and corresponding Data Acquisition software version 7.1 were used (FortéBio). For all experiments, buffers were loaded into a 96-well black bottom plate (Greiner Bio-One) at 200 µL per well. The biosensor tips (FortéBio) used were anti-GST (18-5097), anti-Penta-His (18-5120), Ni-NTA (18-5101) or streptavidin (18-5019) and were equilibrated in buffer containing 10 mM HEPES, 10 mM MES and 100 mM NaCl (Octet buffer) at pH 7.0 for at least 10 minutes prior to running any experiment.

To determine sub-saturating conditions for loading biosensors with ligand protein biosensors were loaded with either wild-type MaSp1 GST-NTD, NTD-His_6 or biotinylated NTD-His_6 protein at concentrations ranging from 1.22 µM to 50 nM for 10 minutes in Octet pH 7.0 buffer. Biosensor tips were then washed with Octet buffer. From this experiment, a loading concentration was chosen based on visual inspection of loading curves. Non-hyperbolic traces indicate sub-saturated ligand binding/loading.

To determine general analyte concentrations to use for association steps, equilibrated biosensors were loaded with wild-type MaSp1 GST-NTD, NTD-His_6 or biotinylated NTD-His_6 protein. Biosensors were then washed in Octet buffer and a baseline was taken. Biosensors were then moved to the association step were wild-type

NTD protein, purified from GST-NTD protein, had been added to the wells containing Octet buffer in concentrations ranging from about 300 µM to 10 nM. After association, biosensors were allowed to dissociate in Octet buffer (Fig. 3.1). Appropriate concentrations for further experiments were chosen based on visual curation of the sensor traces. Traces that visually showed extreme noise, due to low signal, and those showing saturation were excluded. The resultant traces were analyzed to provide a preliminary K_d based on a grouping of K_d values over multiple octet concentrations.

To more accurately determine K_d, the same experiment was performed using the NTD concentrations for the association step ranging from ~10X above and ~10X below the determined preliminary K_d.

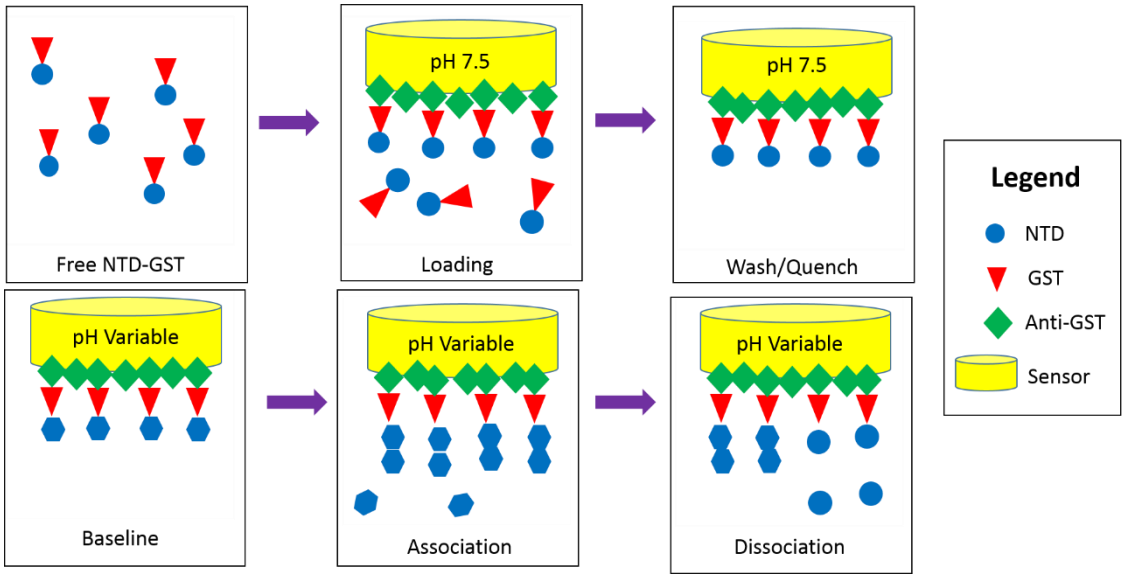

Figure 3.1 Example of basic Octet experiment using anti-GST biosensors. Wild-type MaSp1 GST-NTD protein is loaded onto anti-GST biosensors at pH 7.5 and washed at pH 7.5. Then baseline, association and dissociation steps are completed at the same pH (from 5.5 to 7.5). Wild-type MaSp1 NTD was used in association steps.

Experiments performed using the basic Octet setup presented in Fig. 3.1 revealed several problems related to GST contamination and non-specific binding but served as the foundation for troubleshooting. Troubleshooting efforts for both are detailed in the Results section.

b. Experimental setup-final

The Octet RED96 instrument, associated Data Acquisition software and plates used were the same as mentioned in section III-2-a. Streptavidin biosensors (FortéBio catalog number 18-5019) were used and were equilibrated for at least 10 min at pH 7.0 in Octet buffer containing 10 mM HEPES, 10 mM MES, 100 mM NaCl, 2% BSA and 0.02% Tween 20.

Plates were loaded with 200 µL, per well, of Octet buffer at either pH 5.5 or 7.0. Biosensors were loaded with 50 nM biotinylated NTD-His_6 ligand for 10 minutes in Octet buffer pH 7.0 after equilibration. Biosensors were then moved into Octet buffer pH 7.0 containing 5 µM free biotin (Sigma-Aldrich B4501). Then sensors were washed twice for 5 minutes each in Octet buffer of either pH 7.0 or 5.5. The buffer pH was kept consistent at either 5.5 or 7.0 for the rest of the experiment. A baseline was taken for 3 minutes and biosensors were moved to the association step for 50 seconds containing wild-type MaSp1 NTD. Concentrations for MaSp1 NTD in association step were 300 µM, 150 µM, 75 µM, 38 µM, 19 µM, and 9 µM for pH 7.0 and 75 µM, 38 µM, 19 µM, 9 µM, 5 µM, and 2 µM for pH 5.5. For both experiments a biosensor with loaded protein

only was used as a reference. Sensors were then placed in Octet buffer and allowed to dissociate for 2.5 minutes.

c. Processing data

Completed experiments were processed using Data Analysis software version 7.1 (FortéBio). The reference sensor data was subtracted from each of the experimental sensors to account for noise and drift. Traces were aligned to the y-axis at the baseline step. Inter-step correction was used and data was processed using Savitzky-Golay filtering. Data was analyzed using a 1:1 model for association and dissociation steps. The dissociation step length was truncated to 50 seconds and local full fitting was used to visually curate data with excesses noise and low R^2 values. Three to four traces that grouped around a K_d value were chosen and then analyzed together using global full fit to obtain a final K_d.

IV. Results

1. Protein purification

GST-NTD fusion protein and both wild-type MaSp1 NTD (from GST-NTD fusion) and NTD-His_6 were expressed and purified. NTD and NTD-His_6 protein samples were subjected to duplicate SDS-PAGE and separately stained with Coomassie Brilliant Blue and probed by immunodetection (Fig. 3.2).

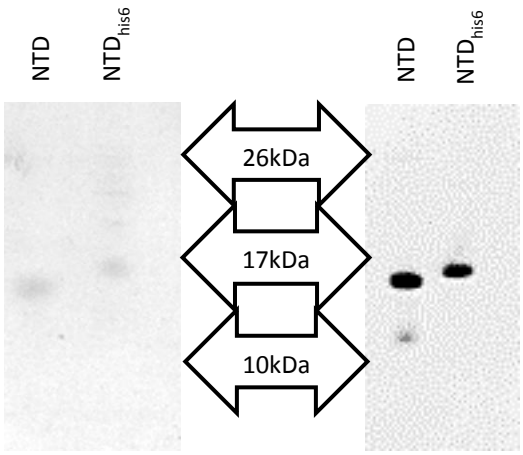

Figure 3.2 Coomassie-stained SDS-PAGE gel (left) and immunodetection membrane using anti-NTD primary antibody (right) showing purified 1 µg NTD (15 kDa) and 1µg NTD-His_6 (16 kDa).

2. Octet experiments

a. Anti-GST Biosensors

Experiments involving anti-GST biosensors used GST-NTD fusion protein for the loading step and free NTD, purified from GST-NTD, for the association step. Initial experiments revealed that 50 nM GST-NTD resulted in a linear (non-hyperbolic) trace, indicative of sub-saturation loading conditions (see dark blue trace in Fig. 3.3). Association was then performed using free NTD concentrations between 150 µM and 10 nM; followed by dissociation. Interestingly, the trace did not plateau during the association step as would be expected (see medium blue trace in Fig. 3.3) but rather continued to rise and thus the data generated was consistent with a 2:1 binding model. Since it is known through crystal structure and size exclusion studies that the MaSp1 NTD forms a 1:1 dimer, another explanation for 2:1 binding behavior was considered

(Askarieh,G. 2010; Gaines,W.A. 2010). Using immunodetection with anti-GST primary antibody, it was determined that the purified NTD contained a small amount of residual GST (≤ 1% of protein concentration) that could have been binding to unoccupied anti-GST antibodies immobilized on the biosensors. This additional GST binding and would be expected to alter the signal detected during the association step and give a more 2:1 binding profile.

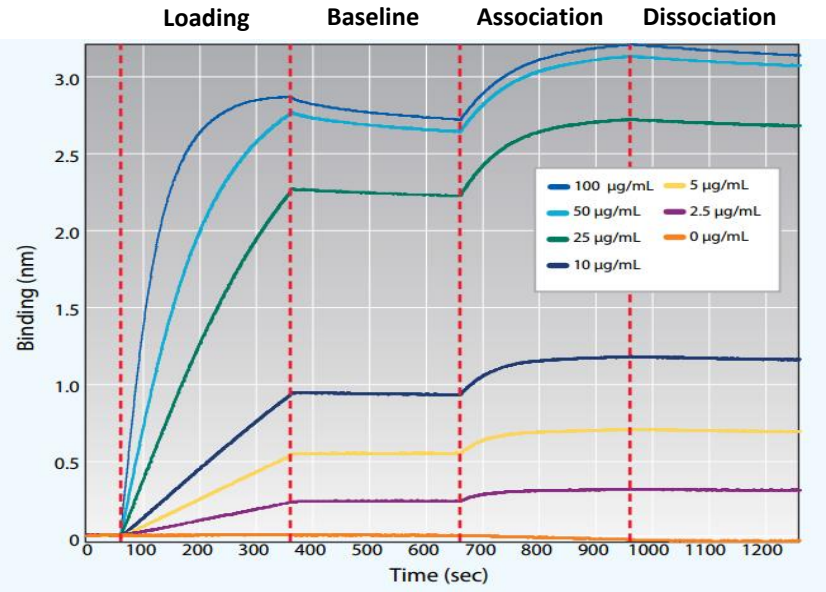

Figure 3.3 Example ligand loading optimization experiment. 100 µg/ml shows the signal leveling off which is indicative of saturation of tip. 10 µg/ml shows what the signal should look like at a proper loading concentration modified from (Tobias and Kumaraswamy, 2014)

In an effort to circumvent this problem, a blocking step was introduced into the protocol. The blocking step was added between the loading and baseline step with the

goal of preventing the residual GST in the free NTD sample from binding to the sensor thereby providing a more accurate signal for dimerization. Trial experiments were performed to test the concentration and time needed. GST protein (Thermo Fisher) was added to Octet buffer of either pH 5.5 or 7.5, depending on the experiment, and concentrations from 170 nM to 2560 nM were tested. The length of the blocking step was also varied from 2 minutes to 46.7 minutes. The blocking step was followed by one or two wash steps before the baseline was taken.

Addition of 250 nM GST in the blocking step eliminated GST binding to the tip during the association step (compare red and light blue traces in Fig. 3.4). Note that the amount of GST included during association (20 nM) was chosen to approximate the level of contamination in the free NTD sample. Moreover, GST blocking also reduced the signal for NTD binding during association (dimerization) by about 50% (compare orange and dark blue traces in Fig. 3.4). This results in a very low NTD dimerization signal that necessitated increasing NTD concentrations for subsequent experiments. Unfortunately, this also increased the amount of contaminating GST and efforts to block these higher levels were unsuccessful.

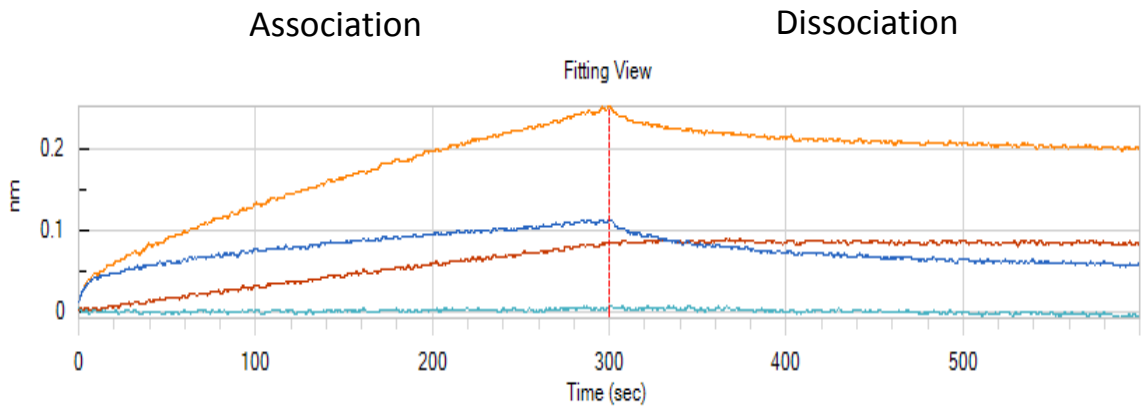

Figure 3.4 Representative graph of association and dissociation with or without GST blocking. Absence of GST in the blocking step and 2000 nM NTD in association step (orange); absence GST in blocking step and 20 nM GST in association step (red); 250 nM GST in blocking step with 2000 nM NTD in association step (dark blue); 250 nM GST in blocking step with 20 nM GST in association step (light blue).

Anti-GST biosensors also had large amounts of non-specific binding, based on experiments using free NTD, in the association step without protein loading, regardless of the presence of blocking GST. BSA and Tween 20 are suggested additives when non-specific binding is observed (FortéBio). However, even when maximum recommended levels of BSA and Tween 20 were included in the Octet buffer, non-specific binding was still observed.

b. Anti-Penta-His and Ni-NTA biosensors

Having eliminated anti-GST biosensors as a viable option for NTD dimerization analysis, anti-Penta-His and Ni-NTA biosensors (FortéBio) were next evaluated using NTD-His_6 for loading and free NTD purified from GST-NTD fusion protein for

association. Unfortunately, both anti-Penta-His and Ni-NTA biosensors displayed poor retention of loaded protein. Once biosensors were moved from the loading step to the Octet buffer wash step, bound NTD-His_6 began to dissociate and continued to dissociate for the remainder of the experiment (Fig. 3.5). These two biosensors also displayed significant non-specific binding of NTD. Addition of Tween 20 and BSA did reduce non-specific binding, but the inability to stably couple the NTD-His_6 protein to the sensors made these also unsuitable for analysis of NTD dimerization.

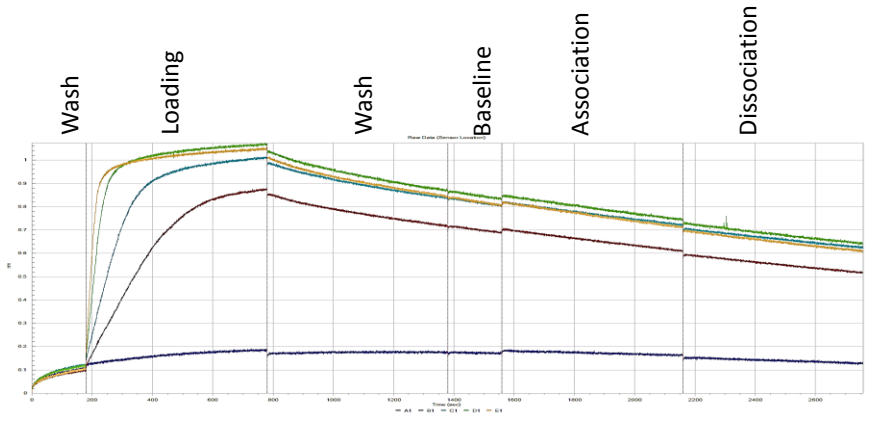

Figure 3.5 Representative graph showing loading of anti-Penta His biosensors, where various concentrations of wild-type MaSp1 NTD-His_6 protein fall off after the loading step.

c. Streptavidin biosensors

NTD-His_6 protein was purified and biotinylated as described in the Materials and Methods section. Streptavidin biosensors used biotinylated NTD-His_6 for loading and free

NTD, from GST-NTD, for association. Streptavidin biosensors showed high affinity binding of ligand during loading and retention during subsequent steps (Fig. 3.6).

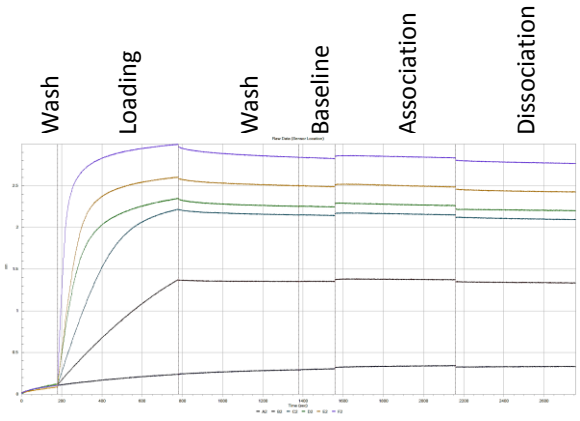

Figure 3.6 Representative graph showing loading of streptavidin biosensors, where various concentrations of biotinylated wild-type MaSp1 NTD-His_6 protein show appropriate loading traces

Streptavidin biosensors also showed the lowest non-specific binding (Fig. 3.7). A blocking step containing free biotin (Sigma-Aldrich B4501) was also included in the protocol to further reduce non-specific binding.

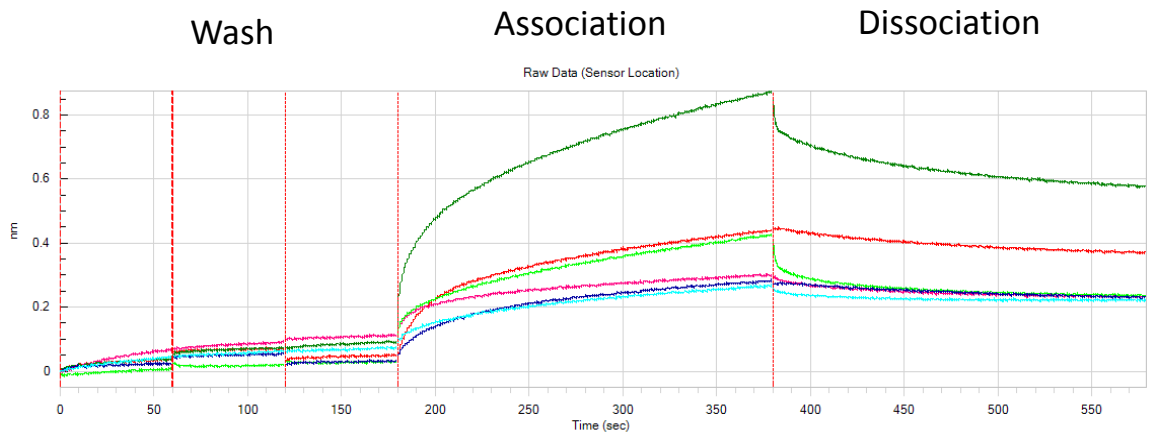

Figure 3.7 Representative graph showing non-specific binding during association step for multiple different biosensors. BSA range from 0.01%-1.0%. Traces shown are for maximum (containing 0.1% BSA) and minimum (containing 1% BSA) non-specific binding signals for each biosensor type in octet buffer at pH 5.5. Ni-NTA maximum (green) and minimum (light green), anti-Penta His maximum (red) and minimum (pink) and streptavidin maximum (blue) and minimum (light blue). MaSp1 NTD concentration for association step 30,000nM.

d. Miscellaneous troubleshooting

During optimization, a variety of additional parameters were evaluated. Association time was evaluated from a maximum time of 50 seconds to 60 minutes to monitor sensor saturation. Dissociation time was evaluated from a maximum time of 2.3 minutes to 60 minutes to ensure near compete dissociation. Dimerization analysis was also limited to pH 7.0 and pH 5.5 for analysis since the NTD goes through intermediate conformations at intermediate pH values.

3. Octet experiments-final

Evaluation of multiple biosensors and optimization of other experimental parameters allowed the development of a protocol to monitor MaSp1 NTD dimerization. Wild-type NTD homodimerization was analyzed using the Octet RED96 instrument and associated software. Affinity constant (K_d), rate of association (k_{on}) and rate of dissociation (k_{dis}) were measured using biotinylated NTD-His_6 as the ligand on streptavidin biosensors and free NTD (purified from GST-NTD) as the analyte at pH 5.5 and 7.0. Details of the final protocol can be found in the Materials and Methods section.

Wild-type MaSp1 NTD showed a 25-fold difference in K_d at acidic pH with a K_d of 36.80 ± 2.92 μM for pH 5.5 and 1.45 ± 0.09 μM for pH 7.0 (Table 3.1). This shows that at pH 5.5 The NTD has a stronger homodimerization than it does at pH 7.0. The rate of dissociation (k_{dis}) for both pH 5.5 and 7 were very similar at $3.01 \times 10^{-2} \pm 6.96 \times 10^{-4}$ s^{-1} and $2.78 \times 10^{-2} \pm 9.95 \times 10^{-4}$ s^{-1}, respectively. However, k_{on} showed a twenty-fold difference with an association of $2.07 \times 10^{4} \pm 1.26 \times 10^{3}$ $M^{-1}s^{-1}$ for pH 5.5 and $1.03 \times 10^{3} \pm 7.68 \times 10^{1}$ $M^{-1}s^{-1}$ for pH 7.0. This agrees with the data for wild-type NTD that show a larger signal during association for pH 5.5 than with 7.0 (Fig. 3.8). The signal during dissociation shows that by about 50 seconds the majority of protein has dissociated. The use of the same association and dissociation times for both pH 5.5 and 7.0 allows for better comparison between the two pHs. Both traces show a good fit to the 1:1 model with R^2 values above 0.9 (Table 3.1).

NTD	pH	K_d (μM)	K_d Error (μM)	k_{on} (1/Ms)	k_{on} Error	k_{dis} (1/s)	k_{dis} Error	R^2
Wild-type	7.0	36.80	2.92	1.03E+03	7.68E+01	2.78E-02	9.95E-04	0.92
	5.5	1.45	0.09	2.07E+04	1.26E+03	3.01E-02	6.96E-04	0.94

Table 3.1 Kinetic analysis of *N. clavipes* wild-type MaSp1 N-terminal domain at pH 5.5 and 7.0.

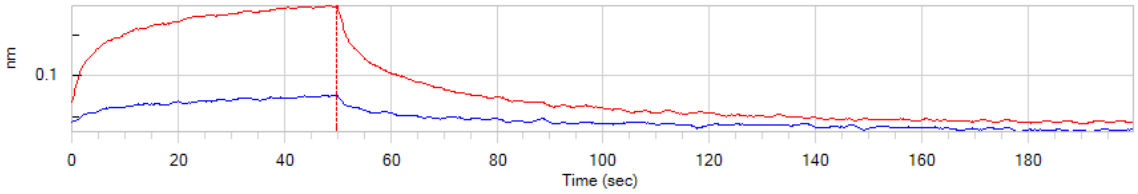

Figure 3.8 Sensogram showing representative trace of wild-type NTD at pH 5.5 (red) and 7.5 (blue) at 75μM

V. Discussion

Wild-type NTD was shown, through tryptophan fluorescence, nuclear magnetic resonance (NMR) spectroscopy and other methods, to undergo a conformational change when transitioning from neutral to acidic pH (Askarieh et al., 2010; Gaines et al., 2010; Jaudzems et al., 2012; Kronqvist et al., 2014). Experiments have also shown that the NTD forms a homodimer through salt bridges at acidic pH. These salt bridges are thought to exist between the positive and negative poles on the NTD, created by clusters of polar amino acid side chains, and under neutral pH conditions the NTDs form weak homodimers that are stabilized at lower a pH (Askarieh et al., 2010; Kronqvist et al., 2014; Rising and Johansson, 2015; Wallace and Shen, 2012). One explanation of this observation is a "trap and trigger" mechanism where the dimer state if favored at all times but only at lower pH does the dimer become more stable (Wallace and Shen, 2012).

Use of BLI by the Octet system and associated software has allowed us to look at wild-type MaSp1 NTD homodimerzation in real time under label free conditions to obtain kinetic information for a more informed picture of the dimerization process.

Before final kinetic experiments could be performed, experimental parameters had to be examined and empirically optimized to allow generation of the most accurate kinetic data. Anti-GST biosensors were the initial choice due to easily produced GST-NTD protein used in previous experiments in our lab (Gaines et al., 2010; Parnham et al., 2011). However, due to the sensitivity of the Octet instrument the residual GST that was left in the purified NTD altered the dimerization signal. Binding during the association step was consistent with a 2:1 interaction instead the 1:1 interaction observed by other studies (Askarieh et al., 2010; Gaines et al., 2010; Jaudzems et al., 2012). This was partly due to binding of residual GST to the anti-GST antibodies and possibly the formation of GST homodimers (Terpe, 2003; Tudyka and Skerra, 1997). Even though the residual GST concentration was small (≤ 1%), at NTD concentrations of ~50 μM the resultant GST concentration would be ~500 nM, which is a higher concentration of GST than is used in the loading step (50 nM). The non NTD-NTD interactions caused the signal to appear to be a 2:1 interaction. Blocking of the anti-GST antibodies did help reduce the GST binding (Fig. 3.4), however, even with apparent saturation in the blocking step, GST binding was still seen in the association step at higher NTD concentrations. This could be due to GST homodimerization.

Due to the inability to use anti-GST biosensors, wild-type NTD was re-cloned with a His_6 tag for use with Ni-NTA and anti-Penta-His biosensors. Anti-Penta-His

biosensors showed low non-specific binding but both those and the Ni-NTA biosensors did not display stable loading of ligand using the NTD-His_6 protein (Fig. 3.5).

Streptavidin biosensors were chosen for final experiments based on the low amount of non-specific binding seen and ability to irreversibly bind biotinylated NTD-His_6 (Fig. 3.6 and 3.7). Biotinylation was done at low pH to preferentially biotinylate the N-terminal α-amino group (Selo et al., 1996). This helped to prevent biotinylation of lysines found in the NTD, at least one of which is believed to be very important in dimerization (Askarieh et al., 2010; Gronau et al., 2013; Jaudzems et al., 2012). Streptavidin sensors were blocked using free biotin to further reduce non-specific binding and this method has been used successfully in other experiments using streptavidin (Abdiche et al., 2009; Abdiche et al., 2011; Fousteri et al., 2012).

BSA and Tween 20 at concentrations of 2% and 0.02%, respectively, were used with the streptavidin biosensors as their use showed an additional and significant decrease in non-specific binding (Fig. 3.6). Association and dissociation step times were kept consistent for pH 5.5 and 7.0 for ease of comparison between pHs and shorter association and dissociation times provided a better fit due to the decrease in time spent at saturation and baseline conditions (Fig. 3.8).

By troubleshooting, we were able to generated robust data that shows a significant 25-fold decrease in the K_d from pH 7.0 to pH 5.5 that leads to the formation of a more stable homodimer (Table 3.1). Since the k_{dis} for both pHs are similar, the majority of the difference in K_d is attributed to the k_{on} (Table 3.1). At pH 7.0, the free wild-type NTD only weakly associates with the NTD attached to the biosensors and once placed in

protein free buffer, dissociates at a rate of $2.78 \times 10^{-2} \pm 9.95 \times 10^{-4}$ s^{-1}. However, at pH 5.5 the free NTDs readily dimerize with NTDs attached to the surface of the biosensors and dissociate at the nearly the same rate as at pH 7.0. The increased dimerization seen at lower pH coincides with tryptophan fluorescence data that shows that wild-type NTD undergoes a conformation change at acidic pH other research has also shown that the NTD forms a more stable dimer at lower pH (Andersson et al., 2014; Askarieh et al., 2010; Gaines et al., 2010; Hagn et al., 2011; Jaudzems et al., 2012; Kronqvist et al., 2014). This difference in dimerization would allow for weak association of NTDs in the gland of the spider, thus facilitating the resolution of knots/tangles that could form if the dimer was more strongly associated. However, as the spidroin proteins flow down the duct the NTD dimers would become more stable, which would help in the formation of multimeric strands of repeating spidroin proteins connected through stable CTD and NTD dimers.

VI. References

Abdiche, Y.N., Lindquist, K.C., Pinkerton, A., Pons, J., and Rajpal, A. (2011). Expanding the ProteOn XPR36 biosensor into a 36-ligand array expedites protein interaction analysis. Anal. Biochem. *411,* 139-151.

Abdiche, Y.N., Malashock, D.S., Pinkerton, A., and Pons, J. (2009). Exploring blocking assays using Octet, ProteOn, and Biacore biosensors. Anal. Biochem. *386,* 172-180.

Andersson, M., Chen, G., Otikovs, M., Landreh, M., Nordling, K., Kronqvist, N., Westermark, P., Jornvall, H., Knight, S., Ridderstrale, Y., *et al.* (2014). Carbonic Anhydrase Generates CO2 and H+ That Drive Spider Silk Formation Via Opposite Effects on the Terminal Domains. PLoS Biol. *12,* e1001921.

Askarieh, G., Hedhammar, M., Nordling, K., Saenz, A., Casals, C., Rising, A., Johansson, J., and Knight, S.D. (2010). Self-assembly of spider silk proteins is controlled by a pH-sensitive relay. Nature *465,* 236-238.

Ayoub, N.A., Garb, J.E., Tinghitella, R.M., Collin, M.A., and Hayashi, C.Y. (2007). Blueprint for a high-performance biomaterial: full-length spider dragline silk genes. PLoS One *2,* e514.

Bell, A.L., and Peakall, D.B. (1969). Changes in fine structure during silk protein production in the ampullate gland of the spider *Araneus sericatus*. J. Cell Biol. *42,* 284-295.

Bittencourt, D., Oliveira, P.F., Prosdocimi, F., and Rech, E.L. (2012). Protein families, natural history and biotechnological aspects of spider silk. Genet. Mol. Res. *11,* 2360-2380.

Breslauer, D.N., Lee, L.P., and Muller, S.J. (2009). Simulation of flow in the silk gland. Biomacromolecules *10,* 49-57.

Chen, X., Knight, D.P., and Vollrath, F. (2002). Rheological characterization of nephila spidroin solution. Biomacromolecules *3,* 644-648.

Eisoldt, L., Hardy, J.G., Heim, M., and Scheibel, T.R. (2010). The role of salt and shear on the storage and assembly of spider silk proteins. J. Struct. Biol. *170,* 413-419.

Fousteri, G., Jasinski, J., Dave, A., Nakayama, M., Pagni, P., Lambolez, F., Juntti, T., Sarikonda, G., Cheng, Y., Croft, M., *et al.* (2012). Following the fate of one insulin-reactive CD4 T cell: conversion into Teffs and Tregs in the periphery controls diabetes in NOD mice. Diabetes *61,* 1169-1179.

Gaines, W.A., Sehorn, M.G., and Marcotte, Jr., W.R. (2010). Spidroin N-terminal domain promotes a pH-dependent association of silk proteins during self-assembly. J. Biol. Chem. *285,* 40745-40753.

Gosline, J.M., DeMont, M.E., and Denny, M.W. (1986). The structure and properties of spider silk. Endeavour *10,* 37-43.

Gosline, J.M., Guerette, P.A., Ortlepp, C.S., and Savage, K.N. (1999). The mechanical design of spider silks: from fibroin sequence to mechanical function. J. Exp. Biol. *202,* 3295-3303.

Greving, I., Cai, M., Vollrath, F., and Schniepp, H.C. (2012). Shear-induced self-assembly of native silk proteins into fibrils studied by atomic force microscopy. Biomacromolecules *13,* 676-682.

Gronau, G., Qin, Z., and Buehler, M.J. (2013). Effect of sodium chloride on the structure and stability of spider silk's N-terminal protein domain. Biomater. Sci. *1,* 276-284.

Hagn, F., Thamm, C., Scheibel, T., and Kessler, H. (2011). pH-dependent dimerization and salt-dependent stabilization of the N-terminal domain of spider dragline silk--implications for fiber formation. Angew. Chem. Int. Ed Engl. *50,* 310-313.

Hayashi, C.Y., Shipley, N.H., and Lewis, R.V. (1999). Hypotheses that correlate the sequence, structure, and mechanical properties of spider silk proteins. Int. J. Biol. Macromol. *24,* 271-275.

Hedhammar, M., Rising, A., Grip, S., Martinez, A.S., Nordling, K., Casals, C., Stark, M., and Johansson, J. (2008). Structural properties of recombinant nonrepetitive and repetitive parts of major ampullate spidroin 1 from *Euprosthenops australis*: implications for fiber formation. Biochemistry *47,* 3407-3417.

Heidebrecht, A., and Scheibel, T. (2013). Recombinant production of spider silk proteins. Adv. Appl. Microbiol. *82,* 115-153.

Heim, M., Keerl, D., and Scheibel, T. (2009). Spider silk: from soluble protein to extraordinary fiber. Angewandte Chemie International Edition *48,* 3584-3596.

Hijirida, D.H., Do, K.G., Michal, C., Wong, S., Zax, D., and Jelinski, L.W. (1996). 13C NMR of *Nephila clavipes* major ampullate silk gland. Biophys. J. *71,* 3442-3447.

Hu, X., Vasanthavada, K., Kohler, K., McNary, S., Moore, A.M., and Vierra, C.A. (2006). Molecular mechanisms of spider silk. Cell Mol. Life Sci. *63,* 1986-1999.

Humenik, M., Scheibel, T., and Smith, A. (2011). Spider silk understanding the structure-function relationship of a natural fiber. Prog. Mol. Biol. Transl. Sci. *103,* 131-185.

Ittah, S., Michaeli, A., Goldblum, A., and Gat, U. (2007). A model for the structure of the C-terminal domain of dragline spider silk and the role of its conserved cysteine. Biomacromolecules *8,* 2768-2773.

Jaudzems, K., Askarieh, G., Landreh, M., Nordling, K., Jörnvall, H., Rising, A., Knight, S.D., and Johansson, J. (2012). pH-Dependent Dimerization of Spider Silk N-Terminal Domain Requires Relocation of a Wedged Tryptophan Side Chain. J. Mol. Biol. *422,* 477-487.

Keten, S., and Buehler, M.J. (2010). Nanostructure and molecular mechanics of spider dragline silk protein assemblies. J. R. Soc. Interface *7,* 1709-1721.

Kluge, J.A., Rabotyagova, O., Leisk, G.G., and Kaplan, D.L. (2008). Spider silks and their applications. Trends Biotechnol. *26,* 244-251.

Knight, D., and Vollrath, F. (1999). Liquid crystals and flow elongation in a spider's silk production line. Proceedings of the Royal Society of London.Series B: Biological Sciences *266,* 519-523.

Knight, D.P., Knight, M.M., and Vollrath, F. (2000). Beta transition and stress-induced phase separation in the spinning of spider dragline silk. Int. J. Biol. Macromol. *27,* 205-210.

Knight, D.D.P. (2001). Changes in element composition along the spinning duct in a Nephila spider. Naturwissenschaften *88,* 179-182.

Kronqvist, N., Otikovs, M., Chmyrov, V., Chen, G., Andersson, M., Nordling, K., Landreh, M., Sarr, M., Jornvall, H., Wennmalm, S., *et al.* (2014). Sequential pH-driven dimerization and stabilization of the N-terminal domain enables rapid spider silk formation. Nat. Commun. *5,* 3254, 1-11.

Leclerc, J., Lefevre, T., Gauthier, M., Gagne, S.M., and Auger, M. (2013). Hydrodynamical properties of recombinant spider silk proteins: Effects of pH, salts and shear, and implications for the spinning process. Biopolymers *99,* 582-593.

Papadopoulos, P., Sölter, J., and Kremer, F. (2009). Hierarchies in the structural organization of spider silk—a quantitative model. Colloid Polym. Sci. *287,* 231-236.

Parnham, S., Gaines, W.A., Duggan, B.M., Marcotte Jr, W.R., and Hennig, M. (2011). NMR assignments of the N-terminal domain of *Nephila clavipes* spidroin 1. Biomolecular NMR Assignments *5,* 131-133.

Rising, A., and Johansson, J. (2015). Toward spinning artificial spider silk. Nature Chemical Biology *11,* 309-315.

Rising, A., Hjalm, G., Engstrom, W., and Johansson, J. (2006). N-terminal nonrepetitive domain common to dragline, flagelliform, and cylindriform spider silk proteins. Biomacromolecules *7,* 3120-3124.

Romer, L., and Scheibel, T. (2008). The elaborate structure of spider silk: structure and function of a natural high performance fiber. Prion *2,* 154-161.

Scheibel, T. (2004). Spider silks: recombinant synthesis, assembly, spinning, and engineering of synthetic proteins. Microb. Cell. Fact. *3,* 14, 1-10.

Selo, I., Negroni, L., Creminon, C., Grassi, J., and Wal, J. (1996). Preferential labeling of α-amino N-terminal groups in peptides by biotin: application to the detection of specific anti-peptide antibodies by enzyme immunoassays. J. Immunol. Methods *199,* 127-138.

Sponner, A., Schlott, B., Vollrath, F., Unger, E., Grosse, F., and Weisshart, K. (2005). Characterization of the protein components of *Nephila clavipes* dragline silk. Biochemistry (N. Y.) *44,* 4727-4736.

Sponner, A., Unger, E., Grosse, F., and Weisshart, K. (2004). Conserved C-termini of Spidroins are secreted by the major ampullate glands and retained in the silk thread. Biomacromolecules *5,* 840-845.

Stauffer, S.L., Coguill, S.L., and Lewis, R.V. (1994). Comparison of Physical Properties of Three Silks from *Nephila clavipes* and Araneus gemmoides. J. Arachnol. *22,* 5-11.

Terpe, K. (2003). Overview of tag protein fusions: from molecular and biochemical fundamentals to commercial systems. Appl. Microbiol. Biotechnol. *60,* 523-533.

Tobias, R., and Kumaraswamy, S. (2014). Biomolecular binding kinetic assays on the octet platform. Forte Bio.Appl.Note *14,* 1-21.

Tokareva, O., Michalczechen-Lacerda, V.A., Rech, E.L., and Kaplan, D.L. (2013). Recombinant DNA production of spider silk proteins. Microb. Biotechnol. *6,* 651-663.

Tudyka, T., and Skerra, A. (1997). Glutathione S-transferase can be used as a C-terminal, enzymatically active dimerization module for a recombinant protease inhibitor, and functionally secreted into the periplasm of *Escherichia coli*. Protein Science *6*, 2180-2187.

Vollrath, F., and Knight, D.P. (1999). Structure and function of the silk production pathway in the spider Nephila edulis. Int. J. Biol. Macromol. *24*, 243-249.

Wallace, J.A., and Shen, J.K. (2012). Unraveling A Trap-and-Trigger Mechanism in the pH-Sensitive Self-Assembly of Spider Silk Proteins. J. Phys. Chem. Lett. *3*, 658-662.

Xu, M., and Lewis, R.V. (1990). Structure of a protein superfiber: spider dragline silk. Proc. Natl. Acad. Sci. U. S. A. *87*, 7120-7124.

CHAPTER 4

DIMERIZATION OF MAJOR AMPULLATE SPIDROIN 1 NTDS

I. Abstract

The way in which spiders form silks is an interesting process that has been the focus of much research. However, the mechanisms responsible for dimerization of one of the silks core components, the NTD, is still under investigation. Here we show, using label-free real-time experiments, that *N. clavipes* wild-type MaSp1 NTD displays a 25-fold increase in homodimerization at pH 5.5 than at pH 7.0. We further examine the dimerization affinities of NTD amino acid variants with the wild-type NTD. Variants D45K and E84K showed low binding affinities with wild-type NTD, comparable to wild-type homodimerization at pH 7.0. Virtually no increase in binding affinity with wild-type NTD at pH 5.5 was observed. K70D and the double variant D45K/K70D, however, show binding affinities with wild-type NTD that are intermediate between that of wild-type NTD homodimerization at pH 7.0 and 5.5. This data supports previous work looking at the conformation change experienced by these variants at decreasing pH and further attests to the link between conformational change and homodimerization.

II. Introduction

While spiders can produce up to seven different types of silk, the most-studied is the major ampullate or dragline silk (Rhisiart and Vollrath, 1994; Hinman et al., 2000; Vollrath, 2000). Major ampullate silk is primarily composed of two proteins termed

major ampullate spidroin 1 (MaSp1) and major ampullate spidroin 2 (MaSp2) (Lewis, 2006).

The MaSp proteins that make up the majority of the proteinaceous spider silk fibers exist as a tripartite domain whose three domains are the N-terminal domain (NTD), repeat domain (R) and C-terminal domain (CTD) (Lewis, 2006). The repeat portion of the MaSp proteins consist of imperfect tandem block units of about 20-40 amino acids that can be repeated more than a hundred times within the protein (Ayoub et al., 2007). These repeat units are characterized by poly-alanine, GA, GGX or GPGXX motifs (Gatesy et al., 2001; Keten and Buehler, 2010; Xu and Lewis, 1990). Both MaSp1 and MaSp2 repeat domains contain a poly-alanine region. MaSp1 and MaSp2 differ in that MaSp1 contains predominately GA and GGX motifs and MaSp2 contains a prominent GPGXX motif. The alanine and glycine residues form β-sheet structures (Hayashi et al., 1999; Papadopoulos et al., 2009; Scheibel, 2004). Unlike the repetitive repeat portion of the protein, the NTD and CTD are non-repetitive, highly-conserved, about 150 kDa in size and consist of 5 α-helices each (Motriuk-Smith et al., 2005; Rising et al., 2006; Romer and Scheibel, 2008; Sponner et al., 2005). The CTD is thought to play a role in protein solubility and has been shown to form homodimers through a disulfide bond (Hedhammar et al., 2008; Ittah et al., 2007; Sponner et al., 2005; Sponner et al., 2004). The NTD was the last major component of the MaSp protein to be characterized due to the challenging nature of cloning and sequencing through the imperfect tandem block repeats (Gaines et al., 2010; Romer and Scheibel, 2008). The most interesting characteristic of the NTD, and focus of this research, is the fact that the NTD has been

show to undergo a pH-dependent conformational change that leads to a more stable homodimer (Andersson et al., 2014; Askarieh et al., 2010; Gaines et al., 2010; Hagn, 2012; Jaudzems et al., 2012; Kronqvist et al., 2014; Schwarze et al., 2013; Wallace and Shen, 2012) All three of the MaSp core components help to form the fiber and give it exceptional mechanical properties, (*i.e.*, great strength and toughness), making it an ideal candidate for use in medical and industrial applications (Gosline et al., 1999; Heidebrecht and Scheibel, 2013; Heim et al., 2009).

Fiber formation starts with the production of spidroin proteins in the gland of the spider where the MaSp proteins are stored at 30-50% w/v concentrations (Chen et al., 2002; Hijirida et al., 1996; Vollrath and Knight, 1999). As the spider needs silk, it pulls on a thread located at the spinneret on its lower abdomen (Humenik et al., 2011; Lewis, 2006). This causes the protein in the gland to be pulled down a narrowing S-shaped duct (Andersson et al., 2013; Knight and Vollrath, 1999; Vollrath and Knight, 1999). Along the duct, the protein is subjected to physical and chemical changes including shear forces, changes in ion concentrations and a drop in pH (Andersson et al., 2014; Breslauer et al., 2009; Knight, 2001). As mentioned previously, the repeats form β-sheets and hydrogen bond with their neighbors and the CTDs form homodimers through disulfide bonds (Hayashi et al., 1999; Papadopoulos et al., 2009; Scheibel, 2004; Hedhammar et al., 2008; Ittah et al., 2007; Sponner et al., 2005; Sponner et al., 2004). The NTD forms stable homodimers at acidic pH thought to be important not only in fiber self-assembly through the formation of long, multimeric strands, but also through inhibition of protein aggregation (Andersson et al., 2014; Askarieh et al., 2010; Hagn et al., 2011; Jaudzems et

al., 2012; Kronqvist et al., 2014; Kurut et al., 2015; Ries et al., 2014; Schwarze et al., 2013; Wallace and Shen, 2012; Xu et al., 2015).

Since the discovery and characterization of the NTD, researchers have looked into the mechanism by which the NTD undergoes this conformational change and dimerization (Andersson et al., 2014; Askarieh et al., 2010; Hagn et al., 2011; Jaudzems et al., 2012; Kronqvist et al., 2014; Kurut et al., 2015; Ries et al., 2014; Schwarze et al., 2013; Wallace and Shen, 2012; Xu et al., 2015). Through tryptophan fluorescence, the NTD was observed to undergo a conformational change at low pH, around 6 to 6.5 (Andersson et al., 2014; Gaines et al., 2010; Jaudzems et al., 2012). Research has also been done using fluorescence, dynamic light scattering, circular dichroism, nuclear magnetic resonance spectroscopy and computer modeling to look at the mechanism behind the conformation change and the rate of NTD-NTD homodimerization (Andersson et al., 2014; Askarieh et al., 2010; Gronau et al., 2013; Hagn, 2012; Jaudzems et al., 2012; Kurut et al., 2015; Ries et al., 2014; Schwarze et al., 2013; Wallace and Shen, 2012; Xu et al., 2015). This research supports the idea of a pH-dependent dimerization event that occurs quickly, with structural/conformational changes that occur on the nano to microsecond scale and that these structural changes are necessary for stable dimer formation. (Ries et al., 2014; Schwarze et al., 2013; Wallace and Shen, 2012).

In this study, we use bio-layer interferometry, via the Octet RED96 system, as a label-free way to look at the dimerization of the NTD in real time. Specifically, we observed the rate of dimerization for wild-type MaSp1 NTD, single variants D45K,

E84K, K70D and double variant D45K/K70D that have been previously analyzed by tryptophan fluorescence. The variants chosen showed strong deviation from wild-type NTD using tryptophan fluorescence and thus were good candidates to observe the effect the NTD conformational change has on homodimerization of the NTD.

III. Material and Methods

1. Wild-Type NTD and Variant Protein Purification

Wild-type NTD and NTD variants D45K, K70D, E84K, and D45K/K70D were cloned and purified as described in Chapter 3. Wild-type NTD containing a His_6 tag was purified and biotinylated as described in Chapter 2.

2. Octet Experiments

Experiments were performed using the Octet RED96 instrument and associated Data Acquisition software version 7.1 (FortéBio). Experiments used 96 well black bottom plates (Greiner Bio-One catalog number 655209) and streptavidin biosensors (FortéBio catalog number 18-5019).

Biosensors were equilibrated in Octet buffer (10 mM HEPES, 10 mM MES, 100 mM NaCl, 2% BSA and 0.02% Tween 20) at either pH 5.5 or 7.0 for at least 10 minutes preceding each experiment. Plate wells were loaded with 200 µL of the appropriate Octet buffer. After equilibration, biosensors were loaded with ligand by immersion for 10 minutes in Octet buffer (pH 7.0) containing 50 nM NTD-His_6, Next, the loaded biosensors were moved into Octet buffer (pH 7.0) containing free biotin (Thermo Scientific 21455) (5 µM) to block remaining streptavidin, washed twice for 5 minutes each in Octet buffer of either pH 7.0 or 5.5, depending on the experiment, and pH was

held constant for all subsequent steps of any given experiment. After acquisition of a 3 minutes baseline reading, the biosensors were moved to the association step for 50 seconds. Association was done in Octet buffer containing wild-type or variant NTD (D45K, K70D, E84K or D45K/K70D) as the analyte. Analyte concentrations were 75 μM, 30 μM, 15 μM, 7.5 μM, 2.75 μM, 1.88 μM, and 0.94 μM. A biosensor with loaded NTD-His_6 only was used as a reference sensor. Sensors were subsequently moved to Octet buffer with no analyte and allowed to dissociate for 2.5 minutes.

Data from experiments was processed by subtracting reference sensor, aligning to the Y-axis value at the baseline step and using Inter-step correction. Data was then processed using Savitzky-Golay filtering and analyzed with a local full fitting 1:1 model (assumes that dissociation would eventually reach 0). Dissociation time values were truncated to 50 seconds and a visual inspection was done on all traces. By visual inspection, traces with excessive noise or low R^2 values were curated. NTD concentrations (3 to 4) that showed a K_d grouping were then analyzed by global full fit.

IV. Results

N. clavipes wild-type MaSp1 NTD and variants were purified and analyzed using the Octet RED96 system to determine rate of association (k_{on}), rate of dissociation (k_{dis}), and the affinity constant (K_d) (Table 4.1). Because of the pH-dependence of dimerization described earlier, these experiments were performed at pH 5.5 and 7.0.

Wild-type NTD showed a 25-fold increase in K_d from pH 5.5 to 7.0 resulting in a more stable homodimer at pH 5.5 (Table 4.1). This is denoted by a change in K_d of 36.80 ± 2.92 μM at pH 7.0 to 1.45 ± 0.09 μM at pH 5.5. The k_{on} also showed a significant

difference from pH 5.5 to 7.0 with values of 2.07 x 10^4 ± 1.26 x 10^3 $M^{-1}s^{-1}$ for pH 5.5 and 1.03 x 10^3 ± 7.68 x 10^1 $M^{-1}s^{-1}$. However, the k_{dis} remained about the same for both pHs. Traces for wild-type NTD show a maximum binding around 2 nm for pH 5.5 and 0.75 for pH 7.0 (Fig. 4.2A).

Kinetic Analysis of Wild-type NTD and Variants								
NTD	**pH**	**K_d (μM)**	**K_d Error (μM)**	**k_{on} (1/Ms)**	**k_{on} Error**	**k_{dis} (1/s)**	**k_{dis} Error**	**R2**
Wild-type	7.0	36.80	2.92	1.03E+03	7.68E+01	2.78E-02	9.95E-04	0.92
	5.5	1.45	0.09	2.07E+04	1.26E+03	3.01E-02	6.96E-04	0.94
D45K	7.0	44.83	4.74	7.29E+02	7.20E+01	2.27E-02	1.24E-03	0.86
	5.5	45.79	7.12	2.41E+03	2.55E+02	1.10E-01	5.56E-03	0.92
K70D	7.0	30.92	2.15	8.82E+02	5.68E+01	2.73E-02	7.09E-04	0.93
	5.5	11.38	1.02	4.18E+03	2.58E+02	4.76E-02	1.31E-03	0.90
E84K	7.0	34.38	2.65	6.75E+02	4.74E+01	2.32E-02	7.38E-04	0.88
	5.5	39.90	5.48	2.24E+03	4.25E+02	1.29E-01	5.22E-03	0.95
D45K/K70D	7.0	32.13	2.65	1.03E+03	1.10E+02	2.32E-02	1.29E-03	0.85
	5.5	22.77	2.68	2.14E+03	2.31E+02	5.09E-02	1.69E-03	0.90

Table 4.1 Kinetic analysis of *N. clavipes* wild-type NTD and variants D45K, K70D, E84K and D45K/K70D at pH 5.5 and 7.0.

Variants D45K, K70D, E84K, and D45K/K70D were similarly evaluated for their ability to associate with wild-type MaSp1-NTD. D45K showed the largest K_d values of 44.83 ± 4.74 μM and 45.79 ± 7.12 μM for pH 7.0 and 5.5, respectively (Table 4.1). These values show a very low binding affinity and are not statistically different from one another or, to that of wild-type at pH 7.0 based on unpaired t-test (Fig. 4.1). Even though the K_d values for both pH 5.5 and 7.0 were almost the same, the k_{on} and k_{dis} rates show an almost one and a half-fold increase in k_{on} for wild-type NTD at pH 7.0 compared to

D45K and an eight and a half-fold increase at pH 5.5 (Table 4.1). For wild-type NTD and D45K the k_{dis} at pH 7.0 are almost the same, however, at pH 5.5 the D45K has about three and a half-fold increase in k_{dis} compared to wild-type. The maximum binding seen for D45K is also only about half that of wild-type, at the same concentration (compare y-axis values in Fig. 4.2). D45K also shows a faster drop in trace signal when placed in protein-free buffer during the dissociation (Fig 4.2 B). This is numerically noted by the k_{dis} value that is over three times higher for D45K at pH 5.5 than that of wild-type (Table 4.1).

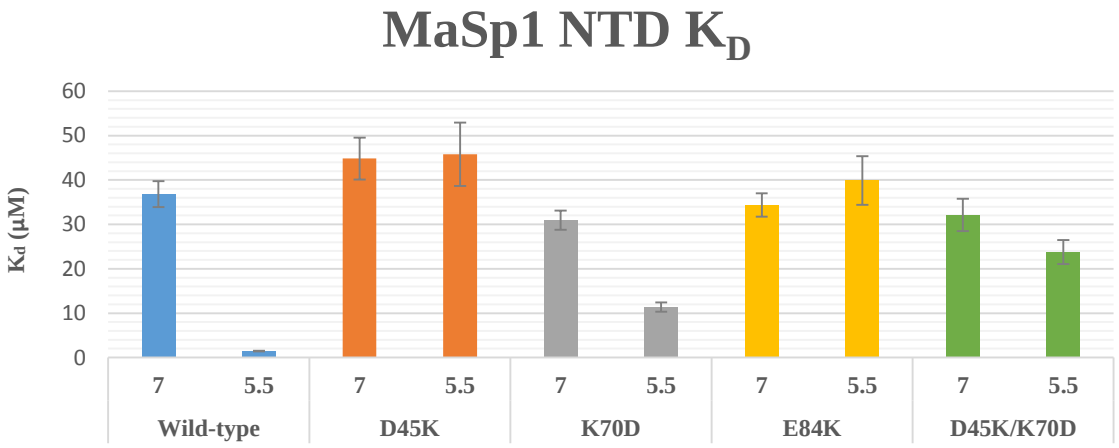

Figure 4.1 Bar graph of K_d values for MaSp1A NTD wild-type, D45K, K70D, E84K and D45K/K70D at pH 7 and 5.5.

The K_d values for E84K also show a very low binding affinity with 34.38 ± 2.65 μM for pH 7.0 and 39.90 ± 5.48 μM for pH 5.5 (Table 4.1). Both these K_d values are indicative of the homodimerization seen for wild-type NTD at pH 7.0 (Fig. 4.1). E84K, has a similar k_{on} to that of D45K at pH 7.0 which is an one and a half-fold less than wild-

type NTD at pH 7.0 and had an almost six and a half-fold decrease at pH 5.5 compared to wild-type NTD (Table 4.1). Wild-type NTD and E84K show similar k_{dis} values at pH 7.0, however, there is an about four-fold increase in k_{dis} for E84K at pH 5.5. E84K and D45K both show a faster dissociation compared to wild-type although maximum binding is higher for E84K than D45K (Fig. 4.2D).

The K_d for variant K70D at pH 7.0 is not statistically different than the K_d for wild-type at the same pH. However, the K_d of 11.38 ± 1.02 μM seen at pH 5.5 is statistically different than both wild-type K_d at 5.5 and 7.0, based on unpaired t-test (Table 4.1). This K_d of 11.38 ± 1.02 μM lies between the two K_ds seen for wild-type and is the lowest K_d, other than wild-type at pH 5.5 (Fig.4.1). K70D has a k_{on} and k_{dis} similar to wild-type at pH 7.0 and 5.5 except for the about five-fold decrease in k_{on} at pH 5.5 (Table 4.1). K70D also shows a high maximum binding, similar to that of wild-type of the same pH, and a more gradual dissociation, which more indicative of wild-type than that of D45K or E84K (Fig. 4.2C).

The double variant D45K/K70D shows a similar K_d value of 32.13 ± 2.65μM, at pH 7.0, to that of wild-type at the same pH (Table 4.1). The K_d value of 22.77 ± 2.68 μM for D45K/K70D at pH 5.5 lies between the wild-type K_d values and is significantly different from both wild-type at pH 7.0 and 5.5. It is also significantly different from the K_d of 11.38 ± 1.02 μM for the K70D variant. This indicates that the double variant has a binding affinity, at pH 5.5, that is between the binding affinities seen for wild-type. This binding affinity is also distinct from the other intermediate binding K_d of the K70D variant (Fig. 4.1). D45K/K70D has k_{on} and k_{dis} similar to wild-type at pH 7.0. At pH 5.5

k_{on} is about nine and a half-fold larger for wild-type and a little more than one and a half-fold smaller for k_{dis}. The maximum binding seen for D45K/K70D is also the lowest of all variants with a maximum binding around 0.06 nm (Fig. 4.2E).

All variants with the exception of K70D and D45K/K70D at pH 5.5, show a binding affinity constant that is not statistically different from wild-type at pH 7.0 (Fig. 4.1). There were, however, differences in the rate of association and dissociation showing that the different variants have different binding profiles even though there K_ds are not statistically different.

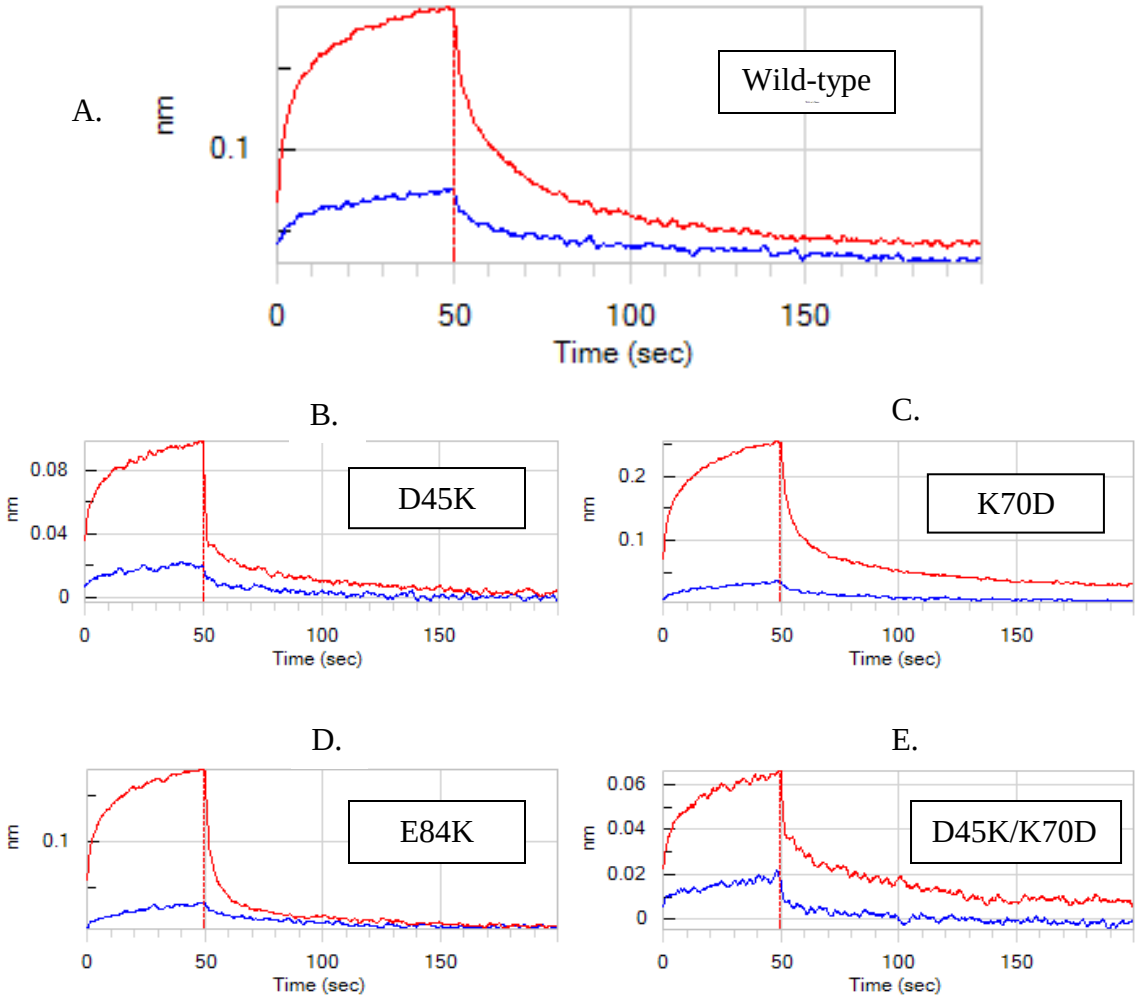

Figure 4.2 Representative graphs showing association (0-50 sec.) and dissociation (50-200sec) of D45K, K70D, E84K and D45K/K70D for 75 µM. Traces shown at pH 7.0 (Blue) and 5.5 (RED). Not all graphs have same Y axis scales and graphs are before time truncation used in analysis.

V. Discussion

Many labs have shown that the wild-type MaSp1 NTD undergoes a conformational change from neutral to acidic pH through tryptophan fluorescence (Askarieh et al., 2010; Gaines et al., 2010; Jaudzems et al., 2012; Kronqvist et al., 2014). This conformational change was shown to be a global change, not localized to micro-

environment around the tryptophan residue, and that this global change is important for homodimer formation (Andersson et al., 2014; Askarieh et al., 2010; Gronau et al., 2013; Hagn, 2012; Jaudzems et al., 2012; Kurut et al., 2015; Parnham et al., 2011; Ries et al., 2014; Schwarze et al., 2013; Wallace and Shen, 2012; Xu et al., 2015). However, previous research has primarily relied on snapshots of NTD, as the protein was only be analyzed at a particular point and time. One study, using intrinsically labeled NTD, however, found that for *E. australis* NTD both D39N and D40N variants abolished dimerization at pH 6.0 (Schwarze et al., 2013), Additionally, while the NTDs are highly conserved, most research was done using the distantly related *Euprosthenops autralis* instead of *Nephila clavipes,* which is used in our research (Gaines and Marcotte, 2008; Garb et al., 2010; Motriuk-Smith et al., 2005; Rising et al., 2006). Based on this knowledge, we believed that having K_d values, of variant NTDs, using label free methods, would give even more insight into the dimerization process.

The four variants chosen were based on their tryptophan fluorescence, which shows a strong deviation from wild-type and other research using tryptophan fluorescence, mass spectrometry, and computational experiments which support for their involvement in NTD homodimerization (Chapter 3) (Kronqvist et al., 2014; Landreh et al., 2010; Schwarze et al., 2013; Wallace and Shen, 2012). The two conformations assumed by the wild-type NTD are termed Conformation I and Conformation II. Conformation I is noted by the tryptophan residue of the NTD being buried within the protein and occurs from pH 7.5 to pH 6.5 for the wild-type MaSp1 NTD from *N. clavipes.* Conformation II is where the protein conformation has changed such that the

tryptophan residue is now solvent-exposed and occurs at pH 6.0 and 5.5 for the wild-type MaSp1 NTD from *N. clavipes*. The homodimerization is stabilized by salt-bridges that form between the negatively and positively charged poles of the NTD (Askarieh et al., 2010; Kronqvist et al., 2014; Rising and Johansson, 2015; Wallace and Shen, 2012). One explanation of the mechanism behind the formation of the NTD homodimer is the formation of a "trap" which favors the dimer state, but is unable to complete the dimerization until certain residues "trigger" its formation (Wallace and Shen, 2012). The residues that make up the positive and negative poles of the NTD are believed to be integral in this "trap and trigger" mechanism (Wallace and Shen, 2012).

There are three exposed residues that are thought to contribute to the positive pole of the NTD, which are H6, R60 and K65 for *E. australis* MaSp1 (Askarieh et al., 2010). However, many other species, including *Nephila clavipes* MaSp1 NTD, do not contain a histidine at residue 6 and contain a lysine instead of an arginine at residue 65 (Askarieh et al., 2010). For *N. clavipes* this would correlate to only two residues K65 and K70 for the positive pole. Conversely there are eight residues thought to be responsible for the negative pole in *E. australis.* Five of these amino acids are exposed, which are D39, D40, E84, E85 and D134. These would equate to D44, D45, E89, and D139, in *N. clavipes*, as there is no E85 equivalent in *N. clavipes.* There are also two residues that, while not exposed, are near the other important negative residues and might be important to dimer formation. For *N. clavipes*, these would be E84 and E124 (Askarieh et al., 2010). From these poles, salt bridges are believed to form, in *E. australis*, between D40-K65 and D39-R60 (Askarieh et al., 2010; Gronau et al., 2013; Kronqvist et al., 2014; Schwarze et al.,

2013). This would translate to D45-K70 and D44-K65 for *N. clavipes*. Thus the variants chosen, D45K, K70D, E84K and D45K/K70D, can help to further clarify the D45-K70 salt bridge formation and dimer significance, as well as help determine if unexposed residues can influence dimer formation.

Data obtained using bio-layer interferometry showed that K_d values ranged from 45.79 ± 7.12 μM to 1.45 ± 0.09 μM with all R^2 values between 0.95 and 0.85. Lower R^2 values were typically seen at higher pH. From other research, D45 has been shown to be integral for formation of the NTD dimer (Askarieh et al., 2010; Jaudzems et al., 2012; Kronqvist et al., 2014; Landreh et al., 2010; Schwarze et al., 2013; Wallace and Shen, 2012). K_d values determined from our kinetics experiments support the importance of D45 as a necessary residue in NTD dimer formation (Table 4.1). Data determined from these experiments shows that the affinity constant for D45K to wild-type NTD at both pH 7.0 and 5.5, at 44.83 ± 4.74 μM and 45.79 ± 7.12 μM respectively, which is similar to that of the wild-type homodimer at pH 7.0 of 36.80 ± 2.92 μM. This is indicative of the NTD being in a more monomeric state and is supported by tryptophan fluorescence data showing no change of D45K into Conformation II, which is believe to be necessary for dimer formation (Chapter 3) ((Gaines et al., 2010). The binding profile also shows a decrease in dimerization, with a fast dissociation (Fig 4.2). The small binding observed could be due to a D44-K65 salt bridge or binding of D45 on the wild-type NTD to the K70 on the D45K variant (Gronau et al., 2013).

D45 is thought to partner with K70 in NTD-NTD salt bridge formation and, like D45, the K70 residue has been shown through other research to be important in dimer

formation (Kronqvist et al., 2014; Landreh et al., 2010; Schwarze et al., 2013; Wallace and Shen, 2012). Based on these studies, K70 stabilizes the monomer, but does not have the same drastic effect on dimer formation as D45 (Kronqvist et al., 2014; Landreh et al., 2010; Schwarze et al., 2013; Wallace and Shen, 2012). Our experiments show that at pH 7.0 the K_d value of variant K70D is analogous to that of wild-type, however, at pH 5.5 the K_d value lies between that of wild-type at 7.0 and 5.5 (Table 4.1). This correlates with what is seen using tryptophan fluorescence ratio data at higher pH, where the K70D variant exhibits Conformation I but at pH 5.5 it shifts into a conformation intermediate to Conformation I and II (Chapter 3 Fig 2.7). K70D at pH 5.5 also shows a binding pattern that is similar to that of wild-type, with a higher maximum binding and more gradual dissociation that differs from D45K and E84K (Figure 4.2).

While E84K was not shown to be an exposed residue, it could still play a part in the overall negative charge of the pole. Other research has shown no change from wild-type, in an E84Q variant (Kronqvist et al., 2014; Landreh et al., 2010; Schwarze et al., 2013). However, based on tryptophan fluorescence and kinetics data, when residue E84 is change to a lysine residue, the change into Conformation II and stable dimerization is prevented (Chapter 3 Fig. 2.5E, Table 4.1). This kinetics data shows K_d values for E84K similar to those of D45K and wild-type at pH 7.0. This is supported by research showing that protonation of the E84 residue is needed for dimer stabilization (Wallace and Shen, 2012). The quick dissociation seen is also similar to that seen in D45K (Fig. 4.2). The binding and dissociation seen at pH 5.5 in some variants could be caused by slight dimerization with wild-type NTD due to its Conformation II arrangement at pH 5.5.

Subsequently, the wild-type NTD is bound but failed to stabilize the dimer, thus when the biosensors are placed in protein free buffer the variant quickly dissociates. This relates to the trap and trigger mechanism that was mentioned earlier (Wallace and Shen, 2012). This would also indicate that for stable homodimerization to occur, like that of wild-type NTD with wild-type NTD at pH 5.5, both proteins have to be in a Conformation II arrangement.

By observing the double variant, we can look at the combined effect of both D45K and K70D. This double variant provides new information involving salt-bridge formation and dimerization. D45K/K70D, at pH 7.0, shows affinity constants similar to those of wild-type and other single variants at pH 7.0 (Table 4.1). However, at pH 5.5 the K_d drops to 22.77 ± 2.68 μM, which is statistically different from all the other K_d values and exists in-between the two K_d values for wild-type. This is correlated with the fact that the tryptophan fluorescence ratios for D45K/K70D show an intermediate conformation between I and II (Chapter 3 Fig. 2.7). This could indicate that at pH 7 the dimer is unable to stabilize as the wild-type NTD is in Conformation I and D45K/K70D is in an intermediate conformation, resulting in a K_d similar to that of wild-type at pH 7.0. When wild-type is in Conformation II, at pH 5.5, the dimerization between wild-type NTD and D45K/K70D is able to become more stable than the wild-type homodimer at pH 5.5. It is also worth noting that the maximum binding of D45K/K70D is the lowest of all the variants which could be due to the complete disruption of the D45K-K70D salt bridges (Fig. 4.2).

Based on the kinetic data, a strong correlation between conformational change and dimerization of the NTDs was observed. We also show the first instance of the use of label-free, real time kinetics to measure the K_d for NTD variants. From our data, we see different binding patterns among the wild-type NTD and variants, even when the K_d values remain similar. The homodimer can exist in between the two extremes seen from wild-type at pH 5.5 and 7.0.

To further our understanding, other residues need to be analyzed to get a more complete idea of dimerization and the residues responsible. Many labs have analyzed other residues in the *E. australis* NTD including, E89, D44, D139 and K65. These would be good residues to examine next in *N. clavipes* (Askarieh et al., 2010; Jaudzems et al., 2012; Kronqvist et al., 2014; Landreh et al., 2010; Schwarze et al., 2013; Wallace and Shen, 2012).

VI. References

Andersson, M., Chen, G., Otikovs, M., Landreh, M., Nordling, K., Kronqvist, N., Westermark, P., Jornvall, H., Knight, S., Ridderstrale, Y., *et al.* (2014). Carbonic Anhydrase Generates CO2 and H+ That Drive Spider Silk Formation Via Opposite Effects on the Terminal Domains. PLoS Biol. *12*, e1001921.

Andersson, M., Holm, L., Ridderstrale, Y., Johansson, J., and Rising, A. (2013). Morphology and composition of the spider major ampullate gland and dragline silk. Biomacromolecules *14*, 2945-2952.

Askarieh, G., Hedhammar, M., Nordling, K., Saenz, A., Casals, C., Rising, A., Johansson, J., and Knight, S.D. (2010). Self-assembly of spider silk proteins is controlled by a pH-sensitive relay. Nature *465*, 236-238.

Ayoub, N.A., Garb, J.E., Tinghitella, R.M., Collin, M.A., and Hayashi, C.Y. (2007). Blueprint for a high-performance biomaterial: full-length spider dragline silk genes. PLoS One *2*, e514.

Breslauer, D.N., Lee, L.P., and Muller, S.J. (2009). Simulation of flow in the silk gland. Biomacromolecules *10*, 49-57.

Chen, X., Knight, D.P., and Vollrath, F. (2002). Rheological characterization of nephila spidroin solution. Biomacromolecules *3*, 644-648.

Gaines, W.A.,4th, and Marcotte, Jr., W.R. (2008). Identification and characterization of multiple Spidroin 1 genes encoding major ampullate silk proteins in *Nephila clavipes*. Insect Mol. Biol. *17*, 465-474.

Gaines, W.A., Sehorn, M.G., and Marcotte, Jr., W.R. (2010). Spidroin N-terminal domain promotes a pH-dependent association of silk proteins during self-assembly. J. Biol. Chem. *285*, 40745-40753.

Garb, J.E., Ayoub, N.A., and Hayashi, C.Y. (2010). Untangling spider silk evolution with spidroin terminal domains. BMC Evol. Biol. *10*, *243*, 1-16.

Gatesy, J., Hayashi, C., Motriuk, D., Woods, J., and Lewis, R. (2001). Extreme diversity, conservation, and convergence of spider silk fibroin sequences. Science *291*, 2603-2605.

Gosline, J.M., Guerette, P.A., Ortlepp, C.S., and Savage, K.N. (1999). The mechanical design of spider silks: from fibroin sequence to mechanical function. J. Exp. Biol. *202*, 3295-3303.

Gronau, G., Qin, Z., and Buehler, M.J. (2013). Effect of sodium chloride on the structure and stability of spider silk's N-terminal protein domain. Biomater. Sci. *1,* 276-284.

Hagn, F. (2012). A structural view on spider silk proteins and their role in fiber assembly. J. Pept. Sci. *18,* 357-365.

Hagn, F., Thamm, C., Scheibel, T., and Kessler, H. (2011). pH-dependent dimerization and salt-dependent stabilization of the N-terminal domain of spider dragline silk--implications for fiber formation. Angew. Chem. Int. Ed Engl. *50,* 310-313.

Hayashi, C.Y., Shipley, N.H., and Lewis, R.V. (1999). Hypotheses that correlate the sequence, structure, and mechanical properties of spider silk proteins. Int. J. Biol. Macromol. *24,* 271-275.

Hedhammar, M., Rising, A., Grip, S., Martinez, A.S., Nordling, K., Casals, C., Stark, M., and Johansson, J. (2008). Structural properties of recombinant nonrepetitive and repetitive parts of major ampullate spidroin 1 from *Euprosthenops australis*: implications for fiber formation. Biochemistry *47,* 3407-3417.

Heidebrecht, A., and Scheibel, T. (2013). Recombinant production of spider silk proteins. Adv. Appl. Microbiol. *82,* 115-153.

Heim, M., Keerl, D., and Scheibel, T. (2009). Spider silk: from soluble protein to extraordinary fiber. Angewandte Chemie International Edition *48,* 3584-3596.

Hijirida, D.H., Do, K.G., Michal, C., Wong, S., Zax, D., and Jelinski, L.W. (1996). 13C NMR of *Nephila clavipes* major ampullate silk gland. Biophys. J. *71,* 3442-3447.

Hinman, M.B., Jones, J.A., and Lewis, R.V. (2000). Synthetic spider silk: a modular fiber. Trends Biotechnol. *18,* 374-379.

Humenik, M., Scheibel, T., and Smith, A. (2011). Spider silk understanding the structure-function relationship of a natural fiber. Prog. Mol. Biol. Transl. Sci. *103,* 131-185.

Ittah, S., Michaeli, A., Goldblum, A., and Gat, U. (2007). A model for the structure of the C-terminal domain of dragline spider silk and the role of its conserved cysteine. Biomacromolecules *8,* 2768-2773.

Jaudzems, K., Askarieh, G., Landreh, M., Nordling, K., Jörnvall, H., Rising, A., Knight, S.D., and Johansson, J. (2012). pH-Dependent Dimerization of Spider Silk N-Terminal Domain Requires Relocation of a Wedged Tryptophan Side Chain. J. Mol. Biol. *422,* 477-487.

Keten, S., and Buehler, M.J. (2010). Nanostructure and molecular mechanics of spider dragline silk protein assemblies. J. R. Soc. Interface *7,* 1709-1721.

Knight, D., and Vollrath, F. (1999). Liquid crystals and flow elongation in a spider's silk production line. Proceedings of the Royal Society of London.Series B: Biological Sciences *266,* 519-523.

Knight, D.D.P. (2001). Changes in element composition along the spinning duct in a Nephila spider. Naturwissenschaften *88,* 179-182.

Kronqvist, N., Otikovs, M., Chmyrov, V., Chen, G., Andersson, M., Nordling, K., Landreh, M., Sarr, M., Jornvall, H., Wennmalm, S., *et al.* (2014). Sequential pH-driven dimerization and stabilization of the N-terminal domain enables rapid spider silk formation. Nat. Commun. *5,* 3254, 1-11.

Kurut, A., Dicko, C., and Lund, M. (2015). Dimerization of Terminal Domains in Spiders Silk Proteins Is Controlled by Electrostatic Anisotropy and Modulated by Hydrophobic Patches. ACS Biomat. Sci. Eng. 1(6), 363-371

Landreh, M., Askarieh, G., Nordling, K., Hedhammar, M., Rising, A., Casals, C., Astorga-Wells, J., Alvelius, G., Knight, S.D., Johansson, J., Jornvall, H., and Bergman, T. (2010). A pH-dependent dimer lock in spider silk protein. J. Mol. Biol. *404,* 328-336.

Lewis, R.V. (2006). Spider silk: ancient ideas for new biomaterials. Chem. Rev. *106,* 3762-3774.

Motriuk-Smith, D., Smith, A., Hayashi, C.Y., and Lewis, R.V. (2005). Analysis of the conserved N-terminal domains in major ampullate spider silk proteins. Biomacromolecules *6,* 3152-3159.

Papadopoulos, P., Sölter, J., and Kremer, F. (2009). Hierarchies in the structural organization of spider silk—a quantitative model. Colloid Polym. Sci. *287,* 231-236.

Parnham, S., Gaines, W.A., Duggan, B.M., Marcotte Jr, W.R., and Hennig, M. (2011). NMR assignments of the N-terminal domain of *Nephila clavipes* spidroin 1. Biomolecular NMR Assignments *5,* 131-133.

Rhisiart, A., and Vollrath, F. (1994). Design features of the orb web of the spider, *Araneus diadematus*. Behav. Ecol. *5,* 280-287.

Ries, J., Schwarze, S., Johnson, C.M., and Neuweiler, H. (2014). Microsecond folding and domain motions of a spider silk protein structural switch. J. Am. Chem. Soc. *136,* 17136-17144.

Rising, A., and Johansson, J. (2015). Toward spinning artificial spider silk. Nature Chemical Biology *11*, 309-315.

Rising, A., Hjalm, G., Engstrom, W., and Johansson, J. (2006). N-terminal nonrepetitive domain common to dragline, flagelliform, and cylindriform spider silk proteins. Biomacromolecules *7*, 3120-3124.

Romer, L., and Scheibel, T. (2008). The elaborate structure of spider silk: structure and function of a natural high performance fiber. Prion *2*, 154-161.

Scheibel, T. (2004). Spider silks: recombinant synthesis, assembly, spinning, and engineering of synthetic proteins. Microb. Cell. Fact. *3*, 14, 1-10.

Schwarze, S., Zwettler, F.U., Johnson, C.M., and Neuweiler, H. (2013). The N-terminal domains of spider silk proteins assemble ultrafast and protected from charge screening. Nat. Commun. 4,2815,1-7

Sponner, A., Vater, W., Rommerskirch, W., Vollrath, F., Unger, E., Grosse, F., and Weisshart, K. (2005). The conserved C-termini contribute to the properties of spider silk fibroins. Biochem. Biophys. Res. Commun. *338*, 897-902.

Sponner, A., Unger, E., Grosse, F., and Weisshart, K. (2004). Conserved C-termini of Spidroins are secreted by the major ampullate glands and retained in the silk thread. Biomacromolecules *5*, 840-845.

Vollrath, F. (2000). Strength and structure of spiders' silks. Reviews in Molecular Biotechnology *74*, 67-83.

Vollrath, F., and Knight, D.P. (1999). Structure and function of the silk production pathway in the spider *Nephila edulis*. Int. J. Biol. Macromol. *24*, 243-249.

Wallace, J.A., and Shen, J.K. (2012). Unraveling A Trap-and-Trigger Mechanism in the pH-Sensitive Self-Assembly of Spider Silk Proteins. J. Phys. Chem. Lett. *3*, 658-662.

Xu, D., Guo, C., and Holland, G.P. (2015). Probing the Impact of Acidification on Spider Silk Assembly Kinetics. Biomacromolecules *16*, 2072-2079.

Xu, M., and Lewis, R.V. (1990). Structure of a protein superfiber: spider dragline silk. Proc. Natl. Acad. Sci. U. S. A. *87*, 7120-7124.

CHAPTER 5
PRODUCTION OF "MINI-SPIDROINS" IN *Saccharomyces cerevisiae*

I. Abstract

Many different organisms have been used to produce recombinant spider silk-like proteins. The ability to use host organisms such as *E. coli* and *Nicotiana tabacum* allows for easy, cheap, and scalable production of proteins that have a myriad of uses. Here we show the first instance of recombinant protein production of spider silk-like proteins termed "mini-spidroins" in *Saccharomyces cerevisiae*. "Mini-spidroins" were produced using glucose, raffinose and glycerol growth media with galactose induction. Aliquots were taken, at various time points, to determine ideal induction time and ideal growth media. Although, these experiments were preliminary, we show that induction times of 24 hrs and 72 hrs have higher protein production, vs. other induction times, in glucose and raffinose media, respectively. While expression was seen at onset of induction, with further refinement, *S. cerevisiae* could be another expression system useful for recombinant spider silk-like protein production.

II. Introduction

Arthropods and silkworms are known for producing silk proteins. The spider has the ability to produce up to seven different types of silk, compared to the one produced by silkworms (Lewis, 2006). Spider silks are used for a variety of purposes including textiles, wound dressings to stop bleeding, and fishing nets (Craig, 1997; Forrest, 1982; Lewis, 1996; Sutherland et al., 2010). More recently, spider silks have expanded utility

including use in optics, cell scaffolding, and adhesives, among others (Omenetto and Kaplan, 2010). This great range of possible applications is partially due to the unique properties of the many different types of spider silks available, each with its own unique properties. For example, flagelliform silk, that is used in the capture spiral of the web, is very extensible and major ampullate silk, that is used for the radials of the web, as well as a lifeline for the spider, is extremely tough (Heidebrecht and Scheibel, 2013; Humenik et al., 2011). Major ampullate silk is composed primarily of two proteins, major ampullate spidroin 1(MaSp1) and major ampullate spidroin 2 (MaSp2).

Due to the cannibalistic nature of spiders, farming is not practical (Kluge et al., 2008; Lewis, 1996). As a result, many research labs have turned to expression of recombinant spider silk-like proteins in different organisms including, *Escherichia coli*, *Pichia pastoris, Bombyx mori* and *Nicotiana tabacum* (Barr et al., 2004; Hedhammar et al., 2008; Huemmerich et al., 2004; Peng et al., 2016; Teulé et al., 2003). An added benefit to making recombinant proteins rather than obtaining them directly from the spider is the ability to modify the protein sequence (Omenetto and Kaplan, 2010; Scheibel, 2004). Modification of the native spider silk protein sequence has the potential to result in novel materials that may be adapted for specific purposes (e.g. medical or industrial fields). In addition, the ability to process recombinant proteins into different forms, including films, gels, and sponges, provides wider application of use than the native fiber form (Kluge et al., 2008; Omenetto and Kaplan, 2010). One such example is the creation of nanoparticles to use as carriers in drug delivery (Lammel et al., 2011; Numata and Kaplan, 2010).

The core components of MaSp proteins are the N-terminal domain (NTD), repeats domain (R), and the C-terminal domain (CTD). The NTD and CTD are non-repetitive domains of about 150 amino acid and both are composed of 5 α-helices (Jaudzems et al., 2012; Huemmerich et al., 2004; Askarieh,G. 2010). The CTDs form homodimers through a disulfide bond, with a tail-to-tail configuration that is thought to be the storage form of spidroins in the lumen of the silk glands (Askarieh et al., 2010; Hedhammar et al., 2008; Ittah et al., 2007; Knight et al., 2000; Lefevre et al., 2008; Sponner et al., 2004).

When the spider needs silk it pulls on the spinneret, located on its lower abdomen and the protein solution in the silk gland is drawn down an S-shaped duct (Hu et al., 2006; Humenik et al., 2011; Knight and Vollrath, 1999). The environment that the protein is exposed to along the duct has a change in ion concentrations, shear forces and most notably a drop in pH (Andersson et al., 2014; Breslauer et al., 2009; Eisoldt et al., 2010; Knight, 2001; Leclerc et al., 2013). The reduction in pH causes the NTD to undergo a conformational change that results in stable homodimerization. NTD homodimers are held together through salt bridges, thus creating "multimeric strands" where both the NTDs and CTDs form homo-dimers (Gaines et al., 2010). The repeats, are the source of the variability in properties of the various types of spider silk. They vary in length and contain poly-alanine motifs (Keten and Buehler, 2010; Xu and Lewis, 1990). The poly-alanine motifs form β-sheets, which form hydrogen bonds with neighboring β-sheets, thus creating beta-crystallites, which facilitate in fiber formation (Hayashi et al., 2004; Papadopoulos et al., 2009; Scheibel, 2004).

Recombinant major ampullate silk-like proteins are often not produced as full length proteins and have one or more of their core components missing (Heidebrecht,A. 2013; Askarieh et al., 2010; Grip et al., 2006; Hedhammar et al., 2008; Sponner et al., 2005; Teule et al., 2009; Xu et al., 2007) and there are many reasons all three full-length core components might not be used in the creation of recombinant spider silk protein. One reason is the large size and repetitive nature of the full-length MaSp proteins (200-350kDa) that complicates molecular cloning and can be difficult for many organisms to produce. Another is the relatively recent discovery of and characterization of the full length NTD (Askarieh et al., 2010; Gaines et al., 2010; Motriuk-Smith et al., 2005)

Truncated versions of recombinant silks are often produced when expressed in *E. coli* (Heidebrecht and Scheibel, 2013). However, *S. cerevisiae*, is better able to process high molecular weight proteins, (Hou et al., 2012; Romanos et al., 1992) which makes it attractive for the production of spider silk proteins. Other characteristics that make *S. cerevisiae* a potentially good choice for recombinant silk production is its low cost, ability to grow at high density, ability to post-translationally modify proteins and the availability of both cytosolic and secretory protein production systems (Hou et al., 2012; Novick et al., 1980). Despite these attractive characteristics, *S. cerevisiae* has never been used to produce spider silk-like proteins that contain all three core components. We chose to use *S. cerevisiae*, to produce recombinant MaSp2-like proteins ("mini-spidroins") that contain native NTD and CTD domains flanking an abbreviated number of block repeat units (eight). Here we show MaSp2 "mini spidroin" proteins expressed in *S. cerevisiae* cells under different culture conditions.

III. Material and Methods

1. "Mini-Spidroins" Protein Purification

a. Cloning

Plasmids containing native MaSp2 NTD and CTD sequences were constructed using DNA isolated from *Nephila clavipes* as previously described (Gaines and Marcotte, 2008; Gaines et al., 2010; Peng et al., 2016). Each part of the "mini spidroin," (NTD, CTD and repeat domain), was amplified separately by PCR using Phusion polymerase (New England Biolabs) and restriction sites were incorporated with each primer for ease of cloning (Table 5.1). A tobacco etch virus (TEV) site was added to the 3' side of the NTD domain through PCR, using primers containing the TEV sequence and six histidines were added after the CTD by PCR. Individual components were confirmed by sequence analysis and incorporated restriction sites were ligated into the MCS of the cloning vector pT7T3α-19 and transformed into DH5α cells. This resulted in a plasmid containing NTD, TEV site, 8 Repeats, CTD and a His_6 tag (N-TEV-R8-C-His_6) schematically shown in (Fig. 5.1). A *Leishmania mexicana* invertase secretion signal (LmexINVSS or ss for short) (Lyda et al., 2015) is present as a result of subsequent cloning steps, upstream of the NTD.

Amino Acid Sequence for MaSp2 Domains in "Mini-Spidroins			
LmexINVSS	**NTD**	**Repeat**	**CTD**
MRRGVILLLVAVAM MAAGALVK	GPLGSPGIPGQNTP WSSTELADAFINAF MNEAGRTGAFTAD QLDDMSTIGDTIKM SAMDKMARSNKSST IKTAMDKMARSNKS SKGKLQALNMAFAS SMAEIAAVEQGGLS VDAKTNALADSLNS AFYQTTGAANPQFV NEIRSLINMFAQSSA NEVSYGG**ENLYFQG**	GPGQQGPGGYGPG QQGPGGYGPGQQG PSGPGSAAAAAAAA	GASAGYGPGSAVAA SAGAGSAGYGPGSQ ASAAASRLASPDSGA RVASAVSNLVSSGPT SSAALSSVISNAVSQI GASNPGLSGCDVLIQ ALLEIVSACVTILSSSS IGQVNYGAASQFAQ VVGQSVLSAF

Table 5.1 Amino acid sequence for MaSp2 domains used to generate "mini-spidroins": NTD, repeat and CTD with TEV site in bold following the NTD sequence. Repeat domain had a total of 8 copies of repeat sequence.

The MaSp2 ss-N-TEV-R8-C-His_6 fragment was cloned into pYES2 using SpeI and NotI restriction sites (Fig. 5.1). To transform pYES2 containing "mini-spidroins" into the INVSc1 strain of *Saccharomyces cerevisiae*, 1 µg of plasmid DNA, along with 100µg of denatured sheared salmon sperm DNA, was added to 100 µl of INVSC1 suspension, per Invitrogen pYES2 manual. Then 700 ul of a solution containing 1x LiAc, 40% PEG-3350, and 1X TE was added. DNA-containing solution was then incubated for 30 minutes at 30°C and 88 µl of DMSO was added. Heat shock (42°C) was applied for 7 min. and cells were spun down, washed in 1X TE, spun down again and resuspended in 100ul 1X TE, which was then plated on synthetic complete (SC) plates minus uracil.

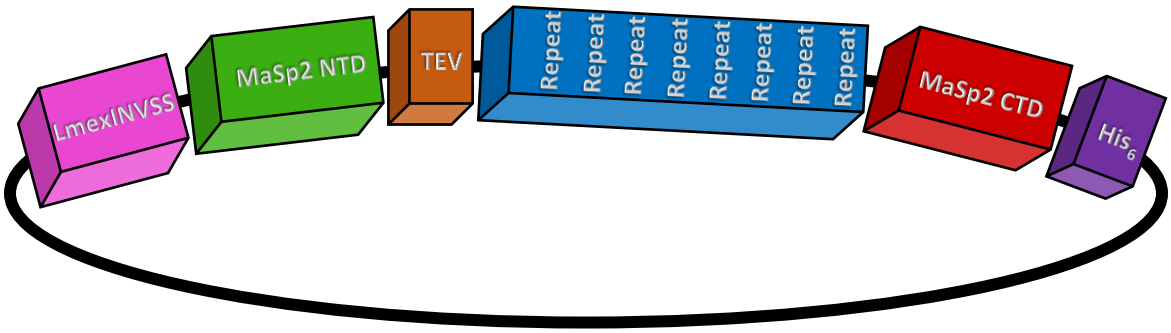

Figure 5.1 Schematic for "mini-spidroin." showing core components. pYes2 plasmid with inserted MaSp2 ss NTD-TEV-R8-CTD-His_6

b. Protein expression

Cells containing MaSp2 ss-N-TEV-R8-C-His_6 were grown overnight at 30°C in synthetic complete medium minus Uracil (SC-U) with 2% glucose, 2% raffinose or 3% glycerol. The OD_{600} was taken and amount of overnight culture was removed to inoculate new culture at OD_{600} of 0.4. Removed sample was spun down and resuspended in SC-U containing sterile galactose at 2% to induce protein expression. Induced cells were grown at 30°C with shaking. Aliquots were removed at 0, 24, 48, and 72 hours post-induction, pelleted and frozen at -20°C until use. Media left from the spun down cells was concentrated using a 3 kDa Amicon centrifugal filter (Millipore). Aliquots were thawed and the OD_{600} was adjusted to an OD_{600} of 50 and cells were lysed, by vortexing with acid-washed glass beads. BCA assay was done on lysate to determine protein concentration and 20 µg of protein from aliquots was run on a 12% SDS-PAGE gel. Gels were stained by Coomassie Brilliant Blue dye or immuodetected using an anti-NTD antibody as described in Chapter 3 materials and methods.

IV. Results

Recombinant protein expression from the *Gal1* promoter contained in *pYES2* is expected to be inhibited by glucose repression and induced once galactose is introduced into the medium (Guthrie and Fink, 1991). However, other catabolite-repressing sugars have been shown to be useful since the strong repression obtained with glucose can be difficult to overcome (Green et al., 2012; Guthrie and Fink, 1991; Lohr et al., 1995; Santangelo, 2006; West et al., 1984). Therefore, INVSc1 cells containing the MaSp2 mini-spidroins expression construct were grown in pre-induction media containing one of three different carbon sources 2% glucose, 2% raffinose, or 3% glycerol. Expression was induced with galactose and aliquots were taken at 0, 24, 48 and 72 hours thereafter. Duplicate polyacrylamide gels were run for staining with Coomassie Brilliant Blue and for immunoblot analysis.

The expected band size for recombinant MaSp2 mini-spidroin (rMaSp2) was 58.2 kDa. The Coomassie-stained gel did not show discernible differences in intensity at that molecular weight with increasing expression time or with the different media (Fig. 5.2).

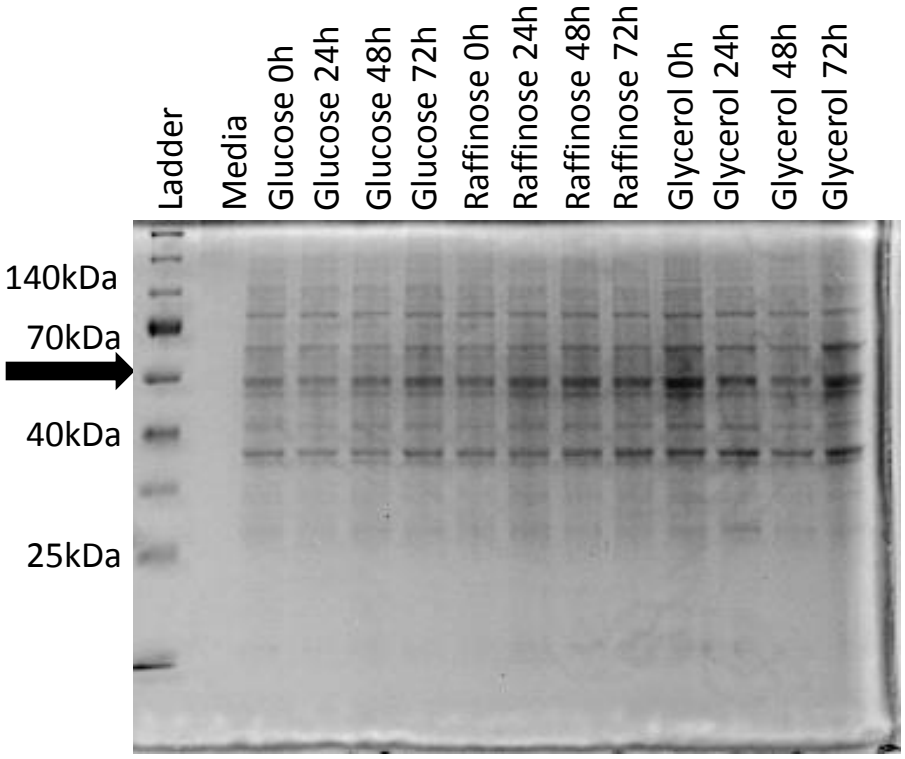

Figure 5.2 Coomassie stained SDS-PAGE gel (12%) of rMaSp2 from *S.cervevisiae* with 20 µg aliquots and ~100X concentrated media. MaSp2 construct (ss-N-TEV-R8-C-His_6) 58. 2kDa noted by black arrow. Aliquots taken at 0, 24, 48 and 72 hours post induction and media is from concentration of supernatant after pelleting of cells.

Immunodetection using a rabbit polyclonal anti-MaSp1 NTD, did show cross-reacting bands at the appropriate molecular weight (Fig. 5.3). Expression in glucose-containing pre-induction medium shows a low level of rMaSp2 that peaks at 24 hours after induction and then decreases at 48 and 72 hours. A similar expression profile is seen with glycerol-containing pre-induction medium (peak expression at 24 hours) but little if

any rMaSp2 mini-spidroin is seen prior to induction. Expression in raffinose-containing pre-induction medium is higher than that seen with glucose but addition of galactose results in decreased expression at 24 and 48 hours that then peaks at 72 hours post-induction. Other lower-molecular weight cross-reacting bands may represent truncated or degraded rMaSp2. Higher molecular weight cross-reacting bands are commonly seen when expressing recombinant spidroin-like proteins (Peng et al., 2016) and have been attributed to aggregation and/or multimerization.

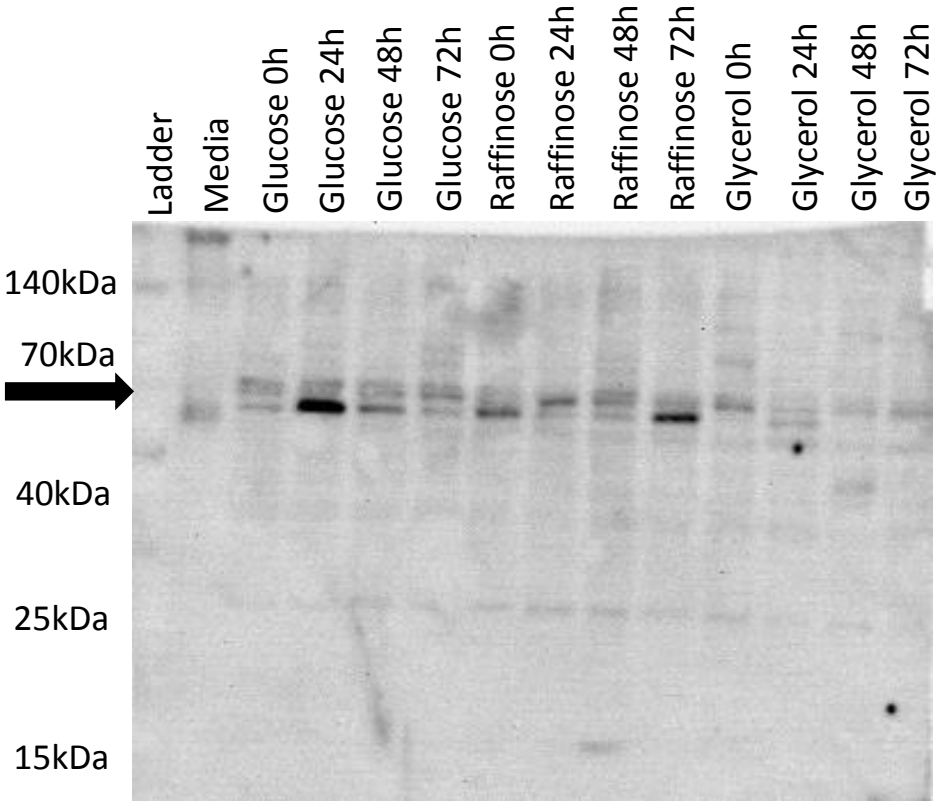

Figure 5.3 Immunodetection of rMaSp2 aliquots (20 µg) and media (`~100x concentrated) using anti-NTD as primary antibody. MaSp2 construct (ss-N-TEV-R8-C-His_6) 58.2 kDa noted by black arrow. Aliquots taken at 0, 24, 48, and 72 hours post induction and media is from concentration of supernatant after pelleting of cells.

While *S. cerevisiae* secretes only 0.5% of native proteins, an essential feature of a functional secretion signal in *S. cerevisiae* is a hydrophobic core of 6-15 amino acids (Romanos et al., 1992). To determine if the *Leishmania mexicana* secretion signal was functional, media from pelleted induced cells was concentrated. No discernable MaSp2 protein secretion can be seen (Fig. 5.2). Immunodetection, however, did reveal a band in the media lane around the 58.2 kDa range that could represent secreted MaSp2 protein (Fig. 5.3).

V. Discussion

Many organisms have been used to produce recombinant spider silk protein. However a perfect system in which full-length spider silk can be produced has not yet been found. While *E. coli* has been the most predominately used expression system, other organisms do offer some advantages. Due to spider silks repetitive nature many organisms have a difficult time producing full-length recombinant protein with a large number of repeat domains. As mentioned, *S. cerevisiae* is able to produce high molecular weight protein, grown at low cost, and can post-translationally modify proteins (Hou et al., 2012; Novick et al., 1980).

Based on immunodetection, using an anti-NTD antibody, we show that we are able to produce full-length rMaSp2 "mini-spidroins" in *S. cerevisiae* (Fig. 5.3). However, there is evidence of protein truncation based on the banding pattern seen below 50 kDa, (Wen et al., 2010; Miao et al., 2006; Zhang et al., 2008) (Fig. 5.2 and Fig. 5.3). (Huemmerich et al., 2004; Miao et al., 2006; Wen et al., 2010; Zhang et al., 2008). The

truncation observed could be due to limitations in translational machinery (Xia et al., 2010; Fahnestock et al., 2000). Another problem that was noted during protein expression was expression of rMaSp2 prior to induction in growth media containing either raffinose or glycerol. Further alteration of the growth conditions are required to reduce the uninduced expression

Of the three pre-induction media types tested, glycerol resulted in the poorest expression (Fig 5.3). Extending the induction time did seem to help with expression of rMaSp2 "mini-spidroins" but higher recombinant protein concentrations were detected at 24hrs and 72hrs in glucose and raffinose, respectively (Fig. 5.3). Further experiments with glycerol and raffinose growth media need to be done to further narrow down the ideal induction time for each to produce the maximum amount of recombinant protein.

The "mini-spidroins" described here contain all three core components of the native full-length spidroin proteins, although the repeat number in our construct is much smaller. Much research has focused on producing recombinant proteins with a large numbers of block repeats but only a few contain the CTD and even fewer the CTD and NTD. With all three components present, experiments can be performed to further delineate the role each component plays in fiber assembly. For example, the recombinant "mini-spidroins" we produced contain a TEV site that allows the NTD to be cleaved off, when desired, for comparative studies. This allows for direct comparison of "mini-spidroins" with and without the NTD to better understand its role in the self-assembly process or in the mechanical and physical properties of the final fiber.

VI. References

Andersson, M., Chen, G., Otikovs, M., Landreh, M., Nordling, K., Kronqvist, N., Westermark, P., Jornvall, H., Knight, S., Ridderstrale, Y., *et al.* (2014). Carbonic Anhydrase Generates CO2 and H+ That Drive Spider Silk Formation Via Opposite Effects on the Terminal Domains. PLoS Biol. *12,* e1001921.

Askarieh, G., Hedhammar, M., Nordling, K., Saenz, A., Casals, C., Rising, A., Johansson, J., and Knight, S.D. (2010). Self-assembly of spider silk proteins is controlled by a pH-sensitive relay. Nature *465,* 236-238.

Barr, L.A., Fahnestock, S.R., and Yang, J. (2004). Production and purification of recombinant DP1B silk-like protein in plants. Mol. Breed. *13,* 345-356.

Breslauer, D.N., Lee, L.P., and Muller, S.J. (2009). Simulation of flow in the silk gland. Biomacromolecules *10,* 49-57.

Craig, C.L. (1997). Evolution of arthropod silks. Annu. Rev. Entomol. *42,* 231-267.

Eisoldt, L., Hardy, J.G., Heim, M., and Scheibel, T.R. (2010). The role of salt and shear on the storage and assembly of spider silk proteins. J. Struct. Biol. *170,* 413-419.

Fahnestock, S.R., Yao, Z., and Bedzyk, L.A. (2000). Microbial production of spider silk proteins. Reviews in Molecular Biotechnology *74,* 105-119.

Forrest, R.D. (1982). Early history of wound treatment. J. R. Soc. Med. *75,* 198-205.

Gaines, W.A.,4th, and Marcotte, Jr.,W.R. (2008). Identification and characterization of multiple Spidroin 1 genes encoding major ampullate silk proteins in *Nephila clavipes*. Insect Mol. Biol. *17,* 465-474.

Gaines, W.A., Sehorn, M.G., and Marcotte, Jr.,W.R. (2010). Spidroin N-terminal domain promotes a pH-dependent association of silk proteins during self-assembly. J. Biol. Chem. *285,* 40745-40753.

Green, E.M., Jiang, Y., Joyner, R., and Weis, K. (2012). A negative feedback loop at the nuclear periphery regulates GAL gene expression. Mol. Biol. Cell *23,* 1367-1375.

Grip, S., Rising, A., Nimmervoll, H., Storckenfeldt, E., Mcqueen-Mason, S.J., Pouchkina-Stantcheva, N., Vollrath, F., Engström, W., and Fernandez-Arias, A. (2006). Transient expression of a major ampullate spidroin 1 gene fragment from *Euprosthenops* sp. in mammalian cells. Cancer Genomics-Proteomics *3,* 83-87.

Guthrie, C., and Fink, G. (1991). Guide to Yeast Genetics and Molecular Biology (Academic, San Diego). 194.3-41

Hayashi, C.Y., Blackledge, T.A., and Lewis, R.V. (2004). Molecular and mechanical characterization of aciniform silk: uniformity of iterated sequence modules in a novel member of the spider silk fibroin gene family. Mol. Biol. Evol. *21,* 1950-1959.

Hedhammar, M., Rising, A., Grip, S., Martinez, A.S., Nordling, K., Casals, C., Stark, M., and Johansson, J. (2008). Structural properties of recombinant nonrepetitive and repetitive parts of major ampullate spidroin 1 from *Euprosthenops australis*: implications for fiber formation. Biochemistry *47,* 3407-3417.

Heidebrecht, A., and Scheibel, T. (2013). Recombinant production of spider silk proteins. Adv. Appl. Microbiol. *82,* 115-153.

Hou, J., Tyo, K.E., Liu, Z., Petranovic, D., and Nielsen, J. (2012). Metabolic engineering of recombinant protein secretion by Saccharomyces cerevisiae. FEMS Yeast Research *12,* 491-510.

Hu, X., Vasanthavada, K., Kohler, K., McNary, S., Moore, A.M., and Vierra, C.A. (2006). Molecular mechanisms of spider silk. Cell Mol. Life Sci. *63,* 1986-1999.

Huemmerich, D., Scheibel, T., Vollrath, F., Cohen, S., Gat, U., and Ittah, S. (2004). Novel assembly properties of recombinant spider dragline silk proteins. Curr. Biol. *14,* 2070-2074.

Humenik, M., Scheibel, T., and Smith, A. (2011). Spider silk understanding the structure-function relationship of a natural fiber. Prog. Mol. Biol. Transl. Sci. *103,* 131-185.

Ittah, S., Michaeli, A., Goldblum, A., and Gat, U. (2007). A model for the structure of the C-terminal domain of dragline spider silk and the role of its conserved cysteine. Biomacromolecules *8,* 2768-2773.

Jaudzems, K., Askarieh, G., Landreh, M., Nordling, K., Jörnvall, H., Rising, A., Knight, S.D., and Johansson, J. (2012). pH-Dependent Dimerization of Spider Silk N-Terminal Domain Requires Relocation of a Wedged Tryptophan Side Chain. J. Mol. Biol. *422,* 477-487.

Keten, S., and Buehler, M.J. (2010). Nanostructure and molecular mechanics of spider dragline silk protein assemblies. J. R. Soc. Interface *7,* 1709-1721.

Kluge, J.A., Rabotyagova, O., Leisk, G.G., and Kaplan, D.L. (2008). Spider silks and their applications. Trends Biotechnol. *26,* 244-251.

Knight, D., and Vollrath, F. (1999). Liquid crystals and flow elongation in a spider's silk production line. Proceedings of the Royal Society of London.Series B: Biological Sciences *266,* 519-523.

Knight, D.P., Knight, M.M., and Vollrath, F. (2000). Beta transition and stress-induced phase separation in the spinning of spider dragline silk. Int. J. Biol. Macromol. *27,* 205-210.

Knight, D.D.P. (2001). Changes in element composition along the spinning duct in a Nephila spider. Naturwissenschaften *88,* 179-182.

Lammel, A., Schwab, M., Hofer, M., Winter, G., and Scheibel, T. (2011). Recombinant spider silk particles as drug delivery vehicles. Biomaterials *32,* 2233-2240.

Leclerc, J., Lefevre, T., Gauthier, M., Gagne, S.M., and Auger, M. (2013). Hydrodynamical properties of recombinant spider silk proteins: Effects of pH, salts and shear, and implications for the spinning process. Biopolymers *99,* 582-593.

Lefevre, T., Boudreault, S., Cloutier, C., and Pézolet, M. (2008). Conformational and orientational transformation of silk proteins in the major ampullate gland of *Nephila clavipes* spiders. Biomacromolecules *9,* 2399-2407.

Lewis, R. (1996). Unraveling the weave of spider silk. Bioscience 636-638.

Lewis, R.V. (2006). Spider silk: ancient ideas for new biomaterials. Chem. Rev. *106,* 3762-3774.

Lohr, D., Venkov, P., and Zlatanova, J. (1995). Transcriptional regulation in the yeast GAL gene family: a complex genetic network. FASEB J. *9,* 777-787.

Lyda, T.A., Joshi, M.B., Andersen, J.F., Kelada, A.Y., Owings, J.P., Bates, P.A., and Dwyer, D.M. (2015). A unique, highly conserved secretory invertase is differentially expressed by promastigote developmental forms of all species of the human pathogen, Leishmania. Mol. Cell. Biochem. *404,* 53-77.

Miao, Y., Zhang, Y., Nakagaki, K., Zhao, T., Zhao, A., Meng, Y., Nakagaki, M., Park, E.Y., and Maenaka, K. (2006). Expression of spider flagelliform silk protein in *Bombyx mori* cell line by a novel Bac-to-Bac/BmNPV baculovirus expression system. Appl. Microbiol. Biotechnol. *71,* 192-199.

Motriuk-Smith, D., Smith, A., Hayashi, C.Y., and Lewis, R.V. (2005). Analysis of the conserved N-terminal domains in major ampullate spider silk proteins. Biomacromolecules *6,* 3152-3159.

Novick, P., Field, C., and Schekman, R. (1980). Identification of 23 complementation groups required for post-translational events in the yeast secretory pathway. Cell *21*, 205-215.

Numata, K., and Kaplan, D.L. (2010). Silk-based delivery systems of bioactive molecules. Adv. Drug Deliv. Rev. *62*, 1497-1508.

Omenetto, F.G., and Kaplan, D.L. (2010). New opportunities for an ancient material. Science *329*, 528-531.

Papadopoulos, P., Sölter, J., and Kremer, F. (2009). Hierarchies in the structural organization of spider silk—a quantitative model. Colloid Polym. Sci. *287*, 231-236.

Peng, C.A., Russo, J., Gravgaard, C., McCartney, H., Gaines, W., and Marcotte Jr, W.R. (2016). Spider silk-like proteins derived from transgenic *Nicotiana tabacum*. Transgenic Res. 1-10.

Romanos, M.A., Scorer, C.A., and Clare, J.J. (1992). Foreign gene expression in yeast: a review. Yeast *8*, 423-488.

Santangelo, G.M. (2006). Glucose signaling in Saccharomyces cerevisiae. Microbiol. Mol. Biol. Rev. *70*, 253-282.

Scheibel, T. (2004). Spider silks: recombinant synthesis, assembly, spinning, and engineering of synthetic proteins. Microb. Cell. Fact. *3*, 14, 1-10.

Sponner, A., Vater, W., Rommerskirch, W., Vollrath, F., Unger, E., Grosse, F., and Weisshart, K. (2005). The conserved C-termini contribute to the properties of spider silk fibroins. Biochem. Biophys. Res. Commun. *338*, 897-902.

Sponner, A., Unger, E., Grosse, F., and Weisshart, K. (2004). Conserved C-termini of Spidroins are secreted by the major ampullate glands and retained in the silk thread. Biomacromolecules *5*, 840-845.

Sutherland, T.D., Young, J.H., Weisman, S., Hayashi, C.Y., and Merritt, D.J. (2010). Insect silk: one name, many materials. Annu. Rev. Entomol. *55*, 171-188.

Teulé, F., Aubé, C., Ellison, M., and Abbott, A. (2003). Biomimetic manufacturing of customized novel fibre proteins for specialised applications. Autex Research Journal *3*, 160-165.

Teule, F., Cooper, A.R., Furin, W.A., Bittencourt, D., Rech, E.L., Brooks, A., and Lewis, R.V. (2009). A protocol for the production of recombinant spider silk-like proteins for artificial fiber spinning. Nat. Protoc. *4*, 341-355.

Wen, H., Lan, X., Zhang, Y., Zhao, T., Wang, Y., Kajiura, Z., and Nakagaki, M. (2010). Transgenic silkworms (Bombyx mori) produce recombinant spider dragline silk in cocoons. Mol. Biol. Rep. *37*, 1815-1821.

West, R.W.,Jr, Yocum, R.R., and Ptashne, M. (1984). Saccharomyces cerevisiae GAL1-GAL10 divergent promoter region: location and function of the upstream activating sequence UASG. Mol. Cell. Biol. *4*, 2467-2478.

Xia, X.X., Qian, Z.G., Ki, C.S., Park, Y.H., Kaplan, D.L., and Lee, S.Y. (2010). Native-sized recombinant spider silk protein produced in metabolically engineered *Escherichia coli* results in a strong fiber. Proc. Natl. Acad. Sci. U. S. A. *107*, 14059-14063.

Xu, H.T., Fan, B.L., Yu, S.Y., Huang, Y.H., Zhao, Z.H., Lian, Z.X., Dai, Y.P., Wang, L.L., Liu, Z.L., Fei, J., and Li, N. (2007). Construct synthetic gene encoding artificial spider dragline silk protein and its expression in milk of transgenic mice. Anim. Biotechnol. *18*, 1-12.

Xu, M., and Lewis, R.V. (1990). Structure of a protein superfiber: spider dragline silk. Proc. Natl. Acad. Sci. U. S. A. *87*, 7120-7124.

Zhang, Y., Hu, J., Miao, Y., Zhao, A., Zhao, T., Wu, D., Liang, L., Miikura, A., Shiomi, K., Kajiura, Z., and Nakagaki, M. (2008). Expression of EGFP-spider dragline silk fusion protein in BmN cells and larvae of silkworm showed the solubility is primary limit for dragline proteins yield. Mol. Biol. Rep. *35*, 329-335.

CHAPTER 6

CONCLUSIONS AND FUTURE DIRECTIONS

Our examination of the *Nephila clavipes* wild-type major ampullate spidroin 1 (MaSp1) N-terminal domain (NTD) gives new information about homodimerization of the NTD. We quantitatively show a 25-fold increase in homodimer stabilization from pH 7.0 to 5.5 based on K_d data obtained from the using biolayer interferometry (BLI) (Chapter 2). This provides label-free, real-time kinetic data for the wild-type MaSp1 NTD. This data is corroborated by other research that has shown the NTD exists primary as a monomer with only weak dimer interaction at neutral pH and exists primarily as a stable homodimer at acidic pH (Andersson et al., 2014; Askarieh et al., 2010; Gaines et al., 2010; Gronau et al., 2013; Hagn, 2012; Jaudzems et al., 2012; Kronqvist et al., 2014; Kurut et al., 2015; Ries et al., 2014; Schwarze et al., 2013; Wallace and Shen, 2012; Xu et al., 2015). We also show that this increase in homodimerization is primarily due to the rate of association vs. the rate of dissociation. This is shown by the 20-fold increase in the rate of association (k_{on}) for wild-type NTD from pH 7.0 to pH 5.5, while the rates of dissociation (k_{dis}) are almost the same.

Because the MaSp1 NTD undergoes homodimerization and conformational changes due to changes in pH, the parameters for BLI experiments were carefully optimized. Specifically four different biosensors, multiple blocking agents, and various different step times and protein concentrations were tested. Streptavidin biosensors, used with buffers containing 2% BSA and 0.02% Tween 20 provided the best combination to analyze the NTD dimerization. We also found that use of a biotin blocking step reduced

the amount of non-specific binding to the biosensors. This setup also required that the NTD_{his6} protein be preferentially biotinylated at the N-terminal α-amino group.

Previous work in our lab showed a conformational change in the wild-type MaSp1 NTD from pH 7.5 to 5.5, specifically between pH 6.0 and pH 6.5 (Gaines et al., 2010). The tryptophan fluorescence data showed that from pH 7.5 to 6.5 the tryptophan residue was buried within the NTD protein resulting in high fluorescence with a maximum signal around 320 nm. This protein arrangement was termed Conformation I. However, at pH 6.0 and 5.5 the tryptophan residue became solvent exposed which quenched the fluorescence signal and shifted the maximum fluorescence to around 338 nm. This protein arrangement was termed Conformation II. Based on this data, we used the same method to look at variants of the NTD in which conserved amino acid with ionizable side chains were altered to determine if they played a role in this conformational change (Chapter 3). From the nine single and two double variants created, we found five residues that showed a similar conformational trend to that of wild-type and six variants that deviated strongly from wild-type. Variants D44N, D58N, E84Q, E124Q, and E139Q displayed fluorescence traces similar to that of wild-type consistent with changes from Conformation I to Conformation II. However, variants D45K and E84K showed complete loss of Conformation II in the pH range of 7.5 to 5.5. Notably, variants that showed intermediate conformations at one or more pHs were observed. K70D showed a Conformation I-like arrangement until pH 5.5 where it entered an intermediate conformation. However, K70E showed an intermediate conformation until pH 6.0 where it shifted into Conformation II. This intermediate conformation shows a

slight red shift but does not shift over as far as Conformation II. Interestingly, the double variant D45K/K70D, showed an intermediate conformation throughout the pH range. The other double variant D45K/K70E, showed a Conformation II-like arrangement over the same pH range. This data coincides with other research that shows that D45 and K70 are important residues and are believed to be involved in the formation of salt bridges, which are necessary for stable homodimer formation (Askarieh et al., 2010; Gronau et al., 2013; Kronqvist et al., 2014; Schwarze et al., 2013; Wallace and Shen, 2012).

Our research and that of others has suggested that dimerization and conformation changes are correlated (Gaines et al., 2010, Andersson et al., 2014; Askarieh et al., 2010; Gronau et al., 2013; Hagn, 2012; Jaudzems et al., 2012; Kurut et al., 2015; Ries et al., 2014; Schwarze et al., 2013; Wallace and Shen, 2012; Xu et al., 2015). The lack of a conformational change seen among some of the variants led us to examine whether this would result in a change in kinetic values compared to wild-type NTD (Chapter 4). Three NTD variants with a single amino acid substitution and one variant with a double substitution were analyzed using BLI, three single and one double, to determine if they could dimerize with the wild-type NTD.

Variants D45K and E84K showed K_d values at both pH 5.5 and 7.0 that were similar to those seen for wild-type at pH 7.0, which indicate a lack of homodimer stabilization at decreased pH. This correlates to the tryptophan fluorescence data showing that D45K does not transition into Conformation II. At pH 7.0 K70D showed a K_d value similar to that of wild-type at the same pH. However, at pH 5.5 K70D displayed an intermediate K_d between that of wild-type at pH 5.5 and 7.0. These data agree with

fluorescence data consistent with Conformation I for K70D until pH 5.5 where it shifts into a more intermediate conformation. The double variant, D45K/K70D, which exhibited an intermediate conformation along the pH range, from pH 5.5 to pH 7.5, showed a K_d at pH 7.0 similar to wild-type at pH 7.0 but an intermediate K_d of 22.77 ± 2.68 μM at pH 5.5, which also fits well with our fluorescence data.

With the wild-type NTD attached to the biosensor, a stable homodimer was unable to form with any of the variants at pH 7.0. We think that for stable NTD homodimerization neither protein can exist in Conformation I. Thus at pH 7.0 the wild-type NTD is in Conformation I the stable homodimer could not form. However, when the experiment was conducted at pH 5.5, the wild-type NTD was in Conformation II and formed an intermediate homodimers, based on K_d, with those variants showing an intermediate conformation. The wild-type NTD was not able to form a stable or intermediate homodimer with variants that still existed in Conformation I at pH 5.5 such as D45K and E84K.

To give us a more complete picture of the NTD homodimerization, other variants need to be produced and measured using tryptophan fluorescence. Based on work from other labs examining the *Euprosthenops australis* NTD, residues E89 and K65 variants in the *Nephila clavipes* NTD would be good places to start (Askarieh et al., 2010; Jaudzems et al., 2012; Kronqvist et al., 2014; Landreh et al., 2010; Schwarze et al., 2013; Wallace and Shen, 2012). When using tryptophan fluorescence residue E84 showed very little visual change from wild-type when changed from a negative-to-neutral charge but abolished Conformation II when changed to a positive charge. Based on this, *N. clavipes*

variants should be created at residues D44, E84, E124 and E139 involving a charge change from negative-to-positive, since these residues are also thought to be involved in conformation change and dimerization. Residues D45 and K70 should also be changed to an amino acid with neutral charge to see if that produces a more wild-like type conformation change.

In the future, kinetics analysis should be done on the aforementioned variants that show a conformational change deviation from wild-type, as well as a few variants that do not like D58N and D84Q. If variants with conformation changes similar to wild-type also showed similar kinetics, it would further support that it is the conformation change resulting from the charge removal that is responsible for homodimerization and not the charge removal alone. Since all of our kinetics data was conducted using wild-type NTD as the dimer partner, it would be interesting to see what type of homodimerizaiton would occur when using two of the same or different variants. For variants like K70D that show an intermediate conformation, we could determine if an intermediately stable homodimer could still be formed if both variants were in an intermediate conformation instead of just one. D45K/K70E would also be of interest since it exists in a Conformation II like arrangement from pH 7.0 to 5.5.

The use of BLI is not limited to the NTDs alone. Our lab is in the process of producing a recombinant protein containing an unstructured linker flanked by the wild-type NTD and CTD. This protein could be used to look at the importance of the combination of the N and C-terminal domains in fiber formation. Since there is a cleavable site following the NTD, the experiment could also look the interaction of the

NTD with the CTD. All of these experiments could also be done at various salt conditions since salt is known to effect conformational change of the NTD (Gaines et al., 2010).

I. References

Andersson, M., Chen, G., Otikovs, M., Landreh, M., Nordling, K., Kronqvist, N., Westermark, P., Jornvall, H., Knight, S., Ridderstrale, Y., *et al.* (2014). Carbonic Anhydrase Generates CO2 and H+ That Drive Spider Silk Formation Via Opposite Effects on the Terminal Domains. PLoS Biol. *12*, e1001921.

Askarieh, G., Hedhammar, M., Nordling, K., Saenz, A., Casals, C., Rising, A., Johansson, J., and Knight, S.D. (2010). Self-assembly of spider silk proteins is controlled by a pH-sensitive relay. Nature *465*, 236-238.

Gaines, W.A., Sehorn, M.G., and Marcotte, Jr.,W.R. (2010). Spidroin N-terminal domain promotes a pH-dependent association of silk proteins during self-assembly. J. Biol. Chem. *285*, 40745-40753.

Gronau, G., Qin, Z., and Buehler, M.J. (2013). Effect of sodium chloride on the structure and stability of spider silk's N-terminal protein domain. Biomater. Sci. *1*, 276-284.

Hagn, F. (2012). A structural view on spider silk proteins and their role in fiber assembly. J. Pept. Sci. *18*, 357-365.

Jaudzems, K., Askarieh, G., Landreh, M., Nordling, K., Jörnvall, H., Rising, A., Knight, S.D., and Johansson, J. (2012). pH-Dependent Dimerization of Spider Silk N-Terminal Domain Requires Relocation of a Wedged Tryptophan Side Chain. J. Mol. Biol. *422*, 477-487.

Kronqvist, N., Otikovs, M., Chmyrov, V., Chen, G., Andersson, M., Nordling, K., Landreh, M., Sarr, M., Jornvall, H., Wennmalm, S., *et al.* (2014). Sequential pH-driven dimerization and stabilization of the N-terminal domain enables rapid spider silk formation. Nat. Commun. *5*, 3254, 1-11.

Kurut, A., Dicko, C., and Lund, M. (2015). Dimerization of Terminal Domains in Spiders Silk Proteins Is Controlled by Electrostatic Anisotropy and Modulated by Hydrophobic Patches. ACS Biomat. Sci. Eng. 1(6), 363-371

Landreh, M., Askarieh, G., Nordling, K., Hedhammar, M., Rising, A., Casals, C., Astorga-Wells, J., Alvelius, G., Knight, S.D., Johansson, J., Jornvall, H., and Bergman, T. (2010). A pH-dependent dimer lock in spider silk protein. J. Mol. Biol. *404*, 328-336.

Ries, J., Schwarze, S., Johnson, C.M., and Neuweiler, H. (2014). Microsecond folding and domain motions of a spider silk protein structural switch. J. Am. Chem. Soc. *136*, 17136-17144.

Schwarze, S., Zwettler, F.U., Johnson, C.M., and Neuweiler, H. (2013). The N-terminal domains of spider silk proteins assemble ultrafast and protected from charge screening. Nat. Commun. 4,2815,1-7

Wallace, J.A., and Shen, J.K. (2012). Unraveling A Trap-and-Trigger Mechanism in the pH-Sensitive Self-Assembly of Spider Silk Proteins. J. Phys. Chem. Lett. *3*, 658-662.

Xu, D., Guo, C., and Holland, G.P. (2015). Probing the Impact of Acidification on Spider Silk Assembly Kinetics. Biomacromolecules *16,* 2072-2079.

APPENDICES

Appendix A

Nephila clavipes Major Ampullate Spidroin 1 N-terminal domain Tryptophan

Fluorescence 320 nm / 338 nm Ratio Graphs

A.

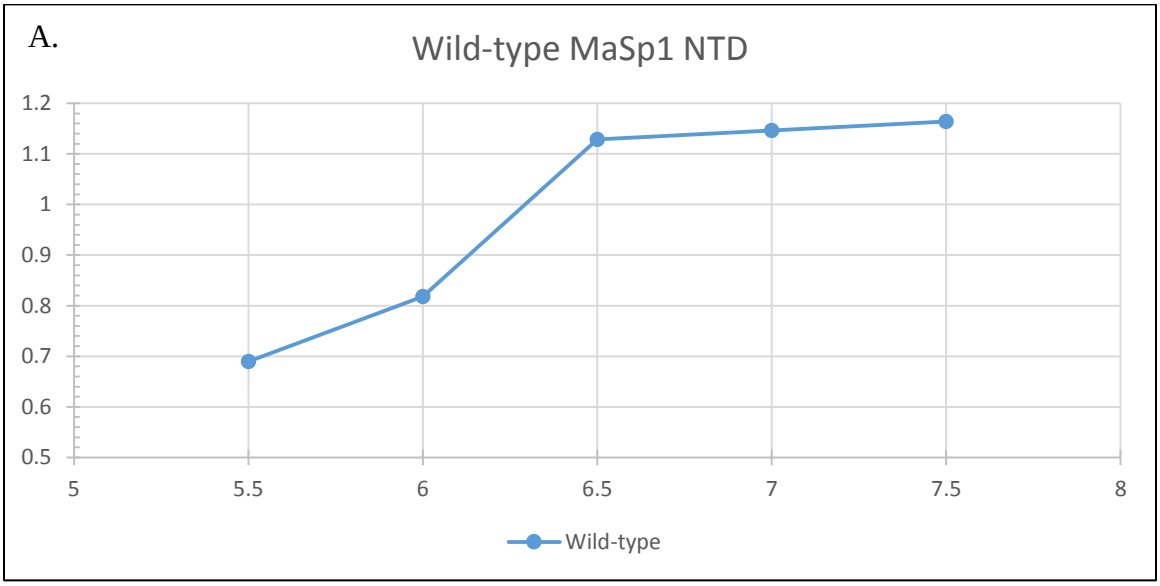

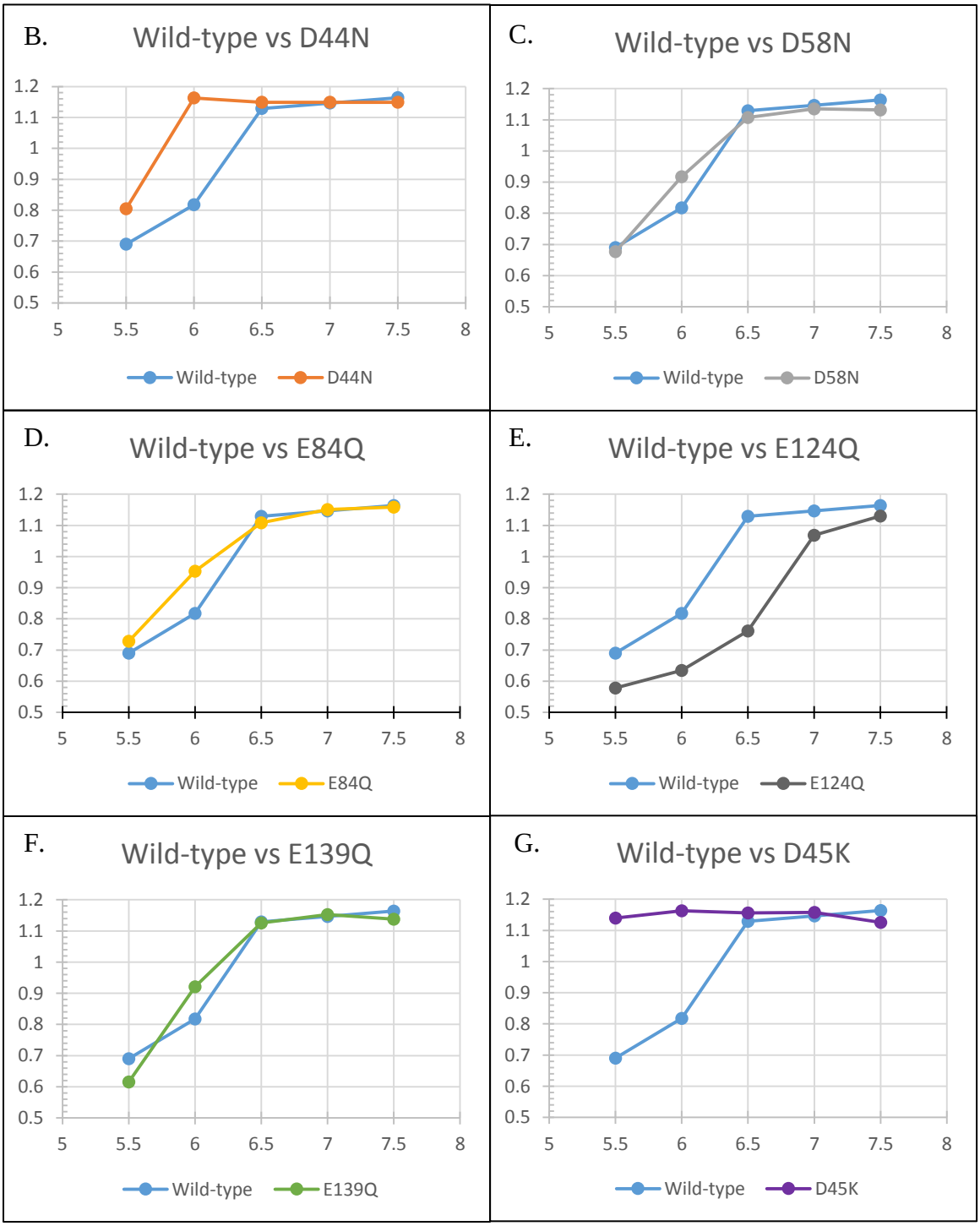
B.
Wild-type vs D44N
1.2
1.1
1
0.9
0.8
0.7
0.6
0.5
5
5.5
6
6.5
7
7.5
8
Wild-type
D44N
C.
Wild-type vs D58N
Wild-type
D58N
D.
Wild-type vs E84Q
Wild-type
E84Q
E.
Wild-type vs E124Q
Wild-type
E124Q
F.
Wild-type vs E139Q
Wild-type
E139Q
G.
Wild-type vs D45K
Wild-type
D45K

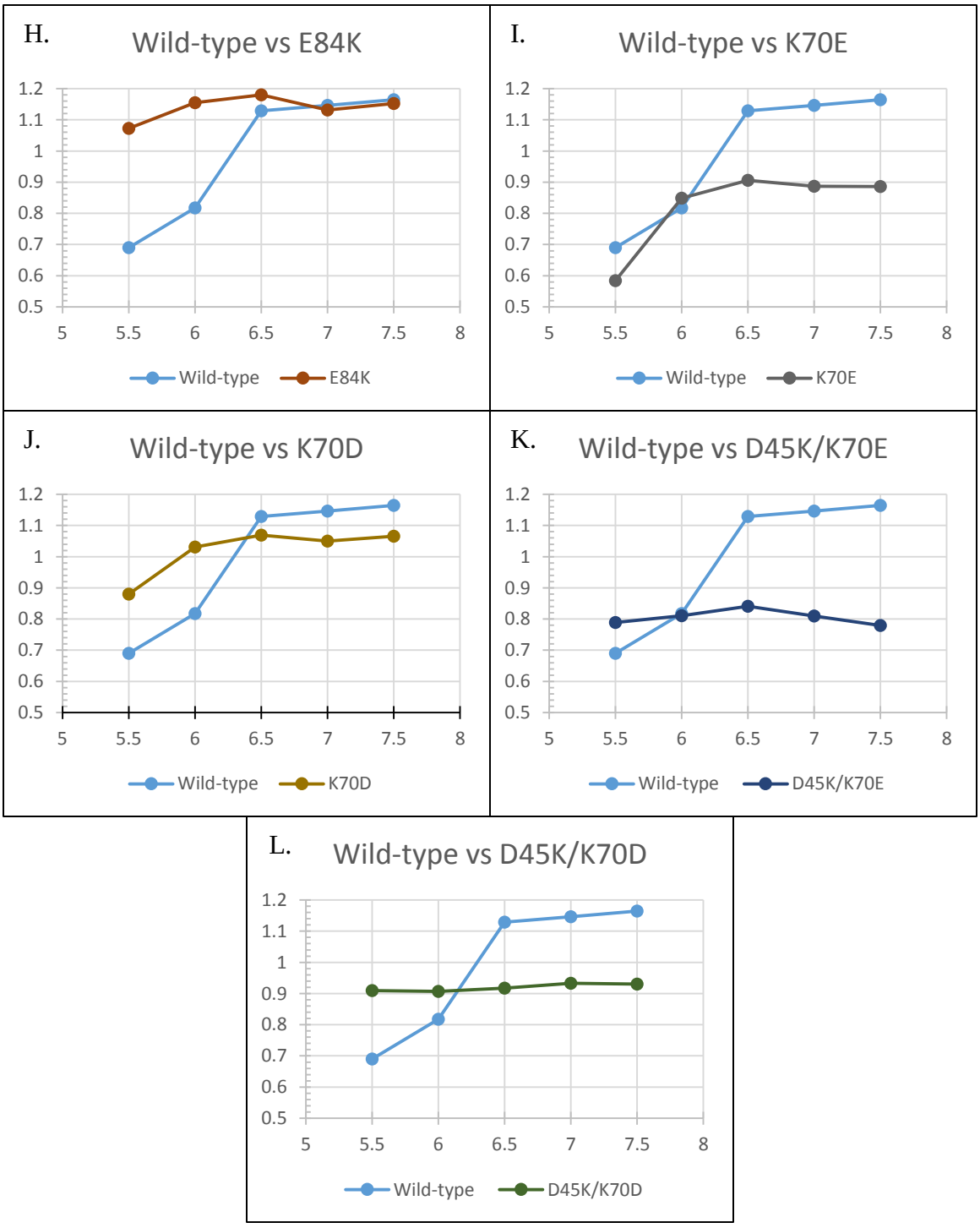

Figure B-1: MaSp1 NTD graphs showing tryptophan fluorescence ratio at 320 nm/338 nm at pH 7.5, 7.0, 6.5, 6.0, and 5.5. A. Wild-type MaSp1 NTD. B.-L. Wild-type MaSp1 NTD vs. NTD variant.

Appendix **B**

ELSEVIER LICENSE
TERMS AND CONDITIONS

Jun 27, 2016

This Agreement between Krystal Cadle ("You") and Elsevier ("Elsevier") consists of your license details and the terms and conditions provided by Elsevier and Copyright Clearance Center.

License Number	3897241070214
License date	Jun 27, 2016
Licensed Content Publisher	Elsevier
Licensed Content Publication	Elsevier Books
Licensed Content Title	Advances in Applied Microbiology
Licensed Content Author	Aniela Heidebrecht,Thomas Scheibel
Licensed Content Date	2013
Licensed Content Pages	39
Start Page	115
End Page	153
Type of Use	reuse in a thesis/dissertation
Portion	figures/tables/illustrations
Number of figures/tables/illustrations	7
Format	both print and electronic
Are you the author of this Elsevier chapter?	No
Will you be translating?	No
Order reference number	
Original figure numbers	Figure 4.1, 4.3 and Table 4.1, 4.2, 4.3, 4.3, 4.5
Title of your thesis/dissertation	The Role the N-Terminal Domain Plays in Spidroin Assembly
Expected completion date	Aug 2016
Estimated size (number of pages)	150
Elsevier VAT number	GB 494 6272 12
Requestor Location	Krystal Cadle 245H Campus Dr. CENTRAL, SC 29630 United States Attn: Krystal Cadle
Total	0.00 USD
Terms and Conditions	

INTRODUCTION

1. The publisher for this copyrighted material is Elsevier. By clicking "accept" in connection

with completing this licensing transaction, you agree that the following terms and conditions apply to this transaction (along with the Billing and Payment terms and conditions established by Copyright Clearance Center, Inc. ("CCC"), at the time that you opened your Rightslink account and that are available at any time at http://myaccount.copyright.com).

GENERAL TERMS

2. Elsevier hereby grants you permission to reproduce the aforementioned material subject to the terms and conditions indicated.

3. Acknowledgement: If any part of the material to be used (for example, figures) has appeared in our publication with credit or acknowledgement to another source, permission must also be sought from that source. If such permission is not obtained then that material may not be included in your publication/copies. Suitable acknowledgement to the source must be made, either as a footnote or in a reference list at the end of your publication, as follows:

"Reprinted from Publication title, Vol /edition number, Author(s), Title of article / title of chapter, Pages No., Copyright (Year), with permission from Elsevier [OR APPLICABLE SOCIETY COPYRIGHT OWNER]." Also Lancet special credit - "Reprinted from The Lancet, Vol. number, Author(s), Title of article, Pages No., Copyright (Year), with permission from Elsevier."

4. Reproduction of this material is confined to the purpose and/or media for which permission is hereby given.

5. Altering/Modifying Material: Not Permitted. However figures and illustrations may be altered/adapted minimally to serve your work. Any other abbreviations, additions, deletions and/or any other alterations shall be made only with prior written authorization of Elsevier Ltd. (Please contact Elsevier at permissions@elsevier.com)

6. If the permission fee for the requested use of our material is waived in this instance, please be advised that your future requests for Elsevier materials may attract a fee.

7. Reservation of Rights: Publisher reserves all rights not specifically granted in the combination of (i) the license details provided by you and accepted in the course of this licensing transaction, (ii) these terms and conditions and (iii) CCC's Billing and Payment terms and conditions.

8. License Contingent Upon Payment: While you may exercise the rights licensed immediately upon issuance of the license at the end of the licensing process for the transaction, provided that you have disclosed complete and accurate details of your proposed use, no license is finally effective unless and until full payment is received from you (either by publisher or by CCC) as provided in CCC's Billing and Payment terms and conditions. If full payment is not received on a timely basis, then any license preliminarily granted shall be deemed automatically revoked and shall be void as if never granted. Further, in the event that you breach any of these terms and conditions or any of CCC's Billing and Payment terms and conditions, the license is automatically revoked and shall be void as if never granted. Use of materials as described in a revoked license, as well as any use of the materials beyond the scope of an unrevoked license, may constitute copyright infringement and publisher reserves the right to take any and all action to protect its copyright in the materials.

9. Warranties: Publisher makes no representations or warranties with respect to the licensed material.

10. Indemnity: You hereby indemnify and agree to hold harmless publisher and CCC, and their respective officers, directors, employees and agents, from and against any and all claims arising out of your use of the licensed material other than as specifically authorized pursuant to this license.

11. No Transfer of License: This license is personal to you and may not be sublicensed, assigned, or transferred by you to any other person without publisher's written permission.

12. No Amendment Except in Writing: This license may not be amended except in a writing signed by both parties (or, in the case of publisher, by CCC on publisher's behalf).

13. Objection to Contrary Terms: Publisher hereby objects to any terms contained in any

purchase order, acknowledgment, check endorsement or other writing prepared by you, which terms are inconsistent with these terms and conditions or CCC's Billing and Payment terms and conditions. These terms and conditions, together with CCC's Billing and Payment terms and conditions (which are incorporated herein), comprise the entire agreement between you and publisher (and CCC) concerning this licensing transaction. In the event of any conflict between your obligations established by these terms and conditions and those established by CCC's Billing and Payment terms and conditions, these terms and conditions shall control.

14. Revocation: Elsevier or Copyright Clearance Center may deny the permissions described in this License at their sole discretion, for any reason or no reason, with a full refund payable to you. Notice of such denial will be made using the contact information provided by you. Failure to receive such notice will not alter or invalidate the denial. In no event will Elsevier or Copyright Clearance Center be responsible or liable for any costs, expenses or damage incurred by you as a result of a denial of your permission request, other than a refund of the amount(s) paid by you to Elsevier and/or Copyright Clearance Center for denied permissions.

LIMITED LICENSE

The following terms and conditions apply only to specific license types:

15. **Translation**: This permission is granted for non-exclusive world **English** rights only unless your license was granted for translation rights. If you licensed translation rights you may only translate this content into the languages you requested. A professional translator must perform all translations and reproduce the content word for word preserving the integrity of the article.

16. **Posting licensed content on any Website**: The following terms and conditions apply as follows: Licensing material from an Elsevier journal: All content posted to the web site must maintain the copyright information line on the bottom of each image; A hyper-text must be included to the Homepage of the journal from which you are licensing at http://www.sciencedirect.com/science/journal/xxxxx or the Elsevier homepage for books at http://www.elsevier.com; Central Storage: This license does not include permission for a scanned version of the material to be stored in a central repository such as that provided by Heron/XanEdu.

Licensing material from an Elsevier book: A hyper-text link must be included to the Elsevier homepage at http://www.elsevier.com . All content posted to the web site must maintain the copyright information line on the bottom of each image.

Posting licensed content on Electronic reserve: In addition to the above the following clauses are applicable: The web site must be password-protected and made available only to bona fide students registered on a relevant course. This permission is granted for 1 year only. You may obtain a new license for future website posting.

17. **For journal authors:** the following clauses are applicable in addition to the above:

Preprints:

A preprint is an author's own write-up of research results and analysis, it has not been peer-reviewed, nor has it had any other value added to it by a publisher (such as formatting, copyright, technical enhancement etc.).

Authors can share their preprints anywhere at any time. Preprints should not be added to or enhanced in any way in order to appear more like, or to substitute for, the final versions of articles however authors can update their preprints on arXiv or RePEc with their Accepted Author Manuscript (see below).

If accepted for publication, we encourage authors to link from the preprint to their formal publication via its DOI. Millions of researchers have access to the formal publications on ScienceDirect, and so links will help users to find, access, cite and use the best available version. Please note that Cell Press, The Lancet and some society-owned have different preprint policies. Information on these policies is available on the journal homepage.

Accepted Author Manuscripts: An accepted author manuscript is the manuscript of an

article that has been accepted for publication and which typically includes author-incorporated changes suggested during submission, peer review and editor-author communications.
Authors can share their accepted author manuscript:

- immediately
  - via their non-commercial person homepage or blog
  - by updating a preprint in arXiv or RePEc with the accepted manuscript
  - via their research institute or institutional repository for internal institutional uses or as part of an invitation-only research collaboration work-group
  - directly by providing copies to their students or to research collaborators for their personal use
  - for private scholarly sharing as part of an invitation-only work group on commercial sites with which Elsevier has an agreement
- after the embargo period
  - via non-commercial hosting platforms such as their institutional repository
  - via commercial sites with which Elsevier has an agreement

In all cases accepted manuscripts should:

- link to the formal publication via its DOI
- bear a CC-BY-NC-ND license - this is easy to do
- if aggregated with other manuscripts, for example in a repository or other site, be shared in alignment with our hosting policy not be added to or enhanced in any way to appear more like, or to substitute for, the published journal article.

Published journal article (JPA): A published journal article (PJA) is the definitive final record of published research that appears or will appear in the journal and embodies all value-adding publishing activities including peer review co-ordination, copy-editing, formatting, (if relevant) pagination and online enrichment.
Policies for sharing publishing journal articles differ for subscription and gold open access articles:
Subscription Articles: If you are an author, please share a link to your article rather than the full-text. Millions of researchers have access to the formal publications on ScienceDirect, and so links will help your users to find, access, cite, and use the best available version.
Theses and dissertations which contain embedded PJAs as part of the formal submission can be posted publicly by the awarding institution with DOI links back to the formal publications on ScienceDirect.
If you are affiliated with a library that subscribes to ScienceDirect you have additional private sharing rights for others' research accessed under that agreement. This includes use for classroom teaching and internal training at the institution (including use in course packs and courseware programs), and inclusion of the article for grant funding purposes.
Gold Open Access Articles: May be shared according to the author-selected end-user license and should contain a CrossMark logo, the end user license, and a DOI link to the formal publication on ScienceDirect.
Please refer to Elsevier's posting policy for further information.
18. **For book authors** the following clauses are applicable in addition to the above:
Authors are permitted to place a brief summary of their work online only. You are not allowed to download and post the published electronic version of your chapter, nor may you scan the printed edition to create an electronic version. **Posting to a repository:** Authors are permitted to post a summary of their chapter only in their institution's repository.
19. **Thesis/Dissertation**: If your license is for use in a thesis/dissertation your thesis may be submitted to your institution in either print or electronic form. Should your thesis be published commercially, please reapply for permission. These requirements include

permission for the Library and Archives of Canada to supply single copies, on demand, of the complete thesis and include permission for Proquest/UMI to supply single copies, on demand, of the complete thesis. Should your thesis be published commercially, please reapply for permission. Theses and dissertations which contain embedded PJAs as part of the formal submission can be posted publicly by the awarding institution with DOI links back to the formal publications on ScienceDirect.

Elsevier Open Access Terms and Conditions

You can publish open access with Elsevier in hundreds of open access journals or in nearly 2000 established subscription journals that support open access publishing. Permitted third party re-use of these open access articles is defined by the author's choice of Creative Commons user license. See our open access license policy for more information.

Terms & Conditions applicable to all Open Access articles published with Elsevier:

Any reuse of the article must not represent the author as endorsing the adaptation of the article nor should the article be modified in such a way as to damage the author's honour or reputation. If any changes have been made, such changes must be clearly indicated.

The author(s) must be appropriately credited and we ask that you include the end user license and a DOI link to the formal publication on ScienceDirect.

If any part of the material to be used (for example, figures) has appeared in our publication with credit or acknowledgement to another source it is the responsibility of the user to ensure their reuse complies with the terms and conditions determined by the rights holder.

Additional Terms & Conditions applicable to each Creative Commons user license:

CC BY: The CC-BY license allows users to copy, to create extracts, abstracts and new works from the Article, to alter and revise the Article and to make commercial use of the Article (including reuse and/or resale of the Article by commercial entities), provided the user gives appropriate credit (with a link to the formal publication through the relevant DOI), provides a link to the license, indicates if changes were made and the licensor is not represented as endorsing the use made of the work. The full details of the license are available at http://creativecommons.org/licenses/by/4.0.

CC BY NC SA: The CC BY-NC-SA license allows users to copy, to create extracts, abstracts and new works from the Article, to alter and revise the Article, provided this is not done for commercial purposes, and that the user gives appropriate credit (with a link to the formal publication through the relevant DOI), provides a link to the license, indicates if changes were made and the licensor is not represented as endorsing the use made of the work. Further, any new works must be made available on the same conditions. The full details of the license are available at http://creativecommons.org/licenses/by-nc-sa/4.0.

CC BY NC ND: The CC BY-NC-ND license allows users to copy and distribute the Article, provided this is not done for commercial purposes and further does not permit distribution of the Article if it is changed or edited in any way, and provided the user gives appropriate credit (with a link to the formal publication through the relevant DOI), provides a link to the license, and that the licensor is not represented as endorsing the use made of the work. The full details of the license are available at http://creativecommons.org/licenses/by-nc-nd/4.0.

Any commercial reuse of Open Access articles published with a CC BY NC SA or CC BY NC ND license requires permission from Elsevier and will be subject to a fee.

Commercial reuse includes:

- Associating advertising with the full text of the Article
- Charging fees for document delivery or access
- Article aggregation
- Systematic distribution via e-mail lists or share buttons

Posting or linking by commercial companies for use by customers of those companies.

20. **Other Conditions**:

v1.8

Questions? customercare@copyright.com or +1-855-239-3415 (toll free in the US) or +1-978-646-2777.

Copyright Clearance Center

Note: Copyright.com supplies permissions but not the copyrighted content itself.

1 PAYMENT 2 REVIEW 3 CONFIRMATION

Step 3: Order Confirmation

Thank you for your order! A confirmation for your order will be sent to your account email address. If you have questions about your order, you can call us at +1.855.239.3415 Toll Free, M-F between 3:00 AM and 6:00 PM (Eastern), or write to us at info@copyright.com. This is not an invoice.

Confirmation Number: 11572873
Order Date: 06/27/2016

If you paid by credit card, your order will be finalized and your card will be charged within 24 hours. If you choose to be invoiced, you can change or cancel your order until the invoice is generated.

Payment Information

Krystal Cadle
kcadle@g.clemson.edu
+1 (229)8942223
Payment Method: CC ending in 0099

Order Details

Journal of experimental biology

Order detail ID:	69890730
Order License Id:	3897250792354
ISSN:	1477-9145
Publication Type:	e-Journal
Volume:	
Issue:	
Start page:	
Publisher:	COMPANY OF BIOLOGISTS LTD.
Author/Editor:	Company of Biologists

Permission Status: Granted

Permission type: Republish or display content
Type of use: Republish in a thesis/dissertation

Requestor type	Academic institution
Format	Print, Electronic
Portion	chart/graph/table/figure
Number of charts/graphs/tables/figures	2
Title or numeric reference of the portion(s)	Fig 1, Table 1
Title of the article or chapter the portion is from	THE MECHANICAL DESIGN OF SPIDER SILKS: FROM FIBROIN SEQUENCE TO MECHANICAL FUNCTION
Editor of portion(s)	N/A
Author of portion(s)	N/A

Volume of serial or monograph	202
Page range of portion	3296
Publication date of portion	16 November 1999
Rights for	Main product
Duration of use	Life of current edition
Creation of copies for the disabled	no
With minor editing privileges	yes
For distribution to	Worldwide
In the following language(s)	Original language of publication
With incidental promotional use	no
Lifetime unit quantity of new product	Up to 499
Made available in the following markets	Education, professional
The requesting person/organization	Krystal Cadle
Order reference number	
Author/Editor	Krystal Cadle
The standard identifier of New Work	KAC2016
Title of New Work	The Role the N-Terminal Domain Plays in Spidroin Assembly
Publisher of New Work	ProQuest
Expected publication date	Aug 2016
Estimated size (pages)	150

Note: This item will be invoiced or charged separately through CCC's **RightsLink** service. More info **$ 3.50**

This is not an invoice.

Total order items: 1

Order Total: 3.50 USD

Confirmation Number: 11572873

Special Rightsholder Terms & Conditions

The following terms & conditions apply to the specific publication under which they are listed

Journal of experimental biology
Permission type: Republish or display content
Type of use: Republish in a thesis/dissertation

TERMS AND CONDITIONS

The following terms are individual to this publisher:

The acknowledgement should state "Reproduced / adapted with permission" and give the source journal name. The acknowledgement should either provide full citation details or refer to the relevant citation in the article reference list. The full citation details should include authors, journal, year, volume, issue and page citation.

Where appearing online or in other electronic media, a link should be provided to the original article (e.g. via DOI):

Development: dev.biologists.org

Disease Models & Mechanisms: dmm.biologists.org

Journal of Cell Science: jcs.biologists.org

The Journal of Experimental Biology: jeb.biologists.org

Other Terms and Conditions:

STANDARD TERMS AND CONDITIONS

1. Description of Service; Defined Terms. This Republication License enables the User to obtain licenses for republication of one or more copyrighted works as described in detail on the relevant Order Confirmation (the "Work(s)"). Copyright Clearance Center, Inc. ("CCC") grants licenses through the Service on behalf of the rightsholder identified on the Order Confirmation (the "Rightsholder"). "Republication", as used herein, generally means the inclusion of a Work, in whole or in part, in a new work or works, also as described on the Order Confirmation. "User", as used herein, means the person or entity making such republication.

2. The terms set forth in the relevant Order Confirmation, and any terms set by the Rightsholder with respect to a particular Work, govern the terms of use of Works in connection with the Service. By using the Service, the person transacting for a republication license on behalf of the User represents and warrants that he/she/it (a) has been duly authorized by the User to accept, and hereby does accept, all such terms and conditions on behalf of User, and (b) shall inform User of all such terms and conditions. In the event such person is a "freelancer" or other third party independent of User and CCC, such party shall be deemed jointly a "User" for purposes of these terms and conditions. In any event, User shall be deemed to have accepted and agreed to all such terms and conditions if User republishes the Work in any fashion.

3. Scope of License; Limitations and Obligations.

3.1 All Works and all rights therein, including copyright rights, remain the sole and exclusive property of the Rightsholder. The license created by the exchange of an Order Confirmation (and/or any invoice) and payment by User of the full amount set forth on that document includes only those rights expressly set forth in the Order Confirmation and in these terms and conditions, and conveys no other rights in the Work(s) to User. All rights not expressly granted are hereby reserved.

3.2 General Payment Terms: You may pay by credit card or through an account with us payable at the end of the month. If you and we agree that you may establish a standing account with CCC, then the following terms apply: Remit Payment to: Copyright Clearance Center, Dept 001, P.O. Box 843006, Boston, MA 02284-3006. Payments Due: Invoices are payable upon their delivery to you (or upon our notice to you that they are available to you for downloading). After 30 days, outstanding amounts will be subject to a service charge of 1-1/2% per month or, if less, the maximum rate allowed by applicable law. Unless otherwise specifically set forth in the Order Confirmation or in a separate written agreement signed by CCC, invoices are due and payable on "net 30" terms. While User may exercise the rights licensed immediately upon issuance of the Order Confirmation, the license is automatically revoked and is null and void, as if it had never been issued, if complete payment for the license is not received on a timely basis either from User directly or through a payment agent, such as a credit card company.

3.3 Unless otherwise provided in the Order Confirmation, any grant of rights to User (i) is "one-time" (including the editions and product family specified in the license), (ii) is non-exclusive and non-transferable and (iii) is subject to

any and all limitations and restrictions (such as, but not limited to, limitations on duration of use or circulation) included in the Order Confirmation or invoice and/or in these terms and conditions. Upon completion of the licensed use, User shall either secure a new permission for further use of the Work(s) or immediately cease any new use of the Work(s) and shall render inaccessible (such as by deleting or by removing or severing links or other locators) any further copies of the Work (except for copies printed on paper in accordance with this license and still in User's stock at the end of such period).

3.4 In the event that the material for which a republication license is sought includes third party materials (such as photographs, illustrations, graphs, inserts and similar materials) which are identified in such material as having been used by permission, User is responsible for identifying, and seeking separate licenses (under this Service or otherwise) for, any of such third party materials; without a separate license, such third party materials may not be used.

3.5 Use of proper copyright notice for a Work is required as a condition of any license granted under the Service. Unless otherwise provided in the Order Confirmation, a proper copyright notice will read substantially as follows: "Republished with permission of [Rightsholder's name], from [Work's title, author, volume, edition number and year of copyright]; permission conveyed through Copyright Clearance Center, Inc. " Such notice must be provided in a reasonably legible font size and must be placed either immediately adjacent to the Work as used (for example, as part of a by-line or footnote but not as a separate electronic link) or in the place where substantially all other credits or notices for the new work containing the republished Work are located. Failure to include the required notice results in loss to the Rightsholder and CCC, and the User shall be liable to pay liquidated damages for each such failure equal to twice the use fee specified in the Order Confirmation, in addition to the use fee itself and any other fees and charges specified.

3.6 User may only make alterations to the Work if and as expressly set forth in the Order Confirmation. No Work may be used in any way that is defamatory, violates the rights of third parties (including such third parties' rights of copyright, privacy, publicity, or other tangible or intangible property), or is otherwise illegal, sexually explicit or obscene. In addition, User may not conjoin a Work with any other material that may result in damage to the reputation of the Rightsholder. User agrees to inform CCC if it becomes aware of any infringement of any rights in a Work and to cooperate with any reasonable request of CCC or the Rightsholder in connection therewith.

4. Indemnity. User hereby indemnifies and agrees to defend the Rightsholder and CCC, and their respective employees and directors, against all claims, liability, damages, costs and expenses, including legal fees and expenses, arising out of any use of a Work beyond the scope of the rights granted herein, or any use of a Work which has been altered in any unauthorized way by User, including claims of defamation or infringement of rights of copyright, publicity, privacy or other tangible or intangible property.

5. Limitation of Liability. UNDER NO CIRCUMSTANCES WILL CCC OR THE RIGHTSHOLDER BE LIABLE FOR ANY DIRECT, INDIRECT, CONSEQUENTIAL OR INCIDENTAL DAMAGES (INCLUDING WITHOUT LIMITATION DAMAGES FOR LOSS OF BUSINESS PROFITS OR INFORMATION, OR FOR BUSINESS INTERRUPTION) ARISING OUT OF THE USE OR INABILITY TO USE A WORK, EVEN IF ONE OF THEM HAS BEEN ADVISED OF THE POSSIBILITY OF SUCH DAMAGES. In any event, the total liability of the Rightsholder and CCC (including their respective employees and directors) shall not exceed the total amount actually paid by User for this license. User assumes full liability for the actions and omissions of its principals, employees, agents, affiliates, successors and assigns.

6. Limited Warranties. THE WORK(S) AND RIGHT(S) ARE PROVIDED "AS IS". CCC HAS THE RIGHT TO GRANT TO USER THE RIGHTS GRANTED IN THE ORDER CONFIRMATION DOCUMENT. CCC AND THE RIGHTSHOLDER DISCLAIM ALL OTHER WARRANTIES RELATING TO THE WORK(S) AND RIGHT(S), EITHER EXPRESS OR IMPLIED, INCLUDING WITHOUT LIMITATION IMPLIED WARRANTIES OF MERCHANTABILITY OR FITNESS FOR A PARTICULAR PURPOSE. ADDITIONAL RIGHTS MAY BE REQUIRED TO USE ILLUSTRATIONS, GRAPHS, PHOTOGRAPHS, ABSTRACTS, INSERTS OR OTHER PORTIONS OF THE WORK (AS OPPOSED TO THE ENTIRE WORK) IN A MANNER CONTEMPLATED BY USER; USER UNDERSTANDS AND AGREES THAT NEITHER CCC NOR THE RIGHTSHOLDER MAY HAVE SUCH ADDITIONAL RIGHTS TO GRANT.

7. Effect of Breach. Any failure by User to pay any amount when due, or any use by User of a Work beyond the scope of the license set forth in the Order Confirmation and/or these terms and conditions, shall be a material breach of the license created by the Order Confirmation and these terms and conditions. Any breach not cured within 30 days of written notice thereof shall result in immediate termination of such license without further notice. Any unauthorized (but licensable) use of a Work that is terminated immediately upon notice thereof may be liquidated by payment of the Rightsholder's ordinary license price therefor; any unauthorized (and unlicensable) use that is not terminated immediately for any reason (including, for example, because materials containing the Work cannot reasonably be recalled) will be subject to all remedies available at law or in equity, but in no event to a payment of less than three times the Rightsholder's ordinary license price for the most closely analogous licensable use plus Rightsholder's and/or CCC's costs and expenses incurred in collecting such payment.

8. **Miscellaneous.**

8.1 User acknowledges that CCC may, from time to time, make changes or additions to the Service or to these terms and conditions, and CCC reserves the right to send notice to the User by electronic mail or otherwise for the purposes of notifying User of such changes or additions; provided that any such changes or additions shall not apply to permissions already secured and paid for.

8.2 Use of User-related information collected through the Service is governed by CCC's privacy policy, available online here: http://www.copyright.com/content/cc3/en/tools/footer/privacypolicy.html.

8.3 The licensing transaction described in the Order Confirmation is personal to User. Therefore, User may not assign or transfer to any other person (whether a natural person or an organization of any kind) the license created by the Order Confirmation and these terms and conditions or any rights granted hereunder; provided, however, that User may assign such license in its entirety on written notice to CCC in the event of a transfer of all or substantially all of

User's rights in the new material which includes the Work(s) licensed under this Service.

8.4 No amendment or waiver of any terms is binding unless set forth in writing and signed by the parties. The Rightsholder and CCC hereby object to any terms contained in any writing prepared by the User or its principals, employees, agents or affiliates and purporting to govern or otherwise relate to the licensing transaction described in the Order Confirmation, which terms are in any way inconsistent with any terms set forth in the Order Confirmation and/or in these terms and conditions or CCC's standard operating procedures, whether such writing is prepared prior to, simultaneously with or subsequent to the Order Confirmation, and whether such writing appears on a copy of the Order Confirmation or in a separate instrument.

8.5 The licensing transaction described in the Order Confirmation document shall be governed by and construed under the law of the State of New York, USA, without regard to the principles thereof of conflicts of law. Any case, controversy, suit, action, or proceeding arising out of, in connection with, or related to such licensing transaction shall be brought, at CCC's sole discretion, in any federal or state court located in the County of New York, State of New York, USA, or in any federal or state court whose geographical jurisdiction covers the location of the Rightsholder set forth in the Order Confirmation. The parties expressly submit to the personal jurisdiction and venue of each such federal or state court.If you have any comments or questions about the Service or Copyright Clearance Center, please contact us at 978-750-8400 or send an e-mail to info@copyright.com.

v 1.1

Close

Confirmation Number: 11572873

Citation Information

Order Detail ID: 69890730

Journal of experimental biology by Company of Biologists Reproduced with permission of COMPANY OF BIOLOGISTS LTD. in the format Republish in a thesis/dissertation via Copyright Clearance Center.

Close

JOHN WILEY AND SONS LICENSE TERMS AND CONDITIONS

Jun 27, 2016

This Agreement between Krystal Cadle ("You") and John Wiley and Sons ("John Wiley and Sons") consists of your license details and the terms and conditions provided by John Wiley and Sons and Copyright Clearance Center.

License Number	3897270622791
License date	Jun 27, 2016
Licensed Content Publisher	John Wiley and Sons
Licensed Content Publication	Angewandte Chemie International Edition
Licensed Content Title	Spider Silk: From Soluble Protein to Extraordinary Fiber
Licensed Content Author	Markus Heim,David Keerl,Thomas Scheibel
Licensed Content Date	Feb 11, 2009
Licensed Content Pages	13
Type of use	Dissertation/Thesis
Requestor type	University/Academic
Format	Print and electronic
Portion	Figure/table
Number of figures/tables	2
Original Wiley figure/table number(s)	Table 1 and Table 2
Will you be translating?	No
Title of your thesis / dissertation	The Role the N-Terminal Domain Plays in Spidroin Assembly
Expected completion date	Aug 2016
Expected size (number of pages)	150
Requestor Location	Krystal Cadle 245H Campus Dr. CENTRAL, SC 29630 United States Attn: Krystal Cadle
Publisher Tax ID	EU826007151
Billing Type	Invoice
Billing Address	Krystal Cadle 245H Campus Dr. CENTRAL, SC 29630 United States Attn: Krystal Cadle
Total	0.00 USD
Terms and Conditions	

TERMS AND CONDITIONS

This copyrighted material is owned by or exclusively licensed to John Wiley & Sons, Inc. or one of its group companies (each a"Wiley Company") or handled on behalf of a society with which a Wiley Company has exclusive publishing rights in relation to a particular work (collectively "WILEY"). By clicking "accept" in connection with completing this licensing transaction, you agree that the following terms and conditions apply to this transaction (along with the billing and payment terms and conditions established by the Copyright Clearance Center Inc., ("CCC's Billing and Payment terms and conditions"), at the time that you opened your RightsLink account (these are available at any time at http://myaccount.copyright.com).

Terms and Conditions

- The materials you have requested permission to reproduce or reuse (the "Wiley Materials") are protected by copyright.

- You are hereby granted a personal, non-exclusive, non-sub licensable (on a stand-alone basis), non-transferable, worldwide, limited license to reproduce the Wiley Materials for the purpose specified in the licensing process. This license, **and any CONTENT (PDF or image file) purchased as part of your order,** is for a one-time use only and limited to any maximum distribution number specified in the license. The first instance of republication or reuse granted by this license must be completed within two years of the date of the grant of this license (although copies prepared before the end date may be distributed thereafter). The Wiley Materials shall not be used in any other manner or for any other purpose, beyond what is granted in the license. Permission is granted subject to an appropriate acknowledgement given to the author, title of the material/book/journal and the publisher. You shall also duplicate the copyright notice that appears in the Wiley publication in your use of the Wiley Material. Permission is also granted on the understanding that nowhere in the text is a previously published source acknowledged for all or part of this Wiley Material. Any third party content is expressly excluded from this permission.

- With respect to the Wiley Materials, all rights are reserved. Except as expressly granted by the terms of the license, no part of the Wiley Materials may be copied, modified, adapted (except for minor reformatting required by the new Publication), translated, reproduced, transferred or distributed, in any form or by any means, and no derivative works may be made based on the Wiley Materials without the prior permission of the respective copyright owner.**For STM Signatory Publishers clearing permission under the terms of the STM Permissions Guidelines only, the terms of the license are extended to include subsequent editions and for editions in other languages, provided such editions are for the work as a whole in situ and does not involve the separate exploitation of the permitted figures or extracts,** You may not alter, remove or suppress in any manner any copyright, trademark or other notices displayed by the Wiley Materials. You may not license, rent, sell, loan, lease, pledge, offer as security, transfer or assign the Wiley Materials on a stand-alone basis, or any of the rights granted to you hereunder to any other person.

- The Wiley Materials and all of the intellectual property rights therein shall at all times remain the exclusive property of John Wiley & Sons Inc, the Wiley Companies, or their respective licensors, and your interest therein is only that of having possession of and the right to reproduce the Wiley Materials pursuant to Section 2 herein during the continuance of this Agreement. You agree that you own no right, title or interest in or to the Wiley Materials or any of the intellectual property rights therein. You shall have no rights hereunder other than the license as provided for above in Section 2. No right,

license or interest to any trademark, trade name, service mark or other branding ("Marks") of WILEY or its licensors is granted hereunder, and you agree that you shall not assert any such right, license or interest with respect thereto

- NEITHER WILEY NOR ITS LICENSORS MAKES ANY WARRANTY OR REPRESENTATION OF ANY KIND TO YOU OR ANY THIRD PARTY, EXPRESS, IMPLIED OR STATUTORY, WITH RESPECT TO THE MATERIALS OR THE ACCURACY OF ANY INFORMATION CONTAINED IN THE MATERIALS, INCLUDING, WITHOUT LIMITATION, ANY IMPLIED WARRANTY OF MERCHANTABILITY, ACCURACY, SATISFACTORY QUALITY, FITNESS FOR A PARTICULAR PURPOSE, USABILITY, INTEGRATION OR NON-INFRINGEMENT AND ALL SUCH WARRANTIES ARE HEREBY EXCLUDED BY WILEY AND ITS LICENSORS AND WAIVED BY YOU.

- WILEY shall have the right to terminate this Agreement immediately upon breach of this Agreement by you.

- You shall indemnify, defend and hold harmless WILEY, its Licensors and their respective directors, officers, agents and employees, from and against any actual or threatened claims, demands, causes of action or proceedings arising from any breach of this Agreement by you.

- IN NO EVENT SHALL WILEY OR ITS LICENSORS BE LIABLE TO YOU OR ANY OTHER PARTY OR ANY OTHER PERSON OR ENTITY FOR ANY SPECIAL, CONSEQUENTIAL, INCIDENTAL, INDIRECT, EXEMPLARY OR PUNITIVE DAMAGES, HOWEVER CAUSED, ARISING OUT OF OR IN CONNECTION WITH THE DOWNLOADING, PROVISIONING, VIEWING OR USE OF THE MATERIALS REGARDLESS OF THE FORM OF ACTION, WHETHER FOR BREACH OF CONTRACT, BREACH OF WARRANTY, TORT, NEGLIGENCE, INFRINGEMENT OR OTHERWISE (INCLUDING, WITHOUT LIMITATION, DAMAGES BASED ON LOSS OF PROFITS, DATA, FILES, USE, BUSINESS OPPORTUNITY OR CLAIMS OF THIRD PARTIES), AND WHETHER OR NOT THE PARTY HAS BEEN ADVISED OF THE POSSIBILITY OF SUCH DAMAGES. THIS LIMITATION SHALL APPLY NOTWITHSTANDING ANY FAILURE OF ESSENTIAL PURPOSE OF ANY LIMITED REMEDY PROVIDED HEREIN.

- Should any provision of this Agreement be held by a court of competent jurisdiction to be illegal, invalid, or unenforceable, that provision shall be deemed amended to achieve as nearly as possible the same economic effect as the original provision, and the legality, validity and enforceability of the remaining provisions of this Agreement shall not be affected or impaired thereby.

- The failure of either party to enforce any term or condition of this Agreement shall not constitute a waiver of either party's right to enforce each and every term and condition of this Agreement. No breach under this agreement shall be deemed waived or excused by either party unless such waiver or consent is in writing signed by the party granting such waiver or consent. The waiver by or consent of a party to a breach of any provision of this Agreement shall not operate or be construed as a waiver of or consent to any other or subsequent breach by such other party.

- This Agreement may not be assigned (including by operation of law or otherwise) by you without WILEY's prior written consent.

- Any fee required for this permission shall be non-refundable after thirty (30) days from receipt by the CCC.

- These terms and conditions together with CCC's Billing and Payment terms and conditions (which are incorporated herein) form the entire agreement between you and WILEY concerning this licensing transaction and (in the absence of fraud) supersedes all prior agreements and representations of the parties, oral or written. This Agreement may not be amended except in writing signed by both parties. This Agreement shall be binding upon and inure to the benefit of the parties' successors, legal representatives, and authorized assigns.

- In the event of any conflict between your obligations established by these terms and conditions and those established by CCC's Billing and Payment terms and conditions, these terms and conditions shall prevail.

- WILEY expressly reserves all rights not specifically granted in the combination of (i) the license details provided by you and accepted in the course of this licensing transaction, (ii) these terms and conditions and (iii) CCC's Billing and Payment terms and conditions.

- This Agreement will be void if the Type of Use, Format, Circulation, or Requestor Type was misrepresented during the licensing process.

- This Agreement shall be governed by and construed in accordance with the laws of the State of New York, USA, without regards to such state's conflict of law rules. Any legal action, suit or proceeding arising out of or relating to these Terms and Conditions or the breach thereof shall be instituted in a court of competent jurisdiction in New York County in the State of New York in the United States of America and each party hereby consents and submits to the personal jurisdiction of such court, waives any objection to venue in such court and consents to service of process by registered or certified mail, return receipt requested, at the last known address of such party.

WILEY OPEN ACCESS TERMS AND CONDITIONS

Wiley Publishes Open Access Articles in fully Open Access Journals and in Subscription journals offering Online Open. Although most of the fully Open Access journals publish open access articles under the terms of the Creative Commons Attribution (CC BY) License only, the subscription journals and a few of the Open Access Journals offer a choice of Creative Commons Licenses. The license type is clearly identified on the article.

The Creative Commons Attribution License

The Creative Commons Attribution License (CC-BY) allows users to copy, distribute and transmit an article, adapt the article and make commercial use of the article. The CC-BY license permits commercial and non-

Creative Commons Attribution Non-Commercial License

The Creative Commons Attribution Non-Commercial (CC-BY-NC)License permits use, distribution and reproduction in any medium, provided the original work is properly cited and is not used for commercial purposes.(see below)

Creative Commons Attribution-Non-Commercial-NoDerivs License

The Creative Commons Attribution Non-Commercial-NoDerivs License (CC-BY-NC-ND) permits use, distribution and reproduction in any medium, provided the original work is properly cited, is not used for commercial purposes and no modifications or adaptations are made. (see below)

Use by commercial "for-profit" organizations
Use of Wiley Open Access articles for commercial, promotional, or marketing purposes requires further explicit permission from Wiley and will be subject to a fee.
Further details can be found on Wiley Online Library
http://olabout.wiley.com/WileyCDA/Section/id-410895.html

Other Terms and Conditions:

v1.10 Last updated September 2015

Questions? customercare@copyright.com or +1-855-239-3415 (toll free in the US) or +1-978-646-2777.

ELSEVIER LICENSE
TERMS AND CONDITIONS

Jun 27, 2016

This Agreement between Krystal Cadle ("You") and Elsevier ("Elsevier") consists of your license details and the terms and conditions provided by Elsevier and Copyright Clearance Center.

License Number	3897260062940
License date	Jun 27, 2016
Licensed Content Publisher	Elsevier
Licensed Content Publication	Elsevier Books
Licensed Content Title	Progress in Molecular Biology and Translational Science
Licensed Content Author	Martin Humenik,Thomas Scheibel,Andrew Smith
Licensed Content Date	2011
Licensed Content Pages	55
Start Page	131
End Page	185
Type of Use	reuse in a thesis/dissertation
Intended publisher of new work	other
Portion	figures/tables/illustrations
Number of figures/tables/illustrations	1
Format	both print and electronic
Are you the author of this Elsevier chapter?	No
Will you be translating?	No
Order reference number	
Original figure numbers	Figure 3
Title of your thesis/dissertation	The Role the N-Terminal Domain Plays in Spidroin Assembly
Expected completion date	Aug 2016
Estimated size (number of pages)	150
Elsevier VAT number	GB 494 6272 12
Requestor Location	Krystal Cadle 245H Campus Dr. CENTRAL, SC 29630 United States Attn: Krystal Cadle
Total	0.00 USD
Terms and Conditions	

INTRODUCTION

1. The publisher for this copyrighted material is Elsevier. By clicking "accept" in connection with completing this licensing transaction, you agree that the following terms and conditions apply to this transaction (along with the Billing and Payment terms and conditions established by Copyright Clearance Center, Inc. ("CCC"), at the time that you opened your Rightslink account and that are available at any time at http://myaccount.copyright.com).

GENERAL TERMS

2. Elsevier hereby grants you permission to reproduce the aforementioned material subject to the terms and conditions indicated.
3. Acknowledgement: If any part of the material to be used (for example, figures) has appeared in our publication with credit or acknowledgement to another source, permission must also be sought from that source. If such permission is not obtained then that material may not be included in your publication/copies. Suitable acknowledgement to the source must be made, either as a footnote or in a reference list at the end of your publication, as follows:
"Reprinted from Publication title, Vol /edition number, Author(s), Title of article / title of chapter, Pages No., Copyright (Year), with permission from Elsevier [OR APPLICABLE SOCIETY COPYRIGHT OWNER]." Also Lancet special credit - "Reprinted from The Lancet, Vol. number, Author(s), Title of article, Pages No., Copyright (Year), with permission from Elsevier."
4. Reproduction of this material is confined to the purpose and/or media for which permission is hereby given.
5. Altering/Modifying Material: Not Permitted. However figures and illustrations may be altered/adapted minimally to serve your work. Any other abbreviations, additions, deletions and/or any other alterations shall be made only with prior written authorization of Elsevier Ltd. (Please contact Elsevier at permissions@elsevier.com)
6. If the permission fee for the requested use of our material is waived in this instance, please be advised that your future requests for Elsevier materials may attract a fee.
7. Reservation of Rights: Publisher reserves all rights not specifically granted in the combination of (i) the license details provided by you and accepted in the course of this licensing transaction, (ii) these terms and conditions and (iii) CCC's Billing and Payment terms and conditions.
8. License Contingent Upon Payment: While you may exercise the rights licensed immediately upon issuance of the license at the end of the licensing process for the transaction, provided that you have disclosed complete and accurate details of your proposed use, no license is finally effective unless and until full payment is received from you (either by publisher or by CCC) as provided in CCC's Billing and Payment terms and conditions. If full payment is not received on a timely basis, then any license preliminarily granted shall be deemed automatically revoked and shall be void as if never granted. Further, in the event that you breach any of these terms and conditions or any of CCC's Billing and Payment terms and conditions, the license is automatically revoked and shall be void as if never granted. Use of materials as described in a revoked license, as well as any use of the materials beyond the scope of an unrevoked license, may constitute copyright infringement and publisher reserves the right to take any and all action to protect its copyright in the materials.
9. Warranties: Publisher makes no representations or warranties with respect to the licensed material.
10. Indemnity: You hereby indemnify and agree to hold harmless publisher and CCC, and their respective officers, directors, employees and agents, from and against any and all claims arising out of your use of the licensed material other than as specifically authorized pursuant to this license.
11. No Transfer of License: This license is personal to you and may not be sublicensed, assigned, or transferred by you to any other person without publisher's written permission.
12. No Amendment Except in Writing: This license may not be amended except in a writing

signed by both parties (or, in the case of publisher, by CCC on publisher's behalf).
13. Objection to Contrary Terms: Publisher hereby objects to any terms contained in any purchase order, acknowledgment, check endorsement or other writing prepared by you, which terms are inconsistent with these terms and conditions or CCC's Billing and Payment terms and conditions. These terms and conditions, together with CCC's Billing and Payment terms and conditions (which are incorporated herein), comprise the entire agreement between you and publisher (and CCC) concerning this licensing transaction. In the event of any conflict between your obligations established by these terms and conditions and those established by CCC's Billing and Payment terms and conditions, these terms and conditions shall control.
14. Revocation: Elsevier or Copyright Clearance Center may deny the permissions described in this License at their sole discretion, for any reason or no reason, with a full refund payable to you. Notice of such denial will be made using the contact information provided by you. Failure to receive such notice will not alter or invalidate the denial. In no event will Elsevier or Copyright Clearance Center be responsible or liable for any costs, expenses or damage incurred by you as a result of a denial of your permission request, other than a refund of the amount(s) paid by you to Elsevier and/or Copyright Clearance Center for denied permissions.

LIMITED LICENSE

The following terms and conditions apply only to specific license types:
15. **Translation**: This permission is granted for non-exclusive world **English** rights only unless your license was granted for translation rights. If you licensed translation rights you may only translate this content into the languages you requested. A professional translator must perform all translations and reproduce the content word for word preserving the integrity of the article.
16. **Posting licensed content on any Website**: The following terms and conditions apply as follows: Licensing material from an Elsevier journal: All content posted to the web site must maintain the copyright information line on the bottom of each image; A hyper-text must be included to the Homepage of the journal from which you are licensing at http://www.sciencedirect.com/science/journal/xxxxx or the Elsevier homepage for books at http://www.elsevier.com; Central Storage: This license does not include permission for a scanned version of the material to be stored in a central repository such as that provided by Heron/XanEdu.
Licensing material from an Elsevier book: A hyper-text link must be included to the Elsevier homepage at http://www.elsevier.com . All content posted to the web site must maintain the copyright information line on the bottom of each image.

Posting licensed content on Electronic reserve: In addition to the above the following clauses are applicable: The web site must be password-protected and made available only to bona fide students registered on a relevant course. This permission is granted for 1 year only. You may obtain a new license for future website posting.
17. **For journal authors:** the following clauses are applicable in addition to the above:
Preprints:
A preprint is an author's own write-up of research results and analysis, it has not been peer-reviewed, nor has it had any other value added to it by a publisher (such as formatting, copyright, technical enhancement etc.).
Authors can share their preprints anywhere at any time. Preprints should not be added to or enhanced in any way in order to appear more like, or to substitute for, the final versions of articles however authors can update their preprints on arXiv or RePEc with their Accepted Author Manuscript (see below).
If accepted for publication, we encourage authors to link from the preprint to their formal publication via its DOI. Millions of researchers have access to the formal publications on ScienceDirect, and so links will help users to find, access, cite and use the best available version. Please note that Cell Press, The Lancet and some society-owned have different

preprint policies. Information on these policies is available on the journal homepage.
Accepted Author Manuscripts: An accepted author manuscript is the manuscript of an article that has been accepted for publication and which typically includes author-incorporated changes suggested during submission, peer review and editor-author communications.
Authors can share their accepted author manuscript:

- immediately
  - via their non-commercial person homepage or blog
  - by updating a preprint in arXiv or RePEc with the accepted manuscript
  - via their research institute or institutional repository for internal institutional uses or as part of an invitation-only research collaboration work-group
  - directly by providing copies to their students or to research collaborators for their personal use
  - for private scholarly sharing as part of an invitation-only work group on commercial sites with which Elsevier has an agreement
- after the embargo period
  - via non-commercial hosting platforms such as their institutional repository
  - via commercial sites with which Elsevier has an agreement

In all cases accepted manuscripts should:

- link to the formal publication via its DOI
- bear a CC-BY-NC-ND license - this is easy to do
- if aggregated with other manuscripts, for example in a repository or other site, be shared in alignment with our hosting policy not be added to or enhanced in any way to appear more like, or to substitute for, the published journal article.

Published journal article (JPA): A published journal article (PJA) is the definitive final record of published research that appears or will appear in the journal and embodies all value-adding publishing activities including peer review co-ordination, copy-editing, formatting, (if relevant) pagination and online enrichment.
Policies for sharing publishing journal articles differ for subscription and gold open access articles:
Subscription Articles: If you are an author, please share a link to your article rather than the full-text. Millions of researchers have access to the formal publications on ScienceDirect, and so links will help your users to find, access, cite, and use the best available version.
Theses and dissertations which contain embedded PJAs as part of the formal submission can be posted publicly by the awarding institution with DOI links back to the formal publications on ScienceDirect.
If you are affiliated with a library that subscribes to ScienceDirect you have additional private sharing rights for others' research accessed under that agreement. This includes use for classroom teaching and internal training at the institution (including use in course packs and courseware programs), and inclusion of the article for grant funding purposes.
Gold Open Access Articles: May be shared according to the author-selected end-user license and should contain a CrossMark logo, the end user license, and a DOI link to the formal publication on ScienceDirect.
Please refer to Elsevier's posting policy for further information.
18. **For book authors** the following clauses are applicable in addition to the above:
Authors are permitted to place a brief summary of their work online only. You are not allowed to download and post the published electronic version of your chapter, nor may you scan the printed edition to create an electronic version. **Posting to a repository:** Authors are permitted to post a summary of their chapter only in their institution's repository.
19. **Thesis/Dissertation**: If your license is for use in a thesis/dissertation your thesis may be

submitted to your institution in either print or electronic form. Should your thesis be published commercially, please reapply for permission. These requirements include permission for the Library and Archives of Canada to supply single copies, on demand, of the complete thesis and include permission for Proquest/UMI to supply single copies, on demand, of the complete thesis. Should your thesis be published commercially, please reapply for permission. Theses and dissertations which contain embedded PJAs as part of the formal submission can be posted publicly by the awarding institution with DOI links back to the formal publications on ScienceDirect.

Elsevier Open Access Terms and Conditions

You can publish open access with Elsevier in hundreds of open access journals or in nearly 2000 established subscription journals that support open access publishing. Permitted third party re-use of these open access articles is defined by the author's choice of Creative Commons user license. See our open access license policy for more information.

Terms & Conditions applicable to all Open Access articles published with Elsevier:

Any reuse of the article must not represent the author as endorsing the adaptation of the article nor should the article be modified in such a way as to damage the author's honour or reputation. If any changes have been made, such changes must be clearly indicated.

The author(s) must be appropriately credited and we ask that you include the end user license and a DOI link to the formal publication on ScienceDirect.

If any part of the material to be used (for example, figures) has appeared in our publication with credit or acknowledgement to another source it is the responsibility of the user to ensure their reuse complies with the terms and conditions determined by the rights holder.

Additional Terms & Conditions applicable to each Creative Commons user license:

CC BY: The CC-BY license allows users to copy, to create extracts, abstracts and new works from the Article, to alter and revise the Article and to make commercial use of the Article (including reuse and/or resale of the Article by commercial entities), provided the user gives appropriate credit (with a link to the formal publication through the relevant DOI), provides a link to the license, indicates if changes were made and the licensor is not represented as endorsing the use made of the work. The full details of the license are available at http://creativecommons.org/licenses/by/4.0.

CC BY NC SA: The CC BY-NC-SA license allows users to copy, to create extracts, abstracts and new works from the Article, to alter and revise the Article, provided this is not done for commercial purposes, and that the user gives appropriate credit (with a link to the formal publication through the relevant DOI), provides a link to the license, indicates if changes were made and the licensor is not represented as endorsing the use made of the work. Further, any new works must be made available on the same conditions. The full details of the license are available at http://creativecommons.org/licenses/by-nc-sa/4.0.

CC BY NC ND: The CC BY-NC-ND license allows users to copy and distribute the Article, provided this is not done for commercial purposes and further does not permit distribution of the Article if it is changed or edited in any way, and provided the user gives appropriate credit (with a link to the formal publication through the relevant DOI), provides a link to the license, and that the licensor is not represented as endorsing the use made of the work. The full details of the license are available at http://creativecommons.org/licenses/by-nc-nd/4.0.

Any commercial reuse of Open Access articles published with a CC BY NC SA or CC BY NC ND license requires permission from Elsevier and will be subject to a fee.

Commercial reuse includes:

- Associating advertising with the full text of the Article
- Charging fees for document delivery or access
- Article aggregation
- Systematic distribution via e-mail lists or share buttons

Posting or linking by commercial companies for use by customers of those companies.

20. **Other Conditions**:

v1.8

Questions? customercare@copyright.com or +1-855-239-3415 (toll free in the US) or +1-978-646-2777.

NATURE PUBLISHING GROUP LICENSE TERMS AND CONDITIONS

Jun 27, 2016

This Agreement between Krystal Cadle ("You") and Nature Publishing Group ("Nature Publishing Group") consists of your license details and the terms and conditions provided by Nature Publishing Group and Copyright Clearance Center.

License Number	3897260306525
License date	Jun 27, 2016
Licensed Content Publisher	Nature Publishing Group
Licensed Content Publication	Nature
Licensed Content Title	Self-assembly of spider silk proteins is controlled by a pH-sensitive relay
Licensed Content Author	Glareh Askarieh, My Hedhammar, Kerstin Nordling, Alejandra Saenz, Cristina Casals, Anna Rising
Licensed Content Date	May 13, 2010
Licensed Content Volume Number	465
Licensed Content Issue Number	7295
Type of Use	reuse in a dissertation / thesis
Requestor type	academic/educational
Format	print and electronic
Portion	figures/tables/illustrations
Number of figures/tables/illustrations	1
High-res required	no
Figures	Figure 2
Author of this NPG article	no
Your reference number	
Title of your thesis / dissertation	The Role the N-Terminal Domain Plays in Spidroin Assembly
Expected completion date	Aug 2016
Estimated size (number of pages)	150
Requestor Location	Krystal Cadle 245H Campus Dr. CENTRAL, SC 29630 United States Attn: Krystal Cadle
Billing Type	Invoice
Billing Address	Krystal Cadle 245H Campus Dr.

CENTRAL, SC 29630
United States
Attn: Krystal Cadle

Total 0.00 USD

Terms and Conditions

Terms and Conditions for Permissions

Nature Publishing Group hereby grants you a non-exclusive license to reproduce this material for this purpose, and for no other use,subject to the conditions below:

1. NPG warrants that it has, to the best of its knowledge, the rights to license reuse of this material. However, you should ensure that the material you are requesting is original to Nature Publishing Group and does not carry the copyright of another entity (as credited in the published version). If the credit line on any part of the material you have requested indicates that it was reprinted or adapted by NPG with permission from another source, then you should also seek permission from that source to reuse the material.

2. Permission granted free of charge for material in print is also usually granted for any electronic version of that work, provided that the material is incidental to the work as a whole and that the electronic version is essentially equivalent to, or substitutes for, the print version.Where print permission has been granted for a fee, separate permission must be obtained for any additional, electronic re-use (unless, as in the case of a full paper, this has already been accounted for during your initial request in the calculation of a print run).NB: In all cases, web-based use of full-text articles must be authorized separately through the 'Use on a Web Site' option when requesting permission.

3. Permission granted for a first edition does not apply to second and subsequent editions and for editions in other languages (except for signatories to the STM Permissions Guidelines, or where the first edition permission was granted for free).

4. Nature Publishing Group's permission must be acknowledged next to the figure, table or abstract in print. In electronic form, this acknowledgement must be visible at the same time as the figure/table/abstract, and must be hyperlinked to the journal's homepage.

5. The credit line should read:
   Reprinted by permission from Macmillan Publishers Ltd: [JOURNAL NAME] (reference citation), copyright (year of publication)
   For AOP papers, the credit line should read:
   Reprinted by permission from Macmillan Publishers Ltd: [JOURNAL NAME], advance online publication, day month year (doi: 10.1038/sj.[JOURNAL ACRONYM].XXXXX)

   Note: For republication from the *British Journal of Cancer,* the following credit lines apply.
   Reprinted by permission from Macmillan Publishers Ltd on behalf of Cancer Research UK: [JOURNAL NAME] (reference citation), copyright (year of publication)For AOP papers, the credit line should read:
   Reprinted by permission from Macmillan Publishers Ltd on behalf of Cancer Research UK: [JOURNAL NAME], advance online publication, day month year (doi: 10.1038/sj.[JOURNAL ACRONYM].XXXXX)

6. Adaptations of single figures do not require NPG approval. However, the adaptation should be credited as follows:

   Adapted by permission from Macmillan Publishers Ltd: [JOURNAL NAME] (reference citation), copyright (year of publication)

   Note: For adaptation from the *British Journal of Cancer,* the following credit line applies.
   Adapted by permission from Macmillan Publishers Ltd on behalf of Cancer Research UK: [JOURNAL NAME] (reference citation), copyright (year of publication)

7. Translations of 401 words up to a whole article require NPG approval. Please visit http://www.macmillanmedicalcommunications.com for more information.Translations of up to a 400 words do not require NPG approval. The translation should be credited as follows:

   Translated by permission from Macmillan Publishers Ltd: [JOURNAL NAME] (reference citation), copyright (year of publication).

   Note: For translation from the *British Journal of Cancer,* the following credit line applies.
   Translated by permission from Macmillan Publishers Ltd on behalf of Cancer Research UK: [JOURNAL NAME] (reference citation), copyright (year of publication)

We are certain that all parties will benefit from this agreement and wish you the best in the use of this material. Thank you.
Special Terms:
v1.1

Questions? customercare@copyright.com or +1-855-239-3415 (toll free in the US) or +1-978-646-2777.

Title: Morphology and Composition of the Spider Major Ampullate Gland and Dragline Silk

Author: Marlene Andersson, Lena Holm, Yvonne Ridderstråle, et al

Publication: Biomacromolecules

Publisher: American Chemical Society

Date: Aug 1, 2013

PERMISSION/LICENSE IS GRANTED FOR YOUR ORDER AT NO CHARGE

This type of permission/license, instead of the standard Terms & Conditions, is sent to you because no fee is being charged for your order. Please note the following:

- Permission is granted for your request in both print and electronic formats, and translations.
- If figures and/or tables were requested, they may be adapted or used in part.
- Please print this page for your records and send a copy of it to your publisher/graduate school.
- Appropriate credit for the requested material should be given as follows: "Reprinted (adapted) with permission from (COMPLETE REFERENCE CITATION). Copyright (YEAR) American Chemical Society." Insert appropriate information in place of the capitalized words.
- One-time permission is granted only for the use specified in your request. No additional uses are granted (such as derivative works or other editions). For any other uses, please submit a new request.

If credit is given to another source for the material you requested, permission must be obtained from that source.

BACK CLOSE WINDOW

PLOS | BIOLOGY

Carbonic Anhydrase Generates CO_2 and H^+ That Drive Spider Silk Formation Via Opposite Effects on the Terminal Domains

Marlene Andersson, Gefei Chen, Martins Otikovs, Michael Landreh, Kerstin Nordling, Nina Kronqvist, Per Westermark, Hans Jörnvall, Stefan Knight, Yvonne Ridderstråle, Lena Holm, Qing Meng, Kristaps Jaudzems, Mitchell Chesler, Jan Johansson, Anna Rising

Published: August 5, 2014 • http://dx.doi.org/10.1371/journal.pbio.1001921

Abstract

Spider silk fibers are produced from soluble proteins (spidroins) under ambient conditions in a complex but poorly understood process. Spidroins are highly repetitive in sequence but capped by nonrepetitive N- and C-terminal domains (NT and CT) that are suggested to regulate fiber conversion in similar manners. By using ion selective microelectrodes we found that the pH gradient in the silk gland is much broader than previously known. Surprisingly, the terminal domains respond in opposite ways when pH is decreased from 7 to 5: Urea denaturation and temperature stability assays show that NT dimers get significantly stabilized and then lock the spidroins into multimers, whereas CT on the other hand is destabilized and unfolds into ThT-positive β-sheet amyloid fibrils, which can trigger fiber formation. There is a high carbon dioxide pressure (pCO_2) in distal parts of the gland, and a CO_2 analogue interacts with buried regions in CT as determined by nuclear magnetic resonance (NMR) spectroscopy. Activity staining of histological sections and inhibition experiments reveal that the pH gradient is created by carbonic anhydrase. Carbonic anhydrase activity emerges in the same region of the gland as the opposite effects on NT and CT stability occur. These synchronous events suggest a novel CO_2 and proton-dependent lock and trigger mechanism of spider silk formation.

Author Summary

The spinning process of spider silk is crucial for making webs or other complex constructions to catch spider's prey. The main components of the silk are spidroins, which are large and repetitive proteins that have conserved nonrepetitive terminal domains (NT and CT). Spiders manage both to store the highly aggregation-prone spidroins in solution at extreme concentrations in the silk glands and then to rapidly convert these spidroins into a solid fiber within fractions of a second as they spin fibres. This process has been extensively studied and is thought to involve a pH gradient, but how this pH gradient is generated and maintained was not resolved. Here, we measured the pH at locations along the ampullate gland and determined that the pH decreases to 5.7 in the middle of the spinning duct. We also observed that the carbon dioxide pressure is simultaneously increased and that its accumulation may affect the stability of CT. We find that active carbonic anhydrase (CA) is crucial to maintain the pH gradient along the gland. Detailed molecular studies of NT and CT under the disparate conditions present along the gland revealed a lock and trigger mechanism whereby in more neutral pH conditions, precocious spidroin aggregation is prevented, and when in more acidic pH conditions, NT dimers firmly interconnect the spidroins and the CT unfolds into β-sheet nuclei that can trigger rapid polymerization of the spidroins. We conclude that this mechanism enables temporal and spatial control of silk formation and may be harnessed in attempts to produce artificial silk replicas.

Citation: Andersson M, Chen G, Otikovs M, Landreh M, Nordling K, Kronqvist N, et al. (2014) Carbonic Anhydrase Generates CO_2 and H^+ That Drive Spider Silk Formation Via Opposite Effects on the Terminal Domains. PLoS Biol 12(8): e1001921. doi:10.1371/journal.pbio.1001921

Academic Editor: Gregory A. Petsko, Brandeis University, United States of America

Received: January 27, 2014; **Accepted:** June 26, 2014; **Published:** August 5, 2014

Funding: The Swedish Research Council (www.vr.se) and the Chinese Scholarship Council (CSC). The funders had no role in study design, data collection and analysis, decision to publish, or preparation of the manuscript.

Competing interests: The authors have declared that no competing interests exist.

Abbreviations: CA, carbonic anhydrase; CD, circular dichroism; CT, C-terminal domain; DMSO, dimethyl sulfoxide; EM, electron microscopy; ESI, electrospray ionization; HDX-MS, hydrogen-deuterium exchange mass spectrometry; HEPES, hydroxyethyl piperazineethanesulfonic acid; HSQC, heteronuclear single quantum coherence; ISM, ion selective microelectrode; LC-MS/MS, liquid chromatography–tandem mass spectrometry; Ma, major ampullate; MES, morpholineethanesulfonic acid; Mi, minor ampullate; MS, mass spectrometry; NMR, nuclear magnetic resonance; NT, N-terminal domain; pCO_2, carbon dioxide pressure; Sp, spidroin; Spidroin, spider silk protein; ThT, Thioflavin T

11200 Rockville Pike
Suite 302
Rockville, Maryland 20852

August 19, 2011

American Society for Biochemistry and Molecular Biology

To whom it may concern,

It is the policy of the American Society for Biochemistry and Molecular Biology to allow reuse of any material published in its journals (the Journal of Biological Chemistry, Molecular & Cellular Proteomics and the Journal of Lipid Research) in a thesis or dissertation at no cost and with no explicit permission needed. Please see our copyright permissions page on the journal site for more information.

Best wishes,

Sarah Crespi

American Society for Biochemistry and Molecular Biology
11200 Rockville Pike, Rockville, MD
Suite 302
240-283-6616
JBC | MCP | JLR

Thesis/Dissertation Reuse Request

Taylor & Francis is pleased to offer reuses of its content for a thesis or dissertation free of charge contingent on resubmission of permission request if work is published.

BACK | CLOSE WINDOW

THE AMERICAN ASSOCIATION FOR THE ADVANCEMENT OF SCIENCE LICENSE TERMS AND CONDITIONS

Jun 27, 2016

This Agreement between Krystal Cadle ("You") and The American Association for the Advancement of Science ("The American Association for the Advancement of Science") consists of your license details and the terms and conditions provided by The American Association for the Advancement of Science and Copyright Clearance Center.

License Number	3897261371600
License date	Jun 27, 2016
Licensed Content Publisher	The American Association for the Advancement of Science
Licensed Content Publication	Science
Licensed Content Title	New Opportunities for an Ancient Material
Licensed Content Author	Fiorenzo G. Omenetto,David L. Kaplan
Licensed Content Date	Jul 30, 2010
Licensed Content Volume Number	329
Licensed Content Issue Number	5991
Volume number	329
Issue number	5991
Type of Use	Thesis / Dissertation
Requestor type	Scientist/individual at a research institution
Format	Print and electronic
Portion	Figure
Number of figures/tables	1
Order reference number	
Title of your thesis / dissertation	The Role the N-Terminal Domain Plays in Spidroin Assembly
Expected completion date	Aug 2016
Estimated size(pages)	150
Requestor Location	Krystal Cadle 245H Campus Dr. CENTRAL, SC 29630 United States Attn: Krystal Cadle
Publisher Tax ID	53-0196568
Billing Type	Invoice
Billing Address	Krystal Cadle 245H Campus Dr. CENTRAL, SC 29630 United States

	Attn: Krystal Cadle
Total	0.00 USD

Terms and Conditions

American Association for the Advancement of Science TERMS AND CONDITIONS
Regarding your request, we are pleased to grant you non-exclusive, non-transferable permission, to republish the AAAS material identified above in your work identified above, subject to the terms and conditions herein. We must be contacted for permission for any uses other than those specifically identified in your request above.
The following credit line must be printed along with the AAAS material: "From [Full Reference Citation]. Reprinted with permission from AAAS."
All required credit lines and notices must be visible any time a user accesses any part of the AAAS material and must appear on any printed copies and authorized user might make.
This permission does not apply to figures / photos / artwork or any other content or materials included in your work that are credited to non-AAAS sources. If the requested material is sourced to or references non-AAAS sources, you must obtain authorization from that source as well before using that material. You agree to hold harmless and indemnify AAAS against any claims arising from your use of any content in your work that is credited to non-AAAS sources.
If the AAAS material covered by this permission was published in Science during the years 1974 - 1994, you must also obtain permission from the author, who may grant or withhold permission, and who may or may not charge a fee if permission is granted. See original article for author's address. This condition does not apply to news articles.
The AAAS material may not be modified or altered except that figures and tables may be modified with permission from the author. Author permission for any such changes must be secured prior to your use.
Whenever possible, we ask that electronic uses of the AAAS material permitted herein include a hyperlink to the original work on AAAS's website (hyperlink may be embedded in the reference citation).
AAAS material reproduced in your work identified herein must not account for more than 30% of the total contents of that work.
AAAS must publish the full paper prior to use of any text.
AAAS material must not imply any endorsement by the American Association for the Advancement of Science.
This permission is not valid for the use of the AAAS and/or Science logos.
AAAS makes no representations or warranties as to the accuracy of any information contained in the AAAS material covered by this permission, including any warranties of merchantability or fitness for a particular purpose.
If permission fees for this use are waived, please note that AAAS reserves the right to charge for reproduction of this material in the future.
Permission is not valid unless payment is received within sixty (60) days of the issuance of this permission. If payment is not received within this time period then all rights granted herein shall be revoked and this permission will be considered null and void.
In the event of breach of any of the terms and conditions herein or any of CCC's Billing and Payment terms and conditions, all rights granted herein shall be revoked and this permission will be considered null and void.
AAAS reserves the right to terminate this permission and all rights granted herein at its discretion, for any purpose, at any time. In the event that AAAS elects to terminate this permission, you will have no further right to publish, publicly perform, publicly display, distribute or otherwise use any matter in which the AAAS content had been included, and all fees paid hereunder shall be fully refunded to you. Notification of termination will be sent to the contact information as supplied by you during the request process and termination shall be immediate upon sending the notice. Neither AAAS nor CCC shall be liable for any costs, expenses, or damages you may incur as a result of the termination of this permission, beyond

the refund noted above.
This Permission may not be amended except by written document signed by both parties.
The terms above are applicable to all permissions granted for the use of AAAS material.
Below you will find additional conditions that apply to your particular type of use.

FOR A THESIS OR DISSERTATION

If you are using figure(s)/table(s), permission is granted for use in print and electronic versions of your dissertation or thesis. A full text article may be used in print versions only of a dissertation or thesis.
Permission covers the distribution of your dissertation or thesis on demand by ProQuest / UMI, provided the AAAS material covered by this permission remains in situ.
If you are an Original Author on the AAAS article being reproduced, please refer to your License to Publish for rules on reproducing your paper in a dissertation or thesis.

FOR JOURNALS:

Permission covers both print and electronic versions of your journal article, however the AAAS material may not be used in any manner other than within the context of your article.

FOR BOOKS/TEXTBOOKS:

If this license is to reuse figures/tables, then permission is granted for non-exclusive world rights in all languages in both print and electronic formats (electronic formats are defined below).
If this license is to reuse a text excerpt or a full text article, then permission is granted for non-exclusive world rights in English only. You have the option of securing either print or electronic rights or both, but electronic rights are not automatically granted and do garner additional fees. Permission for translations of text excerpts or full text articles into other languages must be obtained separately.
Licenses granted for use of AAAS material in electronic format books/textbooks are valid only in cases where the electronic version is equivalent to or substitutes for the print version of the book/textbook. The AAAS material reproduced as permitted herein must remain in situ and must not be exploited separately (for example, if permission covers the use of a full text article, the article may not be offered for access or for purchase as a stand-alone unit), except in the case of permitted textbook companions as noted below.
You must include the following notice in any electronic versions, either adjacent to the reprinted AAAS material or in the terms and conditions for use of your electronic products: "Readers may view, browse, and/or download material for temporary copying purposes only, provided these uses are for noncommercial personal purposes. Except as provided by law, this material may not be further reproduced, distributed, transmitted, modified, adapted, performed, displayed, published, or sold in whole or in part, without prior written permission from the publisher."
If your book is an academic textbook, permission covers the following companions to your textbook, provided such companions are distributed only in conjunction with your textbook at no additional cost to the user:

- Password-protected website
- Instructor's image CD/DVD and/or PowerPoint resource
- Student CD/DVD

All companions must contain instructions to users that the AAAS material may be used for non-commercial, classroom purposes only. Any other uses require the prior written permission from AAAS.
If your license is for the use of AAAS Figures/Tables, then the electronic rights granted herein permit use of the Licensed Material in any Custom Databases that you distribute the electronic versions of your textbook through, so long as the Licensed Material remains within the context of a chapter of the title identified in your request and cannot be downloaded by a user as an independent image file.
Rights also extend to copies/files of your Work (as described above) that you are required to provide for use by the visually and/or print disabled in compliance with state and federal

laws.

This permission only covers a single edition of your work as identified in your request.

FOR NEWSLETTERS:

Permission covers print and/or electronic versions, provided the AAAS material reproduced as permitted herein remains in situ and is not exploited separately (for example, if permission covers the use of a full text article, the article may not be offered for access or for purchase as a stand-alone unit)

FOR ANNUAL REPORTS:

Permission covers print and electronic versions provided the AAAS material reproduced as permitted herein remains in situ and is not exploited separately (for example, if permission covers the use of a full text article, the article may not be offered for access or for purchase as a stand-alone unit)

FOR PROMOTIONAL/MARKETING USES:

Permission covers the use of AAAS material in promotional or marketing pieces such as information packets, media kits, product slide kits, brochures, or flyers limited to a single print run. The AAAS Material may not be used in any manner which implies endorsement or promotion by the American Association for the Advancement of Science (AAAS) or Science of any product or service. AAAS does not permit the reproduction of its name, logo or text on promotional literature.

If permission to use a full text article is permitted, The Science article covered by this permission must not be altered in any way. No additional printing may be set onto an article copy other than the copyright credit line required above. Any alterations must be approved in advance and in writing by AAAS. This includes, but is not limited to, the placement of sponsorship identifiers, trademarks, logos, rubber stamping or self-adhesive stickers onto the article copies.

Additionally, article copies must be a freestanding part of any information package (i.e. media kit) into which they are inserted. They may not be physically attached to anything, such as an advertising insert, or have anything attached to them, such as a sample product. Article copies must be easily removable from any kits or informational packages in which they are used. The only exception is that article copies may be inserted into three-ring binders.

FOR CORPORATE INTERNAL USE:

The AAAS material covered by this permission may not be altered in any way. No additional printing may be set onto an article copy other than the required credit line. Any alterations must be approved in advance and in writing by AAAS. This includes, but is not limited to the placement of sponsorship identifiers, trademarks, logos, rubber stamping or self-adhesive stickers onto article copies.

If you are making article copies, copies are restricted to the number indicated in your request and must be distributed only to internal employees for internal use.

If you are using AAAS Material in Presentation Slides, the required credit line must be visible on the slide where the AAAS material will be reprinted

If you are using AAAS Material on a CD, DVD, Flash Drive, or the World Wide Web, you must include the following notice in any electronic versions, either adjacent to the reprinted AAAS material or in the terms and conditions for use of your electronic products: "Readers may view, browse, and/or download material for temporary copying purposes only, provided these uses are for noncommercial personal purposes. Except as provided by law, this material may not be further reproduced, distributed, transmitted, modified, adapted, performed, displayed, published, or sold in whole or in part, without prior written permission from the publisher." Access to any such CD, DVD, Flash Drive or Web page must be restricted to your organization's employees only.

FOR CME COURSE and SCIENTIFIC SOCIETY MEETINGS:

Permission is restricted to the particular Course, Seminar, Conference, or Meeting indicated in your request. If this license covers a text excerpt or a Full Text Article, access to the reprinted AAAS material must be restricted to attendees of your event only (if you have

been granted electronic rights for use of a full text article on your website, your website must be password protected, or access restricted so that only attendees can access the content on your site).

If you are using AAAS Material on a CD, DVD, Flash Drive, or the World Wide Web, you must include the following notice in any electronic versions, either adjacent to the reprinted AAAS material or in the terms and conditions for use of your electronic products: "Readers may view, browse, and/or download material for temporary copying purposes only, provided these uses are for noncommercial personal purposes. Except as provided by law, this material may not be further reproduced, distributed, transmitted, modified, adapted, performed, displayed, published, or sold in whole or in part, without prior written permission from the publisher."

FOR POLICY REPORTS:

These rights are granted only to non-profit organizations and/or government agencies. Permission covers print and electronic versions of a report, provided the required credit line appears in both versions and provided the AAAS material reproduced as permitted herein remains in situ and is not exploited separately.

FOR CLASSROOM PHOTOCOPIES:

Permission covers distribution in print copy format only. Article copies must be freestanding and not part of a course pack. They may not be physically attached to anything or have anything attached to them.

FOR COURSEPACKS OR COURSE WEBSITES:

These rights cover use of the AAAS material in one class at one institution. Permission is valid only for a single semester after which the AAAS material must be removed from the Electronic Course website, unless new permission is obtained for an additional semester. If the material is to be distributed online, access must be restricted to students and instructors enrolled in that particular course by some means of password or access control.

FOR WEBSITES:

You must include the following notice in any electronic versions, either adjacent to the reprinted AAAS material or in the terms and conditions for use of your electronic products: "Readers may view, browse, and/or download material for temporary copying purposes only, provided these uses are for noncommercial personal purposes. Except as provided by law, this material may not be further reproduced, distributed, transmitted, modified, adapted, performed, displayed, published, or sold in whole or in part, without prior written permission from the publisher."

Permissions for the use of Full Text articles on third party websites are granted on a case by case basis and only in cases where access to the AAAS Material is restricted by some means of password or access control. Alternately, an E-Print may be purchased through our reprints department (brocheleau@rockwaterinc.com).

REGARDING FULL TEXT ARTICLE USE ON THE WORLD WIDE WEB IF YOU ARE AN ‘ORIGINAL AUTHOR’ OF A SCIENCE PAPER

If you chose "Original Author" as the Requestor Type, you are warranting that you are one of authors listed on the License Agreement as a "Licensed content author" or that you are acting on that author's behalf to use the Licensed content in a new work that one of the authors listed on the License Agreement as a "Licensed content author" has written.

Original Authors may post the ‘Accepted Version’ of their full text article on their personal or on their University website and not on any other website. The ‘Accepted Version’ is the version of the paper accepted for publication by AAAS including changes resulting from peer review but prior to AAAS’s copy editing and production (in other words not the AAAS published version).

FOR MOVIES / FILM / TELEVISION:

Permission is granted to use, record, film, photograph, and/or tape the AAAS material in connection with your program/film and in any medium your program/film may be shown or heard, including but not limited to broadcast and cable television, radio, print, world wide web, and videocassette.

The required credit line should run in the program/film's end credits.

FOR MUSEUM EXHIBITIONS:

Permission is granted to use the AAAS material as part of a single exhibition for the duration of that exhibit. Permission for use of the material in promotional materials for the exhibit must be cleared separately with AAAS (please contact us at permissions@aaas.org).

FOR TRANSLATIONS:

Translation rights apply only to the language identified in your request summary above. The following disclaimer must appear with your translation, on the first page of the article, after the credit line: "This translation is not an official translation by AAAS staff, nor is it endorsed by AAAS as accurate. In crucial matters, please refer to the official English-language version originally published by AAAS."

FOR USE ON A COVER:

Permission is granted to use the AAAS material on the cover of a journal issue, newsletter issue, book, textbook, or annual report in print and electronic formats provided the AAAS material reproduced as permitted herein remains in situ and is not exploited separately

By using the AAAS Material identified in your request, you agree to abide by all the terms and conditions herein.

Questions about these terms can be directed to the AAAS Permissions department permissions@aaas.org.

Other Terms and Conditions:

v 2

Kumaraswamy, Sriram Jul 2

to Hope, Todd, me

Correction - Rejane has asked for the high resolution image from our tech team, to give to Krystal. That may still be in process.

Krystal- you have our permission to share this image. Please note in the dissertation that this was published with permission from Pall ForteBio LLC. Reason is that your dissertation may be copyrighted to you or your university and all content will also belong to you or them. In such a situation, we may not even be able to use our image without their permission.